SYNTHETIC CARBON FIXATION FOR IMPROVED

MICROBIAL FERMENTATION YIELDS

by

Ellinor Dorothee Carlson

A dissertation submitted to the Faculty of the University of Delaware in partial fulfillment of the requirements for the degree of Doctor of Philosophy in Chemical Engineering

Summer 2017

SYNTHETIC CARBON FIXATION FOR IMPROVED

MICROBIAL FERMENTATION YIELDS

by

Ellinor Dorothee Carlson

Approved: _____
Abraham M. Lenhoff, Ph.D.
Chair of the Department of Chemical & Biomolecular Engineering

Approved: _____
Babatunde A. Ogunnaike, Ph.D.
Dean of the College of Engineering

Approved: _____
Ann L. Ardis, Ph.D.
Senior Vice Provost for Graduate and Professional Education

I certify that I have read this dissertation and that in my opinion it meets the academic and professional standard required by the University as a dissertation for the degree of Doctor of Philosophy.

Signed: _____

Eleftherios T. Papoutsakis, Ph.D.
Professor in charge of dissertation

I certify that I have read this dissertation and that in my opinion it meets the academic and professional standard required by the University as a dissertation for the degree of Doctor of Philosophy.

Signed: _____

Maciek R. Antoniewicz, Ph.D.
Member of dissertation committee

I certify that I have read this dissertation and that in my opinion it meets the academic and professional standard required by the University as a dissertation for the degree of Doctor of Philosophy.

Signed: _____

Wilfred Chen, Ph.D.
Member of dissertation committee

I certify that I have read this dissertation and that in my opinion it meets the academic and professional standard required by the University as a dissertation for the degree of Doctor of Philosophy.

Signed: _____

Shawn W. Jones, Ph.D.
Member of dissertation committee

Dedicated to my late grandfather

Dr. Karlheinz Richard Schmidt

ACKNOWLEDGMENTS

First, I'd like to thank my family for their immense love and support throughout this journey. I would not have made it this far without my parents' encouragement and their constant emphasis on the importance of education. Thank you for never telling me to stop asking "why?" and continuously fostering my curiosity ever since I was a child. Thank you for everything that you have done for me. I would not be the person I am today without your support throughout my life. As my parents provided me with everything to embark on pursuing my Ph.D., my husband provided me with the necessary support throughout the graduate research journey. Thank you, Torren, for always being there for me at the end of a tough day. Thanks for all the hugs and warm meals that gave me a mental break from my doctorial work. Thank you for forcing me to take breaks and reminding me that there is more to life than running experiments with microbes. Thank you for listening to my research problems, and letting me pick your brain on gas chromatography! Your love and support gave me the strength to stick it out. Thanks for never losing confidence in me. I am so lucky to have had you by my side to share this experience with me. It wouldn't have been the same without you.

Second, a big thanks to all the friends I have made throughout graduate school. I am so proud to be part of the Chemical Engineering community at the University of Delaware, and grateful for the camaraderie and friendships I have made throughout the department. Thanks to Erik Munsell for being the best homework buddy during the first year of graduate school, and later the best climbing buddy to de-stress from a long

day in lab. Thanks to Sarah Mastroianni for pulling me into the Delaware Saengerbund, it was fun singing together and catching up on Wednesdays. Your friendship means a lot to me. Thanks to all my classmates for sharing the grueling experience of first year graduate classes with me. Thanks to our 'girl lunches' during the first few semesters, which were instrumental in creating this sense of community that I now feel part of. The countless happy hours with peers, the Colburn Club and all their work associated with creating the graduate student environment are some of the memories I will cherish from my graduate time.

Third, the Papoutsakis Group and all the lasting friendships I made. Sergios, Stefan, Mohab, Kyle, Keerthi, Nich, Jinlin, Alan, Stephanie, Lisa, Kyle, Chen-Yuan, Julia, Kamil, Alex, Matt, Christian, Erica and Hannah, and everyone else who joined the Papoutsakis Group during my tenure here. The office was always a place to share our experiences together, get insightful ideas and suggestions, and provided a space to laugh and sometimes goof of together. Thanks for all the cake and wonderful singing! A special thanks to my lab mate and friend, Alan Fast, who guided me into my research project and provided friendship to me throughout my journey. Alan, I am so grateful that we could share this experience and were able to work so closely together. Much of this work wouldn't have been possible without your willingness to collaborate. Thanks also to Bryan and Shawn for their friendship and mentorship, as well as their interest in collaborating on the work with acetogens. I learned so many things from both of you, ranging from research knowledge to professional development.

Thanks to my committee members, who all played a much bigger part of my thesis than they realize. Dr. Chen, you set me up on my path towards protein

engineering, from cloning to western blots, your lab provided me with everything necessary to make the switch to biochemical engineering. Maciek, your mentorship on carbon tracers was invaluable to my thesis work. Thank you for all your comments and suggestions, for meeting with me and taking the time to guide me during my research endeavors. Thanks to Jennifer Au and Jacqueline Gonzalez for their constant willingness to run samples for the Papoutsakis Lab. The collaboration between our two labs has been wonderful. Shawn, thank you for being a mentor and friend during my graduate research. Collaborating with you taught me how to be a better researcher. Your mentorship was invaluable in guiding my thesis work.

Last, but not least, I would like to thank my advisor, Terry Papoutsakis, for letting me join his research group and making my graduate research project possible. Thank you for never giving up on me, and thank you for always providing a positive outlook on my research results. Thank you for pushing me when I needed it most, and thank you for giving me space and time when I required independence. Your mentorship and guidance helped me to put my best foot forward, and encouraged me to always exceed my own expectations. Your hard work provides the foundation for all of us to excel at the research we are doing as part of your lab group. I am so grateful to have been part of your research group and complete my doctoral degree under your guidance.

TABLE OF CONTENTS

LIST OF TABLES

LIST OF FIGURES

xvi

ABSTRACT

Microbial fermentation is a well-established conversion technology to utilize our cheap and abundant renewable carbohydrate resources for the production of fuels and chemicals. However, these processes are inherently limited by the decarboxylation reactions occurring during traditional fermentations (glycolysis) leading to low feedstock conversion and product yield. In general, a maximum of two-thirds of the carbon contained in the feedstock can be recovered in useful fermentation products, the rest being lost as undesirable CO_2. With recent advances in synthetic biology, the evolved CO_2 can be utilized as a carbon feedstock by native or engineered organisms, avoiding the loss of CO_2 and increasing overall yield of fuels and chemicals.

A promising CO_2 utilization route is the Wood-Ljungdahl pathway as it is the most efficient pathway for non-phototrophic CO_2 fixation. In this pathway, two molecules of CO_2 are reduced with 8 reducing equivalents to form one molecule of acetyl-CoA, a primordial biological building block for cellular components. The acetyl-CoA molecule can be used in the various downstream pathways to produce the desired products. Through theoretical modeling, the increased product yield when coupling glycolysis to the Wood-Ljungdahl pathway has been shown.

In order to validate this concept, five microorganisms, which natively contain the Wood-Ljungdahl pathway, were grown in the presence of carbohydrates and exogenous gases, and were shown to improve product mass yields. Using carbon-tracing experiments, we demonstrated gaseous carbon uptake was continuous and

independent of the presence of higher-energy carbohydrate substrates. Therefore, this type of anaerobic, non-photosynthetic mixotrophic fermentation can be used to overcome some of the challenges associated with the current production of biofuels via traditional fermentations.

To utilize mixotrophic fermentation for the successful production of biobutanol in an industrially relevant strain, *Clostridium acetobutylicum* was engineered to reduce CO_2 by the heterologous expression of two key enzymes used in autotrophic CO_2 fixation. The CO dehydrogenase (CODH) and acetyl-CoA synthase (ACS) are two essential proteins of the Wood-Ljungdahl pathway and form a bifunctional heterotetrameric complex. The CODH/ACS enzyme can reversibly catalyze CO_2 to CO, effectively enabling a biological water-gas shift reaction at ambient temperatures and pressures. Functional expression of the *C. carboxidivorans* CODH/ACS complex was demonstrated in the solventogen *C. acetobutylicum*, and the strain exhibited both CO_2 reduction and CO oxidation activities. The CODH reactions were studied using isotopic labeling to verify that CO was a direct product of CO_2 reduction and vice versa. The CODH enzyme was hypothesized to use a native *C. acetobutylicum* ferredoxin as the electron carrier for CO_2 reduction. Heterologous CODH activity depended on actively growing cells and required the addition of nickel, which is inserted into CODH without the need to express the native Ni insertase protein. Increasing CO concentrations in the gas phase inhibited CODH activity and altered the metabolite profile of the CODH-expressing cells. This work provides the foundation for engineering a complete and functional Wood-Ljungdahl pathway in non-native host organisms, thereby allowing the application of mixotrophic fermentation to an industrially relevant organism to achieve 100% feedstock conversion.

Chapter 1

INTRODUCTION

1.1   Increasing Demand for Energy Requires New Technologies to Combat Climate Change

Earth's climate has significantly changed since the advent of the industrial revolution due to the accumulation of greenhouse gases such as carbon dioxide, methane, and nitrogen oxides (IEA 2016). The level of atmospheric carbon dioxide (CO_2) has increased to almost 399 ppm, causing an increase in global average surface air temperatures, disrupted weather patterns, and acidified oceans (IEA 2016, Obama 2017). Compared to the pre-industrial revolution levels of atmospheric CO_2 , the current levels are 40% higher and still growing at an alarming rate of 2 ppm per year (IEA 2016). 65% of the total CO_2 emission for the year 2014 were produced by the electricity & heat and energy sector (IEA 2016). This has caused concern among both scientists and politicians and led to a focus on the development of sustainable energy technologies to combat climate change. The demand for energy is increasing while at the same time the availability of fossil fuels is decreasing. Therefore, finding alternative and sustainable energy sources is now more important than ever. Technologies that harness alternative energy sources such as solar, wind, geothermal, hydroelectric and biomass need to achieve economic and technological viability to replace our current, unsustainable sources. One approach in particular, the simultaneous production of alternative fuels along with CO_2 sequestration, is strongly desired (Aresta 2010, Tracy, Jones et al. 2012). This fuel could replace current

petroleum based fuels, and would be carbon neutral if the carbohydrate sources are derived from biomass and/or through microbial carbon fixation. This work investigates the metabolic engineering of *Clostridium acetobutylicum* as a microbial host for the production of fuels and chemicals from the simultaneous use of carbohydrates and CO_2 or CO as feedstock. The fuels and chemicals produced through this bioprocessing approach can be derived from carbon neutral resources and therefore provide an alternative technology to replace current unsustainable, petroleum-based technologies.

1.2   Harnessing the Power of Biology to Produce Fuels and Chemicals

Industrial fermentation utilizes microbial hosts to convert a variety of feedstocks into useful products. *Saccharomyces cerevisiae* (yeast) is one of the most common and well known microbial hosts, which has been used for many centuries to produce alcoholic beverages and bread from simple sugars and starches. With new advancements such as genome sequencing and metabolic engineering approaches, we are expanding our microbial toolbox which has led to the development of new microbial hosts and new bioprocessing technologies to convert a variety of carbohydrate and gaseous feedstocks into fuels and chemicals (Jones and Woods 1986, Clomburg, Crumbley et al. 2017). Feedstocks such as primary and waste biomass as well as syngas (mixture of CO, CO_2 and H_2), derived through the gasification of organic matter or industrial off-gases (Liew, Martin et al. 2016) provide a carbon neutral resource that can be utilized in bioprocessing. The bioprocessing of these feedstocks provides an alternative, "second generation" biofuel that can replace current unsustainable use of petroleum and help combat climate change. The challenge lies in developing the technologies that can compete economically with current

2

technologies. The single most important economic factor in bioprocessing is feedstock cost (Jones, Fast et al. 2016). Modularity in feedstock consumption (i.e. microbial hosts capable of consuming multiple carbohydrate sources), as well as complete feedstock conversion can have a huge impact on the economic competitiveness of bioprocessing. This work shows enhancements in product yields by employing mixotrophic fermentations, which is defined as the combination of traditional, carbohydrate fermentations with that of gaseous fermentations. Increasing product yields is one of the most effective ways to mitigate high feedstock costs (Fast, Schmidt et al. 2015). This work will show that mixotrophy eliminates low biomass and product yields generally found in gaseous only fermentation and achieves higher product diversity than traditional carbohydrate fermentations.

1.2.1 Clostridia Offer the Feedstock Flexibility Necessary for Bioprocessing

Of particular importance are bacteria of the class Clostridia, which are anaerobic, gram$^+$, endospore forming prokaryotes that utilize a wide variety of feedstocks and are capable of producing an assortment of products (Tracy, Jones et al. 2012, Fast, Schmidt et al. 2015). This flexibility and diversity make them ideal candidates for the industrial production of fuels and chemicals from renewable resources, including the greenhouse gas CO_2. They have a unique ability to utilize all complex and simple carbohydrates such as those contained in biomass (i.e. cellulose, xylans, oligo- and polysaccharides), gases (CO_2, CO, H_2), glycerol, and they are also excellent solvent producers (Tracy, Jones et al. 2012). Solventogenic clostridia, such as *Clostridium acetobutylicum*, and *Clostridium beijerinckii*, produce acetone, butanol and ethanol via the metabolic ABE fermentation pathway. *Clostridium acetobutylicum* is characterized by its two-stage growth, termed acidogenesis and solventogenesis.

During the early, exponential stage of growth (acidogenesis), acetate and butyrate accumulate both inside and outside of the cells. In response to this high acid accumulation, the metabolism shifts to stationary phase (solventogenesis), where acetone, butanol and ethanol are produced (in a 3:6:1 ratio). The first large scale biological fermentation process for the industrial production of acetone and butanol was developed using this solvent-producing *Clostridium* strain. During the first world war, Chaim Weizmann utilized CAC to produce acetone, a precursor for cordite, which helped the allies win the war. Later, during World War II, butanol was used as a fuel and precursor for synthetic rubber. The introduction of chemically synthesized solvents in the early 1960s, however, led to commercial fermentation processes becoming nearly obsolete (Jones and Woods 1986). Now with the heightened interest in alternative transportation fuels, commercial biological fermentation is seeing a revival. In particular, butanol and hexanol are superior drop-in fuels as they do not require expensive infrastructure changes and can be used in conventional engines without modification (Fernández-Naveira, Veiga et al. 2017). Currently, butanol is a native fermentation product of *Clostridium acetobutylicum*, *Clostridium carboxidivorans* and *Clostridium kluyveri* , whereas hexanol is currently only known to be produced by *Clostridium carboxidivorans* and *Clostridium kluyveri*. Other products derived through the fermentative alcohol production pathway are isopropanol, 2-pentanol, ethanol, acetone, acetate, and butyrate (Fast, Schmidt et al. 2015). Furthermore, 2-keto acid derived alcohols such as 2,3-butanediol and isobutanol have gained interest as commodity chemicals or fuel substitutions, respectively (Köpke, Mihalcea et al. 2011, Fast, Schmidt et al. 2015). The vast number of different fermentation pathways allows for modularity to produce the fuel of

interest, and engineering efforts have addressed maximizing various product yields making the genus *Clostridium* an attractive microbial platform for bioprocessing.

1.2.2 Acetogens Utilize Gaseous (C1) Feedstocks

Acetogens are obligate anaerobic bacteria characterized by their ability to produce acetate while utilizing gases such as CO_2 along with H_2 or CO as a carbon or energy source (Ragsdale and Pierce 2008). They are autotrophs (deriving energy solely from gases) that use the Wood-Ljungdahl pathway (WLP) to fix CO_2 and incorporate it into biomass and metabolites (Drake, Gössner et al. 2008). Both bacteria and archaea can be considered acetogens. They sequester two molecules of CO_2 using the reducing power of 8 electrons derived either from H_2, CO or other energy-rich carbohydrates. To date, at least eleven organisms with functional WLPs have been sequenced, including *Clostridium ljungdahlii, Clostridium difficile, Clostridium carboxidivorans, Clostridium aceticum, Clostridium autoethanogenum, Acetobacterium woodii, Acetonema longum, Clostridium drakei, Moorella thermoacetica* and *Eubacterium limosum* (Liew, Martin et al. 2016). All of these organisms are part of the class Clostridia; and many are part of the genus *Clostridium*. So far, few have been genetically manipulated (Liew, Martin et al. 2016). The initial discovery of the very first acetogen, *Clostridium aceticum*, occurred in 1936 but the strain was lost shortly thereafter (Drake, Gössner et al. 2008 New light.). The strain was rediscovered years later in the 1980's, but by then *Moorella thermoacetica* (formerly known as *Moorella thermoaceticum*), discovered in 1942, had become the most well-studied model acetogen.

The individual steps in the Wood-Ljungdahl pathway have been elucidated since the late 1980's, but many work remains to understand the metabolic complexity

of acetogens. Because of the inherent energy requirement of CO_2 fixation, (1 ATP molecule per 1 molecule of acetyl-CoA), acetogens have developed ways to overcome the severe energy limitations when grown solely on gases by evolving electron bifurcation (Schuchmann and Müller 2014). Electron bifurcation utilizes the coupling of an exergonic reaction to that of an endergonic reaction, allowing for the conservation of reduction potential while overcoming thermodynamic barriers. These energy conservation mechanisms have been elucidated recently, but more research is underway to understand the how acetogens are able to thrive on gases alone (Schuchmann and Müller 2014). Even with these enhanced, complex energy conservation mechanisms, the biomass yields of many acetogens are quite low, and as a result, acetate remains the major end product as a way to overcome ATP limitations through substrate level phosphorylation. These energy limitations under autotrophic conditions result in a limited product profile and slow growth rates, as reviewed in detail elsewhere (Fast, Schmidt et al. 2015). One way to overcome the limited product profile and energy limitations is to couple the autotrophic metabolism to an energy rich heterotrophic metabolism like the consumption of hexose sugars, termed mixotrophy. This concept of mixotrophic fermentation is discussed in detail below.

1.3   Mixotrophy as a Technology for Achieving High Feedstock Conversion

Mixotrophy, defined as the simultaneous uptake of gaseous and carbohydrate feedstocks, can increase the theoretical carbon conversion as demonstrated by stoichiometric calculations (Fast and Papoutsakis 2012, Fast, Schmidt et al. 2015, Jones, Fast et al. 2016). The cost of feedstock and feedstock pretreatment for bioprocessing and the production of next generation biofuels can often exceed 50% of total operating expenditure (Fast, Schmidt et al. 2015). By converting more of the

supplied feedstock, the economics of bioprocessing become superior to those that cannot achieve complete feedstock conversion. Besides conversion, selectivity is another important parameter, which can be achieved through genetic engineering and process design. Selectivity is defined as the amount of desired product divided by the amounts of undesired side products. The percent conversion of the feedstock and product selectivity can be described by the yield, which is the amount of product formed divided by the amount of feedstock consumed. Due to the decarboxylation reactions occurring in most fermentative pathways, CO_2 becomes an undesirable by-product, thereby lowering the selectivity and yield. Sequestering the CO_2 through CO_2 fixation pathways such as the WLP can have a profound effect on feedstock conversion efficiencies and result in increased yields. The exact mechanisms on how CO_2 can be utilized to increase yields of fermentation products will be discussed in detail below.

1.3.1 The Wood-Ljungdahl Pathway is the Most Energy Efficient CO_2 Fixation Pathway

The Wood-Ljungdahl pathway (WLP), or the reductive acetyl-CoA pathway, reduces two molecules of CO_2 to form one molecule of acetyl-CoA (Figure 1). Acetyl-CoA is then further converted to cellular metabolites or acetate to produce energy via substrate level phosphorylation. The pathway consists of two linear branches, the Eastern (methyl) and the Western (carbonyl) branch. The two branches were discovered in the laboratory of Wood and Ljungdahl (Ljungdahl 2009). The first step is the reduction of CO_2 to formate by formate dehydrogenase (FDH). Subsequently, formate is condensed with tetrahydrofolate to form 10-formyl-THF. This is an ATP dependent step catalyzed by formate-THF-ligase (FTL). The formyl-THF is then

converted to 5,10-methenyl-THF by the methenyl-THF cyclohydrolase (MTC) and reduced to 5,10-methylene-THF by methylene-THF dehydrogenase (MTD) and finally reduced to 5-methyl-THF by a methylene-THF reductase (MTRS) (Ragsdale 1991 , Tracy, Jones et al. 2012). The 5-methyl-THF is transferred by the methyltransferase (MTR) to the cobalt site in the cobalamin cofactor bound to the corrinoid iron–sulfur protein (CFeSP) to form an organometallic methyl-Co(III) intermediate (Ragsdale 1991). In the Western branch, the carbon monoxide dehydrogenase (CODH) catalyzes the conversion of CO_2 to CO to generate CO as a metabolic intermediate. This intermediate, along with the methyl group of the CFeSP from the eastern branch, is combined by the ACS/CODH complex to generate acetyl-CoA (Ragsdale 1991). Compared to other CO_2 fixation pathways, the WLP pathway requires the least amount of ATP (1) and reducing equivalents (NAD(P)H or equivalent) (8), and is therefore the most energy efficient CO_2 fixation pathway (Fast and Papoutsakis 2012).

1.3.2   Glycolysis or the Embden–Meyerhof–Parnas pathway

Typical biological fermentations depend on metabolizing a 5 or 6 carbon carbohydrate source through the Embden–Meyerhof–Parnas (EMP) pathway, in which the decarboxylation of pyruvate results in an overall CO_2 loss. During glycolysis, 6 carbon sugars such as hexose are transformed into 2 molecules of pyruvate through a total of ten enzymatic steps (1.1). In total, 4 molecules of ATP and 4 reducing equivalents become available for the cell to use as energy and reducing power. When 2 molecules of pyruvate are further decarboxylated to yield the metabolic intermediate acetyl-CoA, another 4 reducing equivalents and 2 CO_2 molecules are released. This drastically limits the total theoretical yield that can be achieved from those carbon sources (Fast and Papoutsakis 2012). One way to minimize this carbon loss is to re-

assimilate the CO_2 through the Wood-Ljungdahl pathway (WLP) found in acetogenic bacteria. This was first proposed by Fast *et al* (Fast and Papoutsakis 2012). Other pathways include the non-oxidative glycolysis pathway developed by Bogorad *et al*. but limitations and challenges will be discussed in Chapter 2 (Bogorad, Lin et al. 2013).

1.3.3 Coupling the Wood-Ljungdahl Pathway to the Embden–Meyerhof–Parnas Pathway

The evolved CO_2 from glycolysis can be incorporated back into acetyl-CoA via the WLP, requiring 8 reducing equivalents and 1 molecule of ATP. This coupling between glycolysis and the WLP is depicted in 1.1. At the expense of one molecule of ATP and 8 reducing equivalents, all 6 carbons from hexose can be converted into the metabolic intermediate acetyl-CoA, providing for a much higher carbon yield for products derived through the fermentative alcohol production pathway than when glycolysis is utilized on its own. This so termed mixotrophic fermentation has many advantages when compared to heterotrophic or autotrophic fermentations (sugars or gases only, respectively). Besides the theoretically possible 100% feedstock conversion and increased product yield, energy limitations are alleviated due to the additional energy contained in the carbohydrate feedstock, resulting in higher biomass yields and faster growth rates (Jones, Fast et al. 2016).

1.4 Dissertation Aims and Outline

This work first demonstrates the concept of mixotrophic fermentation by illustrating the improvements in product yield through the development of a stoichiometric Flux Balance Analysis model in MATLAB (Chapter 2). Next, that practical application of mixotrophy is demonstrated by probing five strains of native

acetogens for their ability to increase product yields on glucose when grown under mixotrophic conditions (Chapter 3). The concept is further interrogated by supplying exogenous carbon and electrons to enhance product yields and selectivity. The increase in product yields under these enhanced mixotrophic conditions also demonstrates the ability to shift the native metabolism towards a more reduced product profile (increased selectivity), an inherent requirement for highly reduced molecules such as those required for fuel substitutes.

Second, this work paves the way for achieving synthetic carbon fixation in an industrially relevant strain, *Clostridium acetobutylicum*. This is realized by the heterologous expression of the carbon monoxide dehydrogenase enzyme from the acetogen *Clostridium carboxidivorans* expressed in the closely related *Clostridium acetobutylicum* (Chapter 4). The engineered strain demonstrates the *in vivo* conversion of CO_2 to CO and vice versa. The functionality is probed on an RNA and enzymatic level, as well as on a metabolic level through novel ^{13}C-carbon tracer experiments. The *in vivo* experiments demonstrate the ability of the engineered strain to have the necessary co-factors and low electron potentials to overcome the energetically challenging reaction of CO_2 reduction.

The effect of CO_2 reduction and CO oxidation is further shown to have profound effects on the metabolic profile of the engineered strain, indicating the ability of heterologously expressed genes to influence internal regulatory mechanisms (Chapter 5). The redox balance within cells of *Clostridium acetobutylicum* is tightly regulated and the addition of gases such as CO_2, CO, and H_2 can have a profound impact on product distribution. Most notably, the addition of CO abolishes acetone production, allowing for higher yield in the desired butanol production. The heterologous

expression of the carbon monoxide dehydrogenase enzyme from the acetogen *Clostridium carboxidivorans* expressed in *Clostridium acetobutylicum* showed a reversal to the inhibition of CO, and was capable of detoxifying up to 1 millimole of CO.

Additional hosts for synthetic CO_2 reduction are explored (Chapter 6) and some conclusions and proposals for further work are suggested.
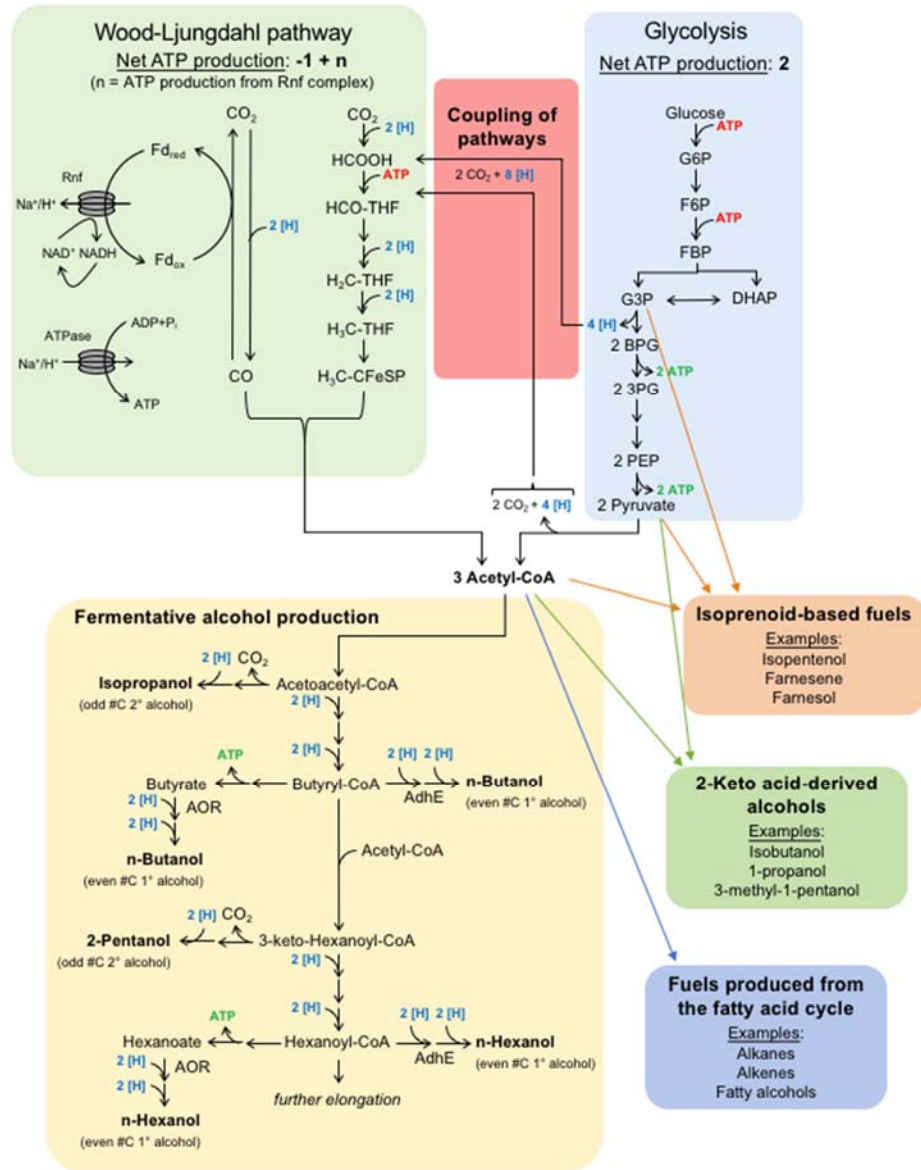
Figure 1.1. Wood-Ljungdahl Pathway coupled to glycolysis and subsequent routes to leading to biofuel production by Clostridia. Glycolysis generates excess ATP, acetyl-CoA, CO_2 and reducing equivalents, while the WLP reassimilates the CO_2 into additional acetyl-CoA, which is fed into downstream pathways. Importantly, acetate does not need to be generated for ATP production. Advanced biofuels can be generated from a number of pathways, as indicated, with different input molecules. A detailed scheme for fermentative alcohol production of long chain alcohols is depicted. Primary (1°) alcohols with an even number of carbon atoms can be generated from one of two routes. One pathway uses an aldehyde:ferredoxin oxidoreductase (AOR) and results in the production of ATP. The other pathway utilizes the bifunctional aldehyde/alcohol dehydrogenase (AdhE) and does not produce ATP. Abbreviations of the different metabolites: G6P, glucose 6-phosphate; F6P, fructose 6-phosphate; FBP, fructose 1,6-bisphosphate; G3P, glyceraldehyde 3-phosphate; DHAP, dihydroxyacetone phosphate; BPG, 1,3-bisphosphoglycerate; 3PG, glycerate 3-phosphate; PEP, phosphoenolpyruvate; 2KIV, 2-ketoisovalerate. Adapted from (Fast, Schmidt et al. 2015)

Chapter 2

THEORETICAL YIELD CALCULATIONS FOR ANAEROBIC, NON-PHOTOSYNTHETIC (ANP) MIXOTROPHIC FERMENTATIONS

2.1 Novel Options for Yield Improvements for the Production of Biofuels and Biochemicals

This Chapter summarizes the theoretical motivation for utilizing mixotrophy for achieving higher product yields for anaerobic fermentations. Much of the foundation of stoichiometric yield calculations has been published by Fast et al. (2012). The concept has been expanded upon in the review by Fast, Schmidt and Jones et al. from which some of the sections are taken (with permission). Figure 2.2 and 2.3 are adopted from Jones, Fast and Carlson et al.

2.2 Novel Options for Yield Improvements for the Production of Biofuels and Biochemicals

Product yields of anaerobic fermentations are often limited by the decarboxylation reactions involved in Embden-Meyerhof-Parnas (EMP) glycolysis. Anaerobic, non-photosynthetic (ANP) mixotrophic fermentation overcomes the low mass yields by recapturing the evolved CO_2 from EMP through the Wood-Ljungdahl Pathway (WLP). In ANP mixotrophic fermentation, two molecules of CO_2 and eight electrons released from glycolysis are fed into the WLP to produce a total of three molecules of acetyl-CoA rather than the two molecules of acetyl-CoA derived from glycolysis alone. The increase in the total acetyl-CoA yields higher product formation

of many fermentative pathway derived products, in particular biofuels like ethanol and butanol. The most significant release of CO_2 results from the decarboxylation of pyruvate, resulting in a third of the carbon moles from sugars to be lost. As a result, the fermentation emits CO_2 and the final theoretical mass yields are lowered. Many desirable products such as ethanol, butanol, hexanol, acetone, isopropanol and 2-pentanol, just to name a few, are derived from the acetyl-CoA intermediate. Thus, these products are especially prone to lower mass yields. In addition, some of these, such as 3-carbon acetone and isopropanol, are produced through an additional decarboxylation reaction, resulting in even lower theoretical mass yields. One way to overcome these significant mass losses is to sequester the CO_2 back into acetyl-CoA. Potential native CO_2 pathways are discussed in Section 2.6 but out of the many CO_2 fixation pathways, the WLP sets itself apart as the ideal CO_2 fixation pathway due to the relatively low requirement of reducing equivalents, ATP, and limited number of enzymes found in the pathway (Fast and Papoutsakis 2012). In addition, the carbon fixation pathway is anaerobic and non-photosynthetic and is widespread throughout many clostridia organisms. Clostridia organisms have a wide substrate as well as product diversity and are therefore of great interest in bioprocessing. To demonstrate the theoretical mass yield improvements, stoichiometric calculations of diverse product pathways are compared during heterotrophic (EMP only), autotrophic (WLP only), and mixotrophic (ANP) fermentations in Section 2.4. The addition of external electrons such as hydrogen or carbon monoxide is also explored in enhanced mixotrophic fermentation calculations in the same Section. The development of the model is discussed in detail in Section 2.3. Limitations under autotrophic conditions are explored in Section 2.5, with additional considerations of the novel energy

conservation mechanisms that acetogens have developed to overcome the challenges of sustaining life on gases alone. Finally, alternative native and synthetic CO_2 fixation pathways are discussed in Section 2.6.

2.3   Flux Balance Analysis Model to Calculate Maximum Product Yields

Flux balance analysis utilizes known metabolic pathways and biochemical networks to calculate the flow of metabolites through the given network (Orth, Thiele et al. 2010). A flux balance model was constructed based on the stoichiometric calculations by Fast *et al.* to calculate the maximum product yield of various metabolites (Fast and Papoutsakis 2012). The stoichiometric model utilizes mass balance equations of biological reactions occurring within the cell, such as i) glycolysis, ii) biomass formation, iii) various fermentative pathways, as well as reaction pathways and iv) products derived through alpha-keto acid intermediates. Maximum theoretical product yields can be calculated by combining these equations into a stoichiometric matrix and solving a linear constraint maximization, or minimization problem. The stoichiometric matrix ($\mathbf{S}$), size m*n, is composed by rows of compounds (m) involved in the reactions and columns (n) of each of the reactions in the network. The flux through all the reactions is denoted as the vector $\mathbf{v}$, (length of n), and the concentrations of all metabolites are represented by a vector $\mathbf{x}$, (length of m). Using the steady state assumption ($d\mathbf{x}/dt = 0$), the final stoichiometric matrix is confined by mass balance constraints as ($\mathbf{Sv}=0$). There are no unique solutions to this system of equations, so constraints are required to create bounds of the solution space, and an objective function is defined which is either maximized or minimized through linear programming. The resulting flux distribution, $\mathbf{v}$, maximizes or minimizes the objective function (see Figure 2.2.).

In this FBA model, reactions shown in Figure 2.1 are incorporated into the columns of **S**, and various metabolites involved make up the rows of this matrix. A schematic to illustrate some of the more common pathways is given in Figure 2.1. The model was constructed in MATLAB using the flux balance model description of Covert *et al.* utilizing the linear solver *linprog* (Covert 2014). The stoichiometric matrix S is concatenated with a matrix that includes the exchange fluxes of the metabolies (See Figure 2.2). The constraints are set through upper and lower bounds for each of the fluxes, and represent the linear equality or in-equality constraints of this system. For example, defining the upper and lower bounds of the external fluxes of NADH to be zero prohibits the accumulation of NADH within the boundary (cell). All other internal metabolites such as acetyl-CoA and pyruvate are treated in a similar fashion. All products (and their respective exchange fluxes) are defined to leave the system (denoted by a negative flux), so the constraint on those fluxes is set to be less than zero. The production of pyruvate from glucose (glycolysis) is irreversible by defining the lower bound of the flux as zero as well. This stoichiometric model can be ued to calculate total product yields for heterotrophic, mixotrophic and enhanced mixotrophic conditions. The results of these calculations are presented in Figure 2.3. The condition which is to be tested (heterotrophy, mixotrophy or enhanced mixotrophy) defines the bounds for the internal fluxes. For example, the default lower and upper bounds for the WLP are set to zero and infinity, respectively, indicating the WLP is irreversible and running in the direction of acetyl-CoA synthesis. If the WLP is desired to be inactive (such as in the case for heterotrophy), the upper and lower bounds for the WLP flux is set to zero. The same has to be true for hydrogen exchange. In the case for mixotrophy and heterotrophy, the hydrogen uptake flux is set

to be greater than zero, defining net hydrogen production (only in the case where extra

NADH is available). In the case of enhanced mixotrophy, the hydrogen flux is allowed

to operate in the reverse, i.e. in the direction of taking up hydrogen. The simple change

of the boundary conditions allows for the product yield calculations under the various

fermentation conditions.

Table 2.1. Stoichiometric Equations from MATLAB flux balance analysis.

Reaction #		Reference
1	glucose $\rightarrow$ 2 pyruvate + 2 ATP + 2 NADH	(Papoutsakis 1984)
2	pyruvate $\rightarrow$ acetyl-CoA + 2 NADH + CO_2	(Papoutsakis 1984)
3	acetyl-CoA $\rightarrow$ acetate + ATP	(Papoutsakis 1984)
4	acetyl-CoA + 2 NADH $\rightarrow$ ethanol	(Papoutsakis 1984)
5	2 acetyl-CoA $\rightarrow$ acetone + CO_2 + ATP	(Papoutsakis 1984)
6	2 acetyl-CoA + 2 NADH $\rightarrow$ butyric acid + ATP	(Papoutsakis 1984)
7	2 acetyl-CoA + 4 NADH $\rightarrow$ butanol	(Papoutsakis 1984)
8	2.43 ATP + 0.3 NADH + 0.5 acetyl-CoA $\rightarrow$ biomass	(Fast and Papoutsakis 2012)
9	NADH $\rightarrow$ H_2	(Papoutsakis 1984)
10	$2CO_2$ + $4H_2$ + ATP $\rightarrow$ acetyl-CoA+ $2H_2O$ + nATP	(Fast, Schmidt et al. 2015)
11	3 acetyl-CoA + 6 NADH $\rightarrow$ hexanol	(Fernández-Naveira, Veiga et al. 2017)
12	pyruvate $\rightarrow$ isobutyrate + 2 CO_2	
13	pyruvate + 2 NADH $\rightarrow$ propionate	

14	2 pyruvate + NADH $\rightarrow$ 2,3-butanediol + 2 CO_2	(Köpke, Mihalcea et al. 2011)
15a	Pyruvate + CO_2 + 2 NADH $\rightarrow$ succinate	(Thakker, Martínez et al. 2012)
15b	succinate + ATP + acetyl-CoA +4 NADH $\rightarrow$ 1,4 butanediol + acetate	(Yim, Haselbeck et al. 2011)
16	2 acetyl-CoA + NADH $\rightarrow$ 3-hydroxybutyrate	
17	2 pyruvate + 2 NADH +$\rightarrow$ isobutanol + 2 CO_2	(Papoutsakis 1984)
18	2 acetyl-CoA + NADH +$\rightarrow$ 2-hydroxyisobutryate	
19	2 acetyl-CoA + NADH $\rightarrow$ isopropanol + CO_2	
20	CO_2 + 2 NADH $\rightarrow$ CO	(Fast and Papoutsakis 2012)

Figure 2.1. Schematic for Stoichiometric Flux Model. The products are defined as leaving the system (indicated by the arrow). CO_2 and H_2 are allowed to either leave or enter the system. Glucose is always consumed.

Figure 2.2. Set up of the Stoichiometric matrix S, with the matrix for the exchange
fluxes (denoted in red arrows).

2.4   Maximum Product Yields for Various Metabolites

The stoichiometric model discussed in Section 2.3 can be used to calculate the

maximum theoretical yield of various metabolites derived through fermentation

pathways found in the genus *Clostridium*. Yield is defined as the total amount of

product(s) produced divided by the total amount of substrate consumed. The models'

calculations are based on directing 5% of the carbon flux towards biomass formation.

Under heterotrophic conditions, the maximum theoretical mass yield of acetate that

can be achieved is 0.62 grams of acetate per gram of glucose. Because the production

of acetate generates energy and is not dependent upon reducing availability, the only

limitation to producing acetate is the total availability of carbon. As another example,

the maximum theoretical mass yield that can be achieved for the production of

butyrate is 0.45 grams per gram of glucose. The lower yield is due to the fact that

butyrate contains 4 carbons rather than 2. So again, the theoretical yield is limited by

the availability of carbons. Under heterotrophic conditions, only 2/3 of the carbon

going into the system can be converted to product. Therefore, if we now include the

WLP in our calculations, as shown for the case of mixotrophy, the maximum

theoretical yield increases. Now, almost 0.94 grams of acetate per gram of glucose can

be formed. This yield indicates that all of the carbon not going towards biomass is

going towards the production of acetate. In comparison, the yield in butyrate is much lower (0.55 g/g glucose). This can be explained by looking at the number of electrons that are required for the production of butyrate. The production of butyrate from acetyl-CoA requires 4 reducing equivalents, compared to none for the production of acetate. The degree of reduction (DOR), which can be calculated by Equation 1, gives an accurate representation of how reduced a certain metabolite is. The higher the DOR, the higher the demand for reducing equivalents, thereby lowering the yield in mixotrophy.

Equation 1 $$DOR = \frac{4(\#C) + \#H - 2(\#O)}{\#C}$$

The DOR of butyrate is higher than the DOR of acetate, which indicates that the production of butyrate requires a higher amount of reducing equivalents. The theoretical yield of butyrate is therefore limited by the availability of electrons in the feedstock. Since the WLP requires electrons to sequester CO_2, the electrons derived through glycolysis from the oxidation of glucose are not sufficient to produce reduced products and at the same time fix CO_2. If we lift the limitation of reducing equivalents by introducing hydrogen into the system, (H_2 supplemented mixotrophy), we see the maximum theoretical yield increases (Figure 2.4). Therefore, both the requirements for CO_2 fixation (ATP and NADH) as well as requirements for the individual products need to be considered when calculating theoretical mass yields. The additional hydrogen that is required to fix all the released CO_2 from the system back into product is shown in Figure 2.4. We can see that the more reduced products such as the alcohols like ethanol, butanol or hexanol, require the most amount of hydrogen. The amount of hydrogen required is correlated to the degree of reduction of each species.

By plotting the degree of reduction versus the hydrogen, we see a linear correlation between the two as can be seen in Figure 2.5.
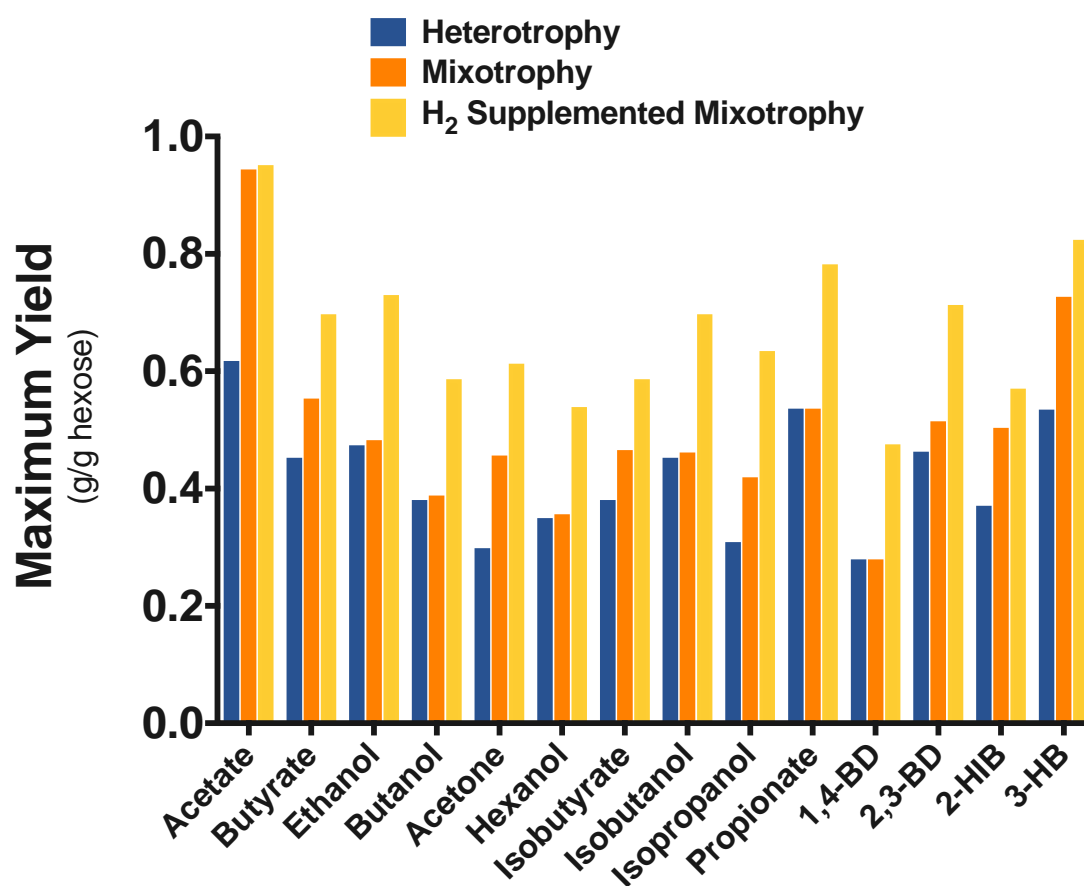
Figure 2.3. Maximum yield for various metabolites under heterotrophic, mixotrophic and hydrogen supplemented mixotrophic conditions.
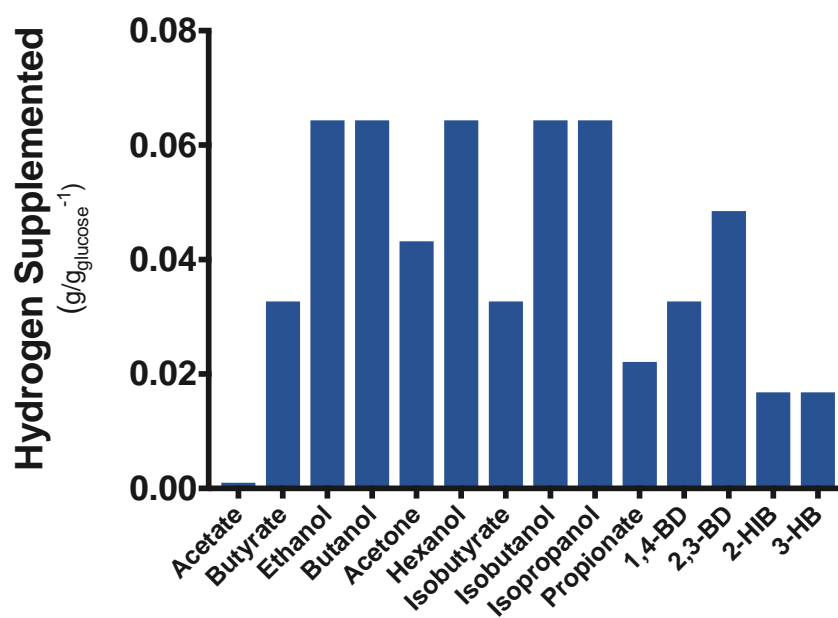
Figure 2.4. Hydrogen required for H$_2$ Supplemented mixotrophy. The amount of hydrogen corresponds to the additional electrons that are required to fix all CO$_2$ evolved from glucose and produce the maximum product yield from Figure 2.3.
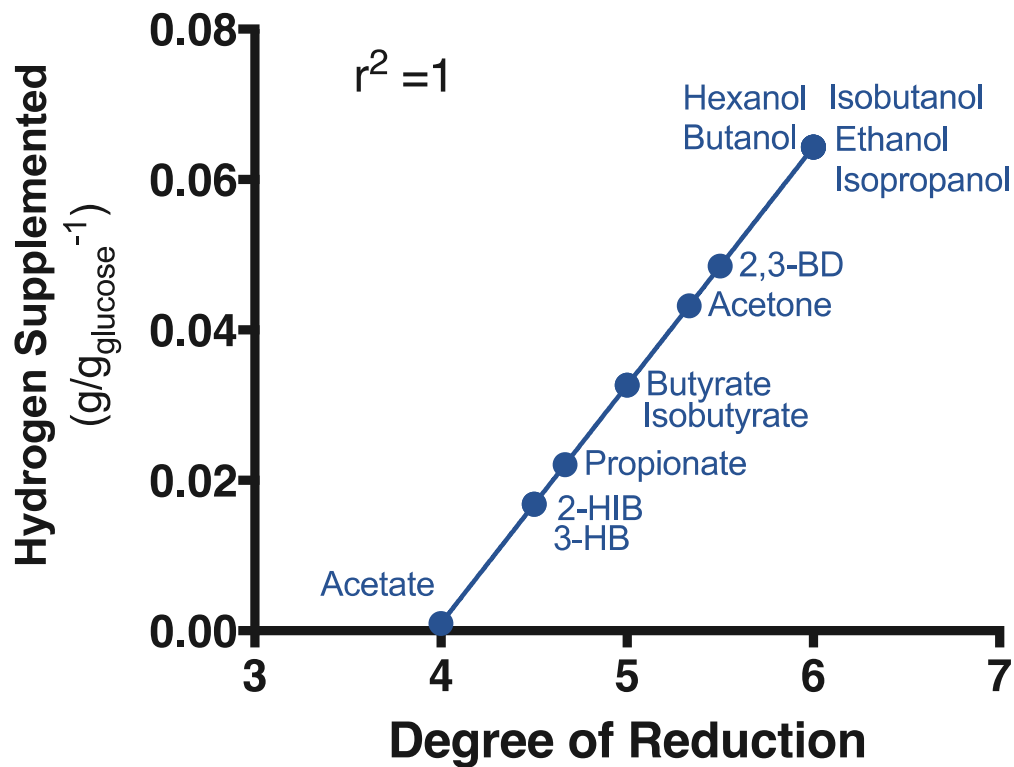
Figure 2.5. Hydrogen supplementation correlated to degree of reduction of various metabolites. There exists a strong correlation between the amount of hydrogen that needs to be supplemented to achieve complete carbon conversion to the degree of reduction of that metabolite.

2.4.1 How Effective is Mixotrophy? The Acetyl-CoA to Reducing Equivalent Ratio Can Give Quick Insight

Generally speaking, the products that are more reduced than the feedstock benefit most greatly from mixotrophy, in particular from hydrogen enhanced mixotrophy. How much benefit can be obtained? The amount of reducing equivalents required per mole of acetyl-CoA can give a good estimate on the potential increase in yield between heterotrophy and mixotrophy. Furthermore, the degree of reduction can indicate the total need of hydrogen required to convert all carbons during H_2

supplemented mixotrophy. The correlation between the NAD(P)H/acetyl-CoA ratio to improvements in product yields with mixotrophy compared to heterotrophy can be seen in Figure 2.6.
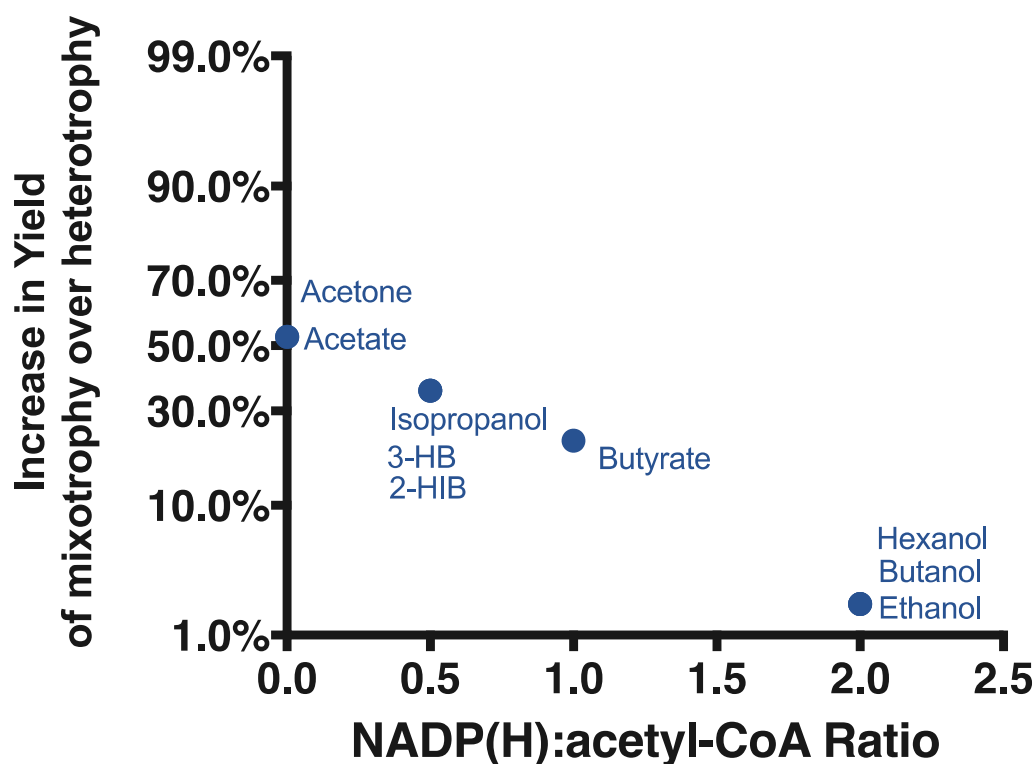
Figure 2.6. The NADP(H) to acetyl-CoA Ratio gives a good estimation on the potential yield increase between heterotrophic and mixotrophic conditions.

2.5   Autotrophic Growth of Acetogens

The maximum yield of any product is limited by the carbon balance, the demand of energy (ATP), as well as the requirements for reducing equivalents (NAD(P)H) for biomass growth and product formation. When grown autotrophically, the limit in ATP is always the bottleneck for achieving higher yields of fermentative

products such as ethanol or butanol. To overcome the energy limitations, acetogens have developed complex mechanisms for energy conservation as discussed in Section 2.5.1. Included in the WLP equations is a constant (n) that accounts for the conservation for ATP generated through membrane gradients (H^+ or Na^+) created by cytochromes or Rnf complexes, as well as through membrane-bound ATPases. The effect of 'n' parameter is discussed in Section 2.5.1.1.

2.5.1 Energetic Challenges in Acetogens during Autotrophic Growth

Autotrophy, defined here as the growth on inorganic gases through the WLP, is characterized by severe energy limitation. Yet the reduction of CO_2 through the WLP can still sustain life as acetogens produce biomass and metabolites through novel energy metabolisms. Acetogens use the universal energy carrier ATP for the synthesis of biomass, fixation of CO_2 and production of energy intensive metabolites and intermediates. The WLP requires one molecule of ATP to fix two molecules of CO_2 to convert into acetyl-CoA. Even with substrate level phosphorylation during the conversion of acetyl-CoA to acetate, which gains one ATP, the net ATP production remains zero. Without a net positive ATP gain, biomass cannot be formed. Clearly, acetogenic bacteria have derived a way to conserve energy to overcome these challenges. Besides substrate level phosphorylation, chemiosmotic gradient driven phosphorylation can provide energy for cells. The translocation of ions across the cell membrane allows membrane-bound ATPases to synthesize ATP. To create the ion gradient, and exergonic reaction (electron transfer reaction) must be coupled to the translocation of ions across the membrane. However, so far none of the enzymes found in the WLP pathway seem to be membrane bound to allow for the coupling of this pathway to the creation of an ion-gradient. Therefore it is hypothesized that the

ion-gradient is created by the accumulation of reduced ferredoxin (Schuchmann and Müller 2014). Acetogens were found to have a membrane bound ferredoxin-NAD^+ oxidoreductase, called the Rnf complex, which catalyzes the electron transfer from reduced ferredoxin to NAD^+, an exergonic reaction, for the translocation of ions across the cell membrane. But how is reduced ferredoxin generated within the cells? Reduced ferredoxin must be derived from the oxidation of hydrogen through hydrogenases. The reduction of ferredoxin with hydrogen is endergonic, so the reaction is coupled to the exergonic reduction of NAD^+, a process called flavin-based electron bifurcation. Some of the produced ferredoxin can be used in the reductive reactions of the WLP (such as the reduction of CO_2 by the carbon monoxide dehydrogenase, discussed more in Chapter 4), while the remaining reducing equivalents can be used by the Rnf complex for the generation of the ion gradient or by the Nfn complex for the interconversion of ferredoxin, NADH and NADPH. Acetogens use different energy metabolisms depending on their transmembrane ion gradient: some use cytochromes and are Na^+ independent (*M. thermoacetica*), others are cytochrome free and Na^+ dependent (such as *A. woodii*), and yet others, such as *Clostridium ljungdahlii*, use neither Na^+ nor cytochromes and rely on proton-dependent ion gradients. The amount of ATP that can be gained through these additional energy conservation mechanisms has been calculated based on various co-factor requirements of the WLP and can range anywhere from 0.13-.63 moles of ATP per molecule of acetyl-CoA (Schuchmann and Müller 2014). Based on biomass yields reported in literature, Fast et al. describe values for 'n' as 1.18 and 2.08 for growth on CO_2/H_2 or CO by *Butyribacterium methylotrophicum*. Even though these energy

conservation mechanisms are widespread throughout clostridia, they have not been found in yeast or *E. coli* (Liew, Martin et al. 2016).

2.5.1.1 Effect of the ATP Coefficient on Product Yields

The effect of the ATP coefficient, denoted as 'n', can be incorporated into the flux balance model by modifying the equation in the WLP as follows:

Equation 2 $\quad\quad 2CO_2 + 4H_2 + ATP \rightarrow$ acetyl-CoA+ $2H_2O$ + nATP

Equation 2 shows the production of acetyl-CoA from two molecules of CO_2 and 4 molecules of hydrogen. The amount of energy that can be derived through electron bifurcation and other energy conservation mechanisms described in Section 2.5.1 is denoted by 'n' which can range from 0.13-0.63, and possibly even higher (Fast and Papoutsakis 2012). The effect of 'n' on product yield can be calculated as shown in Figure 2.7 for the case of maximum ethanol, butanol and acetone production when grown autotrophically. This ATP limit is completely alleviated when grown mixotrophically (see Figure 2.3.)

The range of the ATP coefficient has a tremendous effect on product yield, as can be seen in Figure 2.7. Due to the autotrophic energy limitations, acetate remains one of the main products of acetogenic metabolism. To demonstrate this phenotype using theoretical yield calculations, the effect of the ATP coefficient on product yields that derive from acetyl-CoA intermediates is shown in Figure 2.7. When the objective function of the flux balance model is ethanol, butanol or acetone, the model calculates the co-production of acetate (which produces ATP through substrate level phosphorylation) to compensate the ATP limitation when grown autotrophically. The

higher the ATP coefficient is, the lower the amount of acetate production. In the case of the mixotrophic calculations, no acetate is produced since there are enough energy equivalents available for growth and the reduction of CO_2 through the WLP.
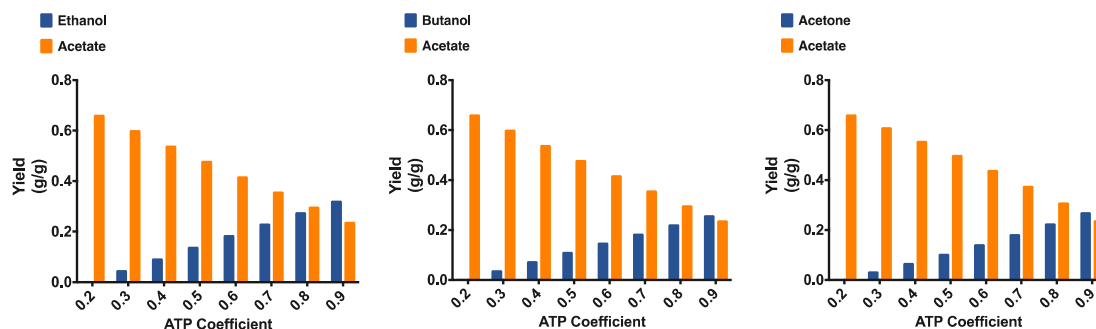
Figure 2.7. Effect of ATP conservation coefficient (n) on maximum yields of ethanol under autotrophic conditions. The total input is 200 moles of CO_2, 3 moles of glucose, and 400 moles of H_2. The biomass demand is defined as 5% of total carbon input (CO_2 and glucose).

Besides ATP limitations, the product yields of many metabolites are also limited by the reducing equivalents available to the cell. When grown autotrophically, cells derive reducing equivalents through the oxidation of hydrogen. Therefore, the more hydrogen is made available to the cell, the higher the amount of internal reducing equivalents. This effect can be seen in Figure 2.8, where the theoretical yield of ethanol reaches a maximum after 600 moles of hydrogen are consumed.
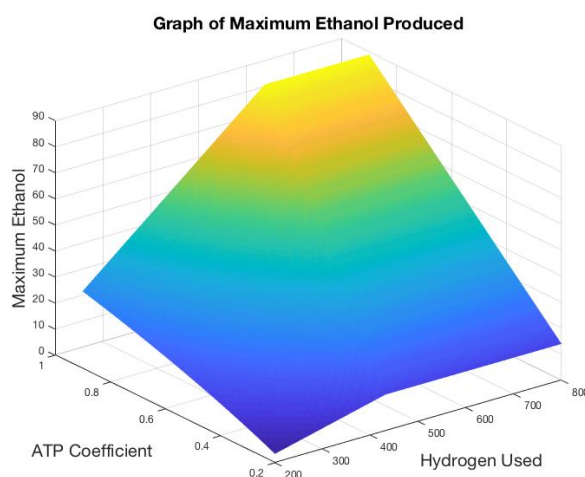
Figure 2.8. Effect of ATP conservation coefficient (n) and available hydrogen on the maximum theoretical ethanol yield (in moles). The carbon input is 200 moles of CO_2, and 3 moles of glucose. The biomass demand is defined as 5% of total carbon input.

2.5.1.2 The AOR Enzyme as Means to Overcome ATP Limitations

Most acetogens produce acetate when reducing CO_2 with H_2 to overcome ATP limitations, however, some acetogens such as *Clostridium autoethanogenum*, *Clostridium ljungdahlii*, and *Clostridium ragsdalei* are able to form large amounts of ethanol despite these ATP limitations. It was found that these acetogens contain an acetaldehyde:ferredoxin oxidoreductase (AOR) enzyme which catalyzes the reversible reduction of acetic acid to acetaldehyde (Mock, Zheng et al. 2015), thereby providing ATP through the acetate kinase reaction. When the AOR is included in the autotrophic yield calculations, the amount of acetate that is produced as a byproduct is reduced significantly, and no acetate is produced for ATP coefficients greater than 0.2, as shown in Figure 2.7 It is clear that the AOR enzyme provides a great evolutionary

30

advantage over acetogens that do not possess one in being able to generate ethanol under autotrophic conditions.
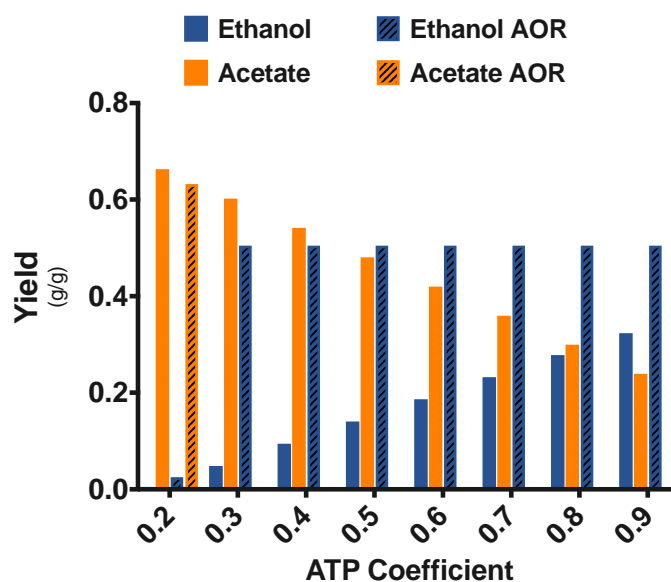
Figure 2.9. Effect of ATP conservation coefficient (n) with and without the AOR (blue with black lines and blue, respectively) on maximum yields of ethanol under autotrophic conditions. The total input is 200 moles of CO_2, 3 moles of glucose, and 400 moles of H_2. The biomass demand is defined as 5% of total carbon input (CO_2 and glucose).

2.5.1.3 Biosynthesis Challenges in Acetogens during Autotrophic Growth

Anabolism is the production of biomolecules used for biosynthesis from various amino acids and fatty acid intermediates. Anabolism often starts from the pyruvate intermediate. In addition to the energy limitations to produce these biomolecules, kinetic implications arise when the WLP is the sole source of carbons and energy. Since acetyl-CoA is the final product in the WLP, the acetyl-CoA needs to further be converted into pyruvate, a common precursor to amino acids such as

alanine, valine and leucine. This occurs through the use of the pyruvate:ferredoxin oxidoreductase (PFOR) that catalyzes the reversible reaction of acetyl-CoA to pyruvate utilizing a ferredoxin. It is therefore necessary to convert acetyl-CoA into pyruvate at reasonable rates for the production of biomass intermediates. It has been shown that the reverse reaction from acetyl-CoA to pyruvate is about 8-fold slower than the forward reaction, which primarily follows glycolysis (Furdui and Ragsdale 2000). Even though it is slower, this rate is estimated to be sufficient for the rate of biosynthesis of growing cells, since only a small amount of flux of metabolites has to go towards biomass synthesis. It is projected that only 4% of substrate consumed during growth on CO_2/H_2 as a sole energy source is recovered in cell biomass compared to 7% when grown on glucose, as has been reported for *M. thermoacetica* (Furdui and Ragsdale 2000). When grown in the presence glucose, pyruvate is an intermediate from glycolysis, rather than acetyl-CoA. Therefore the PFOR does not need to operate in the slower, reverse direction of pyruvate synthesis. The low rate of the reverse PFOR reaction could also attribute to the generally low biomass yields obtained when grown on gases alone.

The combined utilization of CO_2/H_2 and sugars C6 or C5 substrates (mixotrophic fermentation) should therefore alleviate the need to operate the PFOR in the more energetically challenging reaction from pyruvate to acetyl-CoA. This is especially important since some clostridia species, such as *Clostridium acetobutylicum*, have shown that the PFOR does not operate in reverse (Au, Choi et al. 2014). By combining gaseous and carbohydrate fermentation, the need to synthesize pyruvate from acetyl-CoA becomes obsolete, and no biosynthesis challenge arises.

2.5.1.4 Kinetics of Sugar and Gas Consumption

The successful implementation of mixotrophy relies on the uptake rates of both carbohydrates and gases to be at least on the same order of magnitude. So far, the growth rates of many acetogens vary and are often substrate dependent. Here we will focus on those acetogens which have been studied in more detail such as *Clostridium ljungdahlii* and *Moorella thermoacetica*. Nagarajan *et al*. reported an experimentally determined the fructose uptake rate of 1.9 mmol/gDW/h, which also agreed with the proposed metabolic model by the same authors (Nagarajan, Sahin et al. 2013). The CO_2 released during the fermentation can be calculated (3.8 mmol/gDW/h), and fits within the constraints of the model which limited CO_2 uptake rates at 10 mmol/gDW/h. However the paper failed to confirm this growth rate on CO_2 experimentally (Nagarajan, Sahin et al. 2013). Additionally, others reported a gaseous uptake rate for *Clostridium ljungdahlii* as 34.4 mmol CO/gDW/h when grown on a mixture of $CO/CO_2/H_2$ (Mohammadi, Mohamed et al. 2014). Both the computational rates and experimental rates seem to be higher than the rate of CO_2 produced during glycolysis, indicating the feasibility of a mixotrophic fermentation. Braun and Gottschalk showed the simultaneous consumption of both organic substrates (fructose, glucose and lactate) and of H_2/CO_2, by *A. woodii*, with the consumption of gases being almost 26 times higher than the consumption of glucose (Braun and Gottschalk 1981). It was even noted that the gaseous uptake rate varied depending on the co-substrate. The gas uptake rate was higher with glucose than with fructose or lactate. In addition, some clostridia are inhibited by certain amounts of glucose, as in the case of glucose and *Clostridium ljungdahlii*. Interestingly, some acetogens can grow on CO but can also be inhibited by this substrate due to CO binding to the hydrogenase active site. Mohammadi et al. discovered that *Clostridium ljungdahlii* preferentially consumed

CO$_2$/H$_2$ rather than CO, and that higher amounts of CO inhibit growth (Mohammadi, Mohamed et al. 2014). Similar results had previously been shown with cultures of *M. thermoacetica*, although doubling times of the organism in the presence of CO$_2$/H$_2$ or in the presence of CO were dependent upon media conditions (8.5 versus 10 in the undefined and 16 vs. 9 in the defined medium, respectively) (Daniel, Hsu et al. 1990). The authors also found that the hydrogenases and carbon monoxide dehydrogenase in *M. thermoacetica* are upregulated during growth on CO or CO$_2$/H$_2$. Even though more work needs to be done to clearly outline and characterize acetogenic growth and kinetic rates of metabolism, current work suggests that both gaseous uptake and carbohydrate uptake rates occur on the same order of magnitude, proving the potential for mixotrophy to be implemented in many of these acetogens.

2.6   Native and Synthetic CO$_2$ fixation Pathways

In addition to the Wood-Ljungdahl pathway, many more CO$_2$ fixation pathways occur in nature. All of them play a role in the global carbon cycle that supplies the carbon building blocks for all living organisms in terrestrial and marine environments (Müller 2003, Bar-Even, Noor et al. 2012). CO$_2$ is an essential and abundant component within the carbon cycle, and it is sequestered from the atmosphere through autotrophic growth of plants and bacteria by photo- and chemosynthesis, recycling roughly 203 billions tons of CO$_2$ annually (Aresta 2010). In addition to natural carbon emissions stemming from degradation of methane and other hydrocarbons such as plant matter as well as respiration from animals, anthropogenic additions to the carbon cycle from the energy, agricultural and industrial sector account for about 32 billion tons of CO$_2$ annually, as estimated by the International Energy Agency for 2014 (IEA 2016). By exploiting or utilizing existing pathways in the carbon cycle, we can

improve overall carbon fixation or utilize carbon fixation as means to produce valuable products. The majority of organisms use the Calvin-Benson-Bassham cycle for CO_2 fixation. Others use the Wood-Ljungdahl pathway, the reductive citric acid cycle, the 3-Hydroxypropionate/Malyl-CoA Cycle, the 3-Hydroxypropionate/4-Hydroxybutyrate Cycle or the dicarboxylate/4-Hydroxybutyrate Cycle (Aresta 2010, Fast and Papoutsakis 2012). Out of the many carbon fixation pathways, the WLP is the most energy efficient. Because of the wide-spread use of the WLP in both archaea and bacteria, genes and enzymes of this pathway are believed to be quite ancient, and may have been part of the very first biological pathway (Russell, Nitschke et al. 2013). In addition to naturally occuring carbon fixation routes, researchers have established a non-native pathway that avoids the loss of CO_2.

2.6.1 Non-oxidative Glycolysis (NOG) as a Synthetic Route to Preventing CO_2 Losses

Bogorad et al. proposed a synthetic route to avoid the loss of CO_2. In this pathway, glucose is broken down into fructose-6-phosphate (F6P) through phosphorylation and subsequent isomerization at the loss of ATP, similarly to the first two steps of glycolysis. Next, the pathway deviates from glycolysis by irreversibly breaking down 3 molecules of F6P into three acetyl phosphate (AcP) and three erythrose 4-phosphate (E4P) molecules. The three molecules of AcP can be converted into acetyl-CoA, and subsequently into desired molecules. The three E4P molecules enter a carbon rearrangement network to re-form two molecules of F6P, which can then re-enter the pathway in a cyclic manner, avoiding the loss of any carbons throughout the pathway. The authors showed the feasibility of the above scheme *in vitro* utilizing fructose 6-phosphate, ribose 5-phosphate, and glyceraldehyde 3-

phosphate as substrates. *In vivo* the authors were unable to show the utilization of fructose, but were able to show the conversion of xylose into two molecules of AcP and two molecules of glyceraldehyde 3-phosphate (G3P), which was isomerized to form F6P, entering the cyclic manner of NOG. The yield on xylose was 2.2 moles of acetate, which is near the theoretical maximum of 2.5 moles and above the theoretical maximum of 1.67 moles through EMP glycolysis. The only way to generate energy through this pathway is the production of acetate through substrate level phosphorylation, severely limiting the application of the NOG pathway for production of a wide variety of chemicals.

Chapter 3

**ACETOGENIC MIXOTROPHY INCREASES PRODUCT YIELDS AND
INFLUENCES PRODUCT PROFILE DISTRIBUTION**

3.1   Preface

This chapter (including all text, figures, and tables) was adapted from Jones,
Fast, and Carlson (2016) with permission, and describes the effect of mixotrophy
through CO_2 fixation by anaerobic non-photosynthetic acetogens for improved carbon
conversion. Some additional experiments not found in the publication involving
Clostridium carboxidivorans are included to further expand the understanding of
mixotrophy in native acetogens.

3.2   Abstract

Traditional fermentations are often limited by their ability to consume 100% of
the feedstock due to the decarboxylation reactions occurring during glycolysis.
Considering feedstock cost is one of the most important factors in determining
economic feasibility, increasing feedstock conversion has huge impacts on producing
biotechnology platforms that can compete in today's chemical and energy markets. To
achieve superior feedstock conversion rates, CO_2 evolved during traditional
fermentations has to be sequestered back into the fermentation process, thereby
eliminating the mass loss that is usually upwards of 33%. An attractive route to
complete feedstock conversion is the utilization of acetogenic bacteria, which are
capable of fixing two molecules of CO_2 along with a source of electrons by utilizing
the Wood-Ljungdahl pathway. By combining the fermentation of carbohydrates along
with gaseous feedstocks, termed mixotrophic fermentation, superior mass yields can
be achieved. Here we demonstrate the practical application of mixotrophy for five

acetogenic species, *Clostridium ljungdahlii, Clostridium autoethanogenum, Eubacterium limosum, Moorella thermoacetica* and *Clostridium carboxidivorans.* Total mass yields are improved in mixotrophic fermentations compared to traditional fermentations of *Clostridium acetobutylicum*, and carbon tracers are utilized to demonstrate the coinciding uptake of gases and carbohydrates. In depth analysis of the mRNA levels in *Clostridium ljungdahlii* indicates successful transcription of all genes involved in the Wood-Ljungdahl pathway, regardless of the presence or absence of carbohydrates. In addition, the supplementation of electron rich gases into the headspace of mixotrophic fermentations, termed syngas enhanced mixotrophy, has a dramatic effect on product profile distributions. The fermentation behavior of *Clostridium carboxidivorans* is described and yields are compared to previously published literature values. Taken together, these data confirm the theoretical calculations of mixotrophy and demonstrate the successful application of acetogenic mixotrophy.

3.3   Introduction

Acetogens are obligate anaerobic bacteria that employ the Wood-Ljungdahl pathway for the sequestration of CO_2 along with a source of electrons, either from H_2, CO or other energy-rich carbohydrates (Ragsdale and Pierce 2008). The Wood-Ljungdahl pathway converts two molecules of CO_2 and 8 reducing equivalents into acetyl-CoA, a biological pre-cursor and building block. Acetyl-CoA can then further be converted into a variety of fermentative products. A hallmark of acetogens is the production of acetate. The first acetogen was discovered to grow on CO_2/H_2 and produce acetate. This acetogen, *Clostridium aceticum*, was initially discovered in 1936 and shortly thereafter lost, until 40 years later it was re-discovered (Drake, Gössner et

al. 2008). Since then, the most well studied acetogen has become *M. thermoacetica* (formerly *Clostridium thermoaceticum*), but many others have been isolated and sequenced (Liew, Martin et al. 2016). There has been evidence of co-utilization of gases and sugars for cultures of *M. thermoacetica* that were able to produce 2.5 moles of acetate from 1 mole of glucose, indicating the consumption of evolved CO_2 released through glycolysis of the glucose substrate (Fontaine 1942). Since then, this phenomenon has not been further studied or utilized for the application in industrial fermentations to increasing carbon yields. With the recent revival of creating biological platforms for the production of fuels and chemicals, acetogens offer a promising route for the production of chemical from cheap, abundant and alternative C1 feedstocks (industrial waste gases and syngas) (Heijstra, Leang et al. 2017). However, product and biomass yields can be low when grown on gases alone. The concept of mixotrophic fermentation overcomes these limitations and offers a new route to high feedstock conversion and increased yields.

Besides *Moorella thermoacetica*, *Acetobacterium woodii*, *Clostridium ljungdahlii*, *Clostridium autoethanogenum* and *Eubacterium limosum* have been the focus on more recent studies of acetogens. Many strains differ in their ability to synthesize a variety of products (Fast, Schmidt et al. 2015, Liew, Martin et al. 2016), but acetate still remains the major end product during autotrophy (due to the energy limitations as discussed in Chapter 2). However, novel energy conservation mechanism as well as the expression of the acetaldehyde:oxidoreductase enzyme have allowed some acetogens to expand their product profile. Besides acetate, *Clostridium ljungdahlii* and *Clostridium autoethanogenum* can produce ethanol, 2,3 butanediol, and lactate. *Eubacterium limosum* is able to produce butyrate in addition to acetate

(Jeong, Bertsch et al. 2015). Even though these product profiles are promising for implementation of gas fermentation platforms, highly reduced, higher number of carbon (C>3) and/or branched products would be highly desirable. We developed the concept of mixotrophy, defined as the combination of a carbohydrate feedstock with that of a gaseous one to achieve higher product yields and more reduced product profiles (Fast and Papoutsakis 2012, Fast, Schmidt et al. 2015, Jones, Fast et al. 2016).

Because the product profile is known to be affected by the external feedstocks provided, we set out to investigate mixotrophic fermentations for *Clostridium ljungdahlii*, *Clostridium autoethanogenum*, *Moorella thermoacetica*, and *Eubacterium limosum.* We tested their ability confirm our theoretical yield calculations for mixotrophy, and demonstrated the potential of enhanced mixotrophic conditions to improve their product yields beyond what is possible with complete carbohydrate utilization alone. We showed that these acetogenic species were capable of sequestering gaseous carbon while at the same time consuming carbohydrates, suggesting this to be a general trait of acetogens. The enhanced mixotrophic experiment demonstrated the potential for external gases to influence the product profile towards more highly reduced products such as ethanol and butyrate. Furthermore, we studied in detail the concomitant consumption of carbohydrates and ^{13}C-carbon gases through metabolite labeling studies.

3.4   Proof-of-Concept of Mixotrophy: Increasing Product Yields with four Acetogenic Species

To investigate the effect of mixotrophy on the product yields of native acetogens, we tested four strains (*Clostridium ljungdahlii*, *Clostridium autoethanogenum*, *Moorella thermoacetica* and *Eubacterium limosum*) for their ability

to grow under mixotrophic conditions (closed headspace and 5 or 10 g/L fructose) to improve their product yields. The product yield is defined as the total number of carbon moles in the products produced divided by the total number of carbon moles in the substrate consumed given as a percentage (C-moles produced/C-moles consumed). We demonstrated that our control, the non-gas consuming *Clostridium acetobutylicum* (CAC), an anaerobic bacterium closely related to many acetogens, was not able to achieve a product yield above the theoretical maximum of 67% (Figure 3.1). The product yield for this culture was 65%, close to the theoretical maximum due to the large amount of lactate that was formed in the closed headspace. All four acetogenic strains were able to achieve greater than 67% product yields under mixotrophic conditions. *Clostridium ljungdahlii*, *Clostridium autoethanogenum*, *Eubacterium limosum* and *Moorella thermoacetica* produced a product yield of 83%, 72%, 78% and 83%, respectively (Figure 3.1). Interestingly, the lower yields by *Clostridium autoethanogenum* and *Eubacterium limosum* can be attributed to the higher amounts of reduced products that were formed (*Clostridium autoethanogenum* produced more ethanol than *Clostridium ljungdahlii*, and *Eubacterium limosum* produced butyrate). The production of reduced products results in less CO_2 being fixed (See Chapter 2). To further demonstrate the ability of mixotrophy to increase product yields, we conducted experiments with enhanced mixotrophy, which increases the total carbon and reducing equivalents in the system through the addition of exogenous gases. In these experiments, cultures were grown in a closed headspace along with fructose, and electron rich gases such as H_2/CO_2 or CO. *Clostridium ljungdahlii*, *Clostridium autoethanogenum* and *Eubacterium limosum* were all grown under a syngas mixture containing 55% CO, 10% CO_2, 20% H_2 balanced with N_2 at 20-30 psig. Due to the

inability of *Moorella thermoacetica* to grow in the presence of 55% CO, *Moorella thermoacetica* was grown on a mixture of CO_2 and H_2 (20:80). All four strains exhibited significant improvements in their total carbon yield due to the simultaneous utilization of carbohydrates and gases. Both *Clostridium ljungdahlii* and *Clostridium autoethanogenum* made carbon yield improvements of 195% and 165%, respectively. *Eubacterium limosum* achieved a product yield of 110%, whereas *Moorella thermoacetica* only saw a modest improvement of 88%. Still, all four strains were able to achieve superior carbon yields due to the additional carbon and electron source during syngas enhanced mixotrophy, suggesting native mixotrophy is a general trait among acetogens.
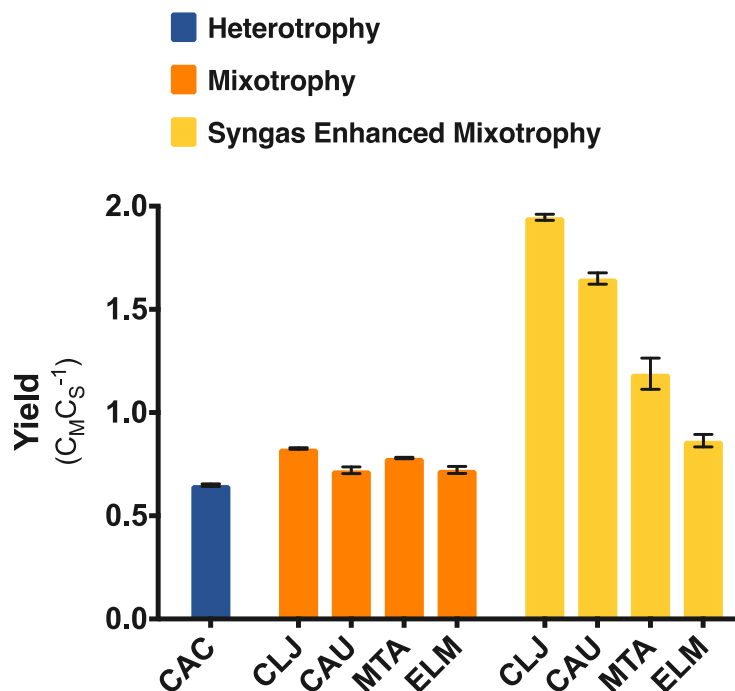
Figure 3.1. Product Yields for Mixotrophy and Syngas Enhanced Mixotrophy of four acetogenic strains**.** The product yield is defined as the yield molar yield of products divided by the molar consumption of substrate. *C. acetobutylicum* (CAC) was used as a heterotophic control. Legend: *C. ljungdahlii* (CLJ), *C. autoethanogenum* (CAU), *M. thermoacetica* (MTA), and *Eubacterium limosum* (ELM). Adapted from (Jones, Fast et al. 2016)

3.5   Product Profile Strongly Affected by External Electron Sources

Besides the highly desirable increase in product yield under mixotrophic conditions, a shift towards more reduced products in the presence of externally added gases is an additional benefit of mixotrophy. When grown on carbohydrate feedstocks in a closed headspace (mixotrophic), the four acetogens tested (*Clostridium ljungdahlii, Clostridium autoethanogenum, Moorella thermoacetica* and *Eubacterium limosum*) demonstrated a varied product profile strongly dependent upon the individual species. For example, *Clostridium ljungdahlii* and *Clostridium*

autoethanogenum, which are quite similar on a genomic and phylogenetic level, show the production of ethanol, a reduced product derived through the conversion of acetate by the AOR enzyme or the reduction of acetyl-CoA using the alcohol dehydrogenase. The production of ethanol under heterotrophic conditions has been reported before (Kopke, Held et al. 2010, Mock, Zheng et al. 2015). Previously, *Clostridium autoethanogenum* had been shown to produce significantly less alcohol when grown on fructose (Mock, Zheng et al. 2015) and also when grown on xylose (Cotter, Chinn et al. 2009). When previous studies attempted to evaluate ethanol production between *Clostridium ljungdahlii* and *Clostridium autoethanogenum*, continuous bioreactor studies showed *Clostridium ljungdahlii* to produce higher amounts of ethanol than *Clostridium autoethanogenum*. In this study, the *Clostridium autoethanogenum* strain was able to produce more ethanol than *Clostridium ljungdahlii* under both mixotrophic and enhanced mixotrophic conditions (1.6 g/L and 3.1 g/L, respectively). In comparison, *Clostridium ljungdahlii* only produced modest amounts of ethanol under both mixotrophic and enhanced mixotrophic conditions (0.3 g/L and 0.4 g/L, respectively). This shows the phenotypic differences between the two strains and also shows the strong effect of varying culture conditions on the outcomes of the yields. One hypothesis to explain the difference in ethanol production under heterotrophic growth is due to difference in cofactor utilization by the AdhE enzyme (Liew, Henstra et al. 2017). Another difference is the number of copies of the AOR enzyme (Martin, Richter et al. 2016).

In comparison, a very different acetogen, *Moorella thermoacetica* had been shown previously to mainly produce acetate when grown autotrophically (Daniel, Hsu et al. 1990), but has been reported to produce ethanol under heterotrophic conditions

(Liew, Martin et al. 2016). For the first time, this study reported the production of lactate by *Moorella thermoacetica* grown mixotrophically. Lactate often indicates an electron imbalance within the cells. Lactate has been shown in engineered *Clostridium autoethanogenum* to provide an electron sink when the cells experience a redox imbalance, such in the double knockout of *Clostridium autoethanogenum* described by Liew et al. (Liew, Henstra et al. 2017). In addition, *Moorella thermoacetica* was the only acetogen in this study that was unable to tolerate 55% CO in the headspace. Therefore, all enhanced mixotrophic experiments were conducted with CO_2/H_2 (20psi). Interestingly, *Moorella thermoacetica* is quite different from *Clostridium ljungdahlii* or *Clostridium autoethanogenum* since it lacks the Rnf complex found in other acetogens to allow energy generation, but instead relies on an energy-converting hydrogenase (Schuchmann and Müller 2014). This hydrogenase could result in the strong inhibition by CO. So far, only *Acetobacterium. woodii* has been shown to contain a carbon monoxide tolerant iron hydrogenase (Ceccaldi, Schuchmann et al. 2017), so it might be possible that the discovery of other CO-tolerant hydrogenases may follow. In comparison to the other three strains, *Eubacterium limosum* was able to synthesize modest amounts of butyrate under the mixotrophic condition (0.5 g/L). When grown under enhanced mixotrophic conditions, *Eubacterium limosum* produced 1.3 g/L of butyrate. Generally speaking, all four acetogenic strains implied an increase in the production of reduced products under the enhanced mixotrophic conditions. *Clostridium ljungdahlii* and *Clostridium autoethanogenum* produced more ethanol and 2,3 butanediol, and *Moorella thermoacetica* produced significantly more lactate but also more ethanol. *Eubacterium limosum* increased the butyrate production by 250% (0.5 g/L versus 1.3 g/L under mixotrophic and enhanced mixotrophic conditions,

respectively). Figure 3.2 illustrates the change in product profile distribution when strains were grown mixotrophically (panel A) and with exogenous gas supplementation (panel B). Clearly, the addition of gases to the fermentation can shift product profiles towards the more desirable, reduced products. These results demonstrate the power of enhanced mixotrophy in shaping final product profiles.
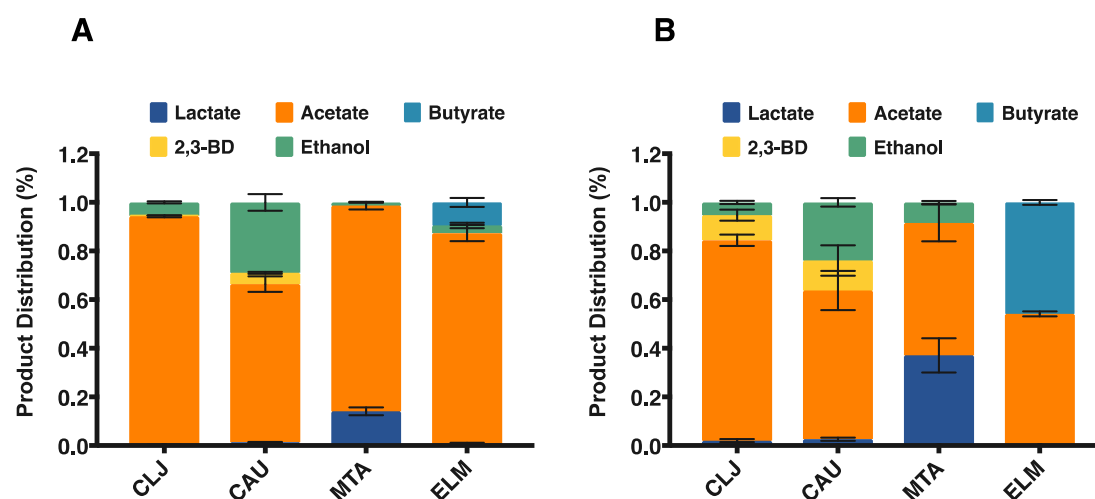
Figure 3.2. Product Profiles under mixotrophic (A) and syngas-enhanced mixotrophic conditions (B) for *C. ljungdahlii* (CLJ), *C. autoethanogenum* (CAU), *M. thermoacetica* (MTA) and *Eubacterium limosum* (ELM).

3.6 ^{13}C-tracing studies show simultaneous utilization of gases and sugars

To demonstrate the concurrent co-utilization of both sugars and gases, we used ^{13}C-tracing to identify if both pathways, glycolysis and the Wood-Ljungdahl pathway, produced metabolites and biomass components at the same time, or sequentially. A common phenomenon, termed catabolite repression, is the preferential uptake of one carbon source over another. The first evidence for co-utilization of glycolysis and the Wood-Ljungdahl pathway was first observed in a *M. thermoacetica* culture that was

capable of producing 2.5 moles of acetate per mole of glucose, which provided the first indication of the potential of acetogens to achieve higher product yields when grown mixotrophically (Fontaine, Peterson et al. 1942). In a later study by Brown and Gottschalk, *Clostridium aceticum* readily consumed H_2/CO_2 in the absence of fructose, but consumed only small amounts of H_2/CO_2 in the presence of fructose (Braun and Gottschalk 1981). In addition, activity measurements of hydrogenases exhibited a reduced activity in the presence of fructose. However, in the same study, *Acetobacterium woodii* was shown to grow on CO_2 and H_2 in the presence of fructose, glucose, and lactate. In all three cases, *A. woodii* readily consumed both the gaseous and organic substrates, resulting in the production of higher yields of acetate than could be produced using the organic substrates alone. Furthermore, the hydrogenase activity of *Acetobacterium woodii* was found to not be differentially regulated in the presence of fructose, in contrast to the hydrogenase of *Clostridium aceticum*. Taken together, these results indicate that the co-utilization might be species dependent.

To demonstrate the co-utilization of sugars and gases in other acetogens using ^{13}C tracers, we chose to study *Clostridium ljungdahlii* and *Clostridium autoethanogenum* as they are the most recently studied acetogens (both in industry and academia), genetically tractable, and about 99% similar on a genetic basis, but still contain a few phenotypic differences (Liew, Martin et al. 2016). A specialized syngas mixture ($^{13}CO/^{13}CO_2/H_2/N_2$, 55:10:20:15) was used to pressurize the headspace in the presence of 10 g/L ^{12}C-fructose. The two acetogenic species, *Clostridium ljungdahlii* and *Clostridium autoethanogenum*, demonstrated very characteristic fermentation profiles during the enhanced mixotrophic experiment (Figure 3.3). Both fermentations consumed fructose while at the same time producing ethanol and acetate. Small

amounts of lactate (data not shown) and 2,3 butanediol were formed as well. Even though the *Clostridium ljungdahlii* culture did not consume all fructose, it did eventually consume more than 50% of the initial fructose (data not shown). During the fermentation, metabolites (acetate and lactate) were analyzed for their ^{13}C carbon content. Both strains consumed gases and sugars simultaneously, as indicated by the consistent labeling throughout the fermentation. Labeling in acetate did not vary with time, and the percent labeling in acetate varied between 73% and 80% for *Clostridium ljungdahlii*, and 51 and 58% for *Clostridium autoethanogenum*. Even at the earlier time points, both strains exhibited a surprisingly large percentage labeling in acetate (73% and 53%, for *Clostridium ljungdahlii* and *Clostridium autoethanogenum* respectively). The unlabeled acetate is derived from the fructose supplemented in the media or from metabolizing the minimal amounts of yeast extract (1 g/L). Because *Clostridium autoethanogenum* consumed more fructose, the labeling in acetate is lower than in the case for *Clostridium ljungdahlii*. Still, the high percentage indicates a large uptake of gases simultaneously to the fructose uptake. We therefore conclude that there is no preference given to the higher energy density of the hexose sugar substrate, and that the presence of this hexose sugar does not repress the functionality of the Wood-Ljungdahl pathway enzymes.
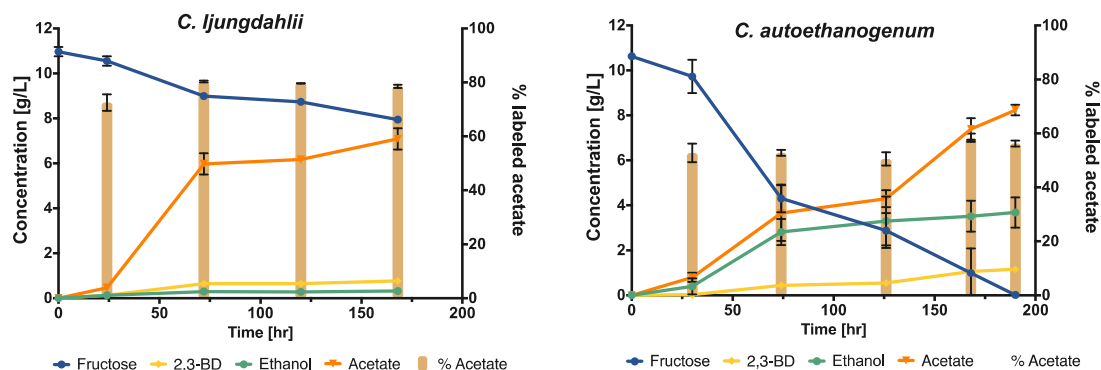
Figure 3.3. ¹³C-labelling fermentation profiles for *Clostridium ljungdahlii* and *Clostridium autoethanogenum* during syngas-enhanced mixotrophy. Fructose (blue line) consumed and metabolites produced during fermentation in the presence of a syngas mixture (^{13}CO, $^{13}CO_2$, H_2 and N_2). The percentage of acetate labelled with ^{13}C is shown in light brown for each time point. The s.d. of two biological replicates is shown in black error bars.

3.6.1 Relative Labeling in Acetyl-CoA derived Products and Pyruvate Derived Products

Because the gaseous headspace contains the labeling alone, any acetate or lactate containing a labeled carbon therefore must be derived from the gases through the Wood-Ljungdahl pathway, so this serves as a good indication of the flux of carbon going through the Wood-Ljungdahl pathway (^{13}C gases) versus through alternative pathways such as glycolysis (^{12}C fructose) or through the uptake of amino acids from yeast extract. Of particular interest is lactate, since unlike acetate, lactate is a pyruvate derived product rather than an acetyl-CoA derived product. Labeled lactate at the 1 or 2 carbon position is as a result of the conversion of labeled acetyl-CoA (derived through the Wood-Ljungdahl pathway) to pyruvate, and labeling at the third carbon is due to a carbon exchange between labeled CO_2 and the acetyl-CoA molecule bound to the pyruvate-ferredoxin enzyme (Amador-Noguez, Feng et al. 2010) (Figure S3.1,

Case V, VI and VII). From Figure 3.4 we can see that the labeling in lactate is very similar between both *Clostridium ljungdahlii* and *Clostridium autoethanogenum* (21 vs 25%, respectively). This indicates the rate of the rPFOR reaction is similar for both organisms. Also, generally speaking the labeling in lactate is much lower than that of acetate, indicating that pyruvate is preferentially derived through glycolysis rather than the Wood-Ljungdahl pathway, as would be expected since the PFOR reaction is believed to be 8 times faster in the direction of acetyl-CoA synthesis rather than pyruvate synthesis (Furdui and Ragsdale 2000) (also see Chapter 2). The acetate is labeled much higher in *Clostridium ljungdahlii* than in *Clostridium autoethanogenum*, as discussed previously.
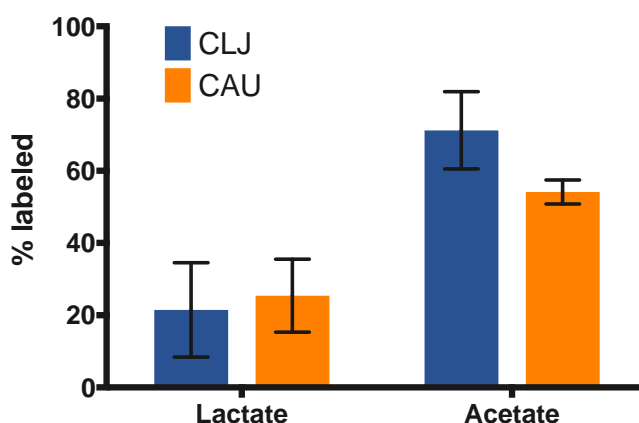
Figure 3.4. ^{13}C-labeling in lactate (left) and acetate (right) for culture of *Clostridium ljungdahlii* (CLJ, blue) and *Clostridium autoethanogenum* (CAU, orange).

Assuming the labeling for acetate is representative of the labeling in ethanol, the final metabolite concentrations derived from the Wood-Ljungdahl pathway alone

are 77mM acetate and 45 mM ethanol in *Clostridium autoethanogenum* (Table S3.1). These values are 2.3 times higher than previous values published, indicating increased carbon flux through the Wood-Ljungdahl pathway in the presence of sugars due to the increase in biomass (OD values were 2.3-3 times higher) (Köpke, Mihalcea et al. 2011). Final labeling in the metabolites of *Clostridium ljungdahlii* were 78% and 21% for acetate and lactate, respectively. Assuming again the labeling for acetate is representative of ethanol, the final metabolite concentrations derived from the Wood-Ljungdahl pathway alone are 113mM acetate and 6mM ethanol in *Clostridium ljungdahlii*. Interestingly, the low amounts of ethanol produced in our experiments in *Clostridium ljungdahlii* have been reported in previous experiments involving *Clostridium autoethanogenum* growing on fructose (Mock, Zheng et al. 2015). It is clear that fermentation and experimental conditions have a big impact on product yields, as can be seen by varying reports on yields in literature.

3.7 mRNA Transcripts and Protein Expression under Mixotrophic Conditions

To further demonstrate the co-current utilization of both the Wood-Ljungdahl pathway and the glycolysis, we set out to quantify RNA levels using q-RT-PCR and analyze the presence of proteins in the Wood-Ljungdahl pathway using western blots under autotrophic and mixotrophic conditions. Previously, various studies have examined the transcription levels of *Clostridium ljungdahlii* in the presence of carbohydrates. One study demonstrated an up-regulation of carbon fixation genes (both from the methyl and carbonyl branches of the Wood-Ljungdahl pathway) under autotrophic conditions (CO/CO_2) compared to heterotrophic conditions (5 g/L fructose) (Tan, Liu et al. 2013). In a different study, there was no differential expression of Wood-Ljungdahl pathway genes between autotrophic or heterotrophic

conditions (Nagarajan, Sahin et al. 2013). The authors postulated that the contrasting

finding was due to a different gas composition for their autotrophic study (CO/CO_2 for

the study showing differential regulation and H_2/CO_2 for the study that showed similar

expression levels for both autotrophic and chemotrophic growth). Nagarajan et al. did

note the downregulation of a few genes involved in fructose metabolism. Another

study that established the importance of the ATP-conserving Rnf complex in the

autotrophic growth of *Clostridium ljungdahlii*, showed through qPCR that

transcription from the Rnf operon was significantly higher in cells grown on H_2/CO_2

as compared to transcription in cells grown on fructose (Tremblay, Zhang et al. 2013).

This indicates the importance of the Rnf complex when grown autotrophically, as

discussed in Chapter 2. Given the conflicting transcriptional analyses, we set out to

measure transcription profiles of major genes involved in the Wood-Ljungdahl

pathway as well as a few genes from glycolysis under autotrophic, mixotrophic as well

as syngas enhanced mixotrophic conditions to determine a general up or

downregulation trend. Our analysis showed no significant up or down regulation in all

three cases. Figure 3.5 represents the 2-fold expression (compared to the autotrophic

case) of 4 major genes involved in the Wood-Ljungdahl pathway. As can be seen from

the figure, none of the values were significantly higher than 1, indicating the

expression of these genes is independent of the presence of sugars or gases.
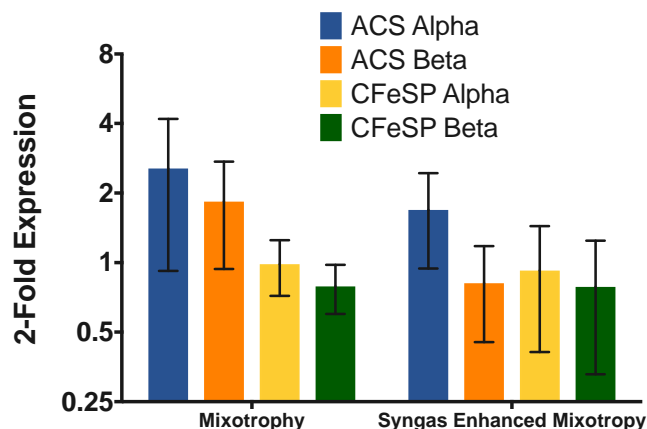
Figure 3.5. q-RT-PCR for *Clostridium ljungdahlii* under mixotrophy and syngas enhanced mixotrophy. No significant up or downregulation was observed between the mixotrophy and syngas enhanced mixotrophy compared to the autotrophy control.

Furthermore, the presence of the CODH gene was tested using a polyclonal antibody raised in rabbits against the CODH subunit. Under all three conditions, the intensity of the bands between autotrophic, mixotrophic or syngas enhanced mixotrophic conditions did not significantly change. Together with the q-RT-PCR experiments, it seems that the transcription and translation of the genes in the Wood-Ljungdahl pathway are unaffected by the presence of sugars.
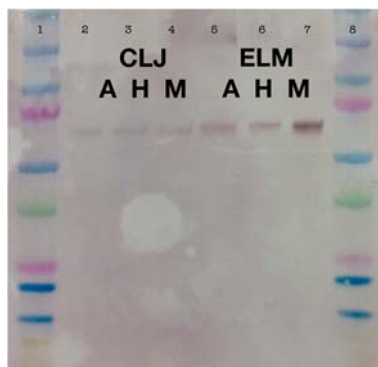
Figure 3.6. Western blot using polyclonal antibody raised against CODH subunit of the ACS/CODH enzyme of *Clostridium ljungdahlii* or *Eubacterium limosum*. Legend: Ladder (1 and 8), *Clostridium ljungdahlii* auto (2), mixo (3), and syngas enhanced mixotrophy (4). *Eubacterium limosum* auto (5), mixo (6), and syngas enhanced mixotrophy (7). There is no difference between the intensity of the bands under the three conditions tested for either of the two strains.

3.8 Characterizing *Clostridium carboxidivorans* Fermentations to Identify its Diverse Product Profile

One acetogen discovered recently has shown promise with a much-expanded product profile compared to the other, previously studied acetogens. The acetogen *Clostridium carboxidivorans* P7^T was isolated in 2005 and exhibits one of the most diverse product profiles, as it can produce 2, 3, 4, and 6 carbon compounds. The fermentation behavior closely resembles the traditional ABE fermentation pathway of *Clostridium acetobutylicum* but lacks the acetone production pathway. Nine years after the initial discovery, researchers first reported the production of hexanol and hexanoic acid in *Clostridium carboxidivorans* (Ramachandriya, Kundiyana et al. 2013). This is the one of two acetogenic strains that is known to produce higher carbon alcohols, like butanol and hexanol. Unlike ethanol, butanol is an excellent drop in fuel substitute, as it does not need a changing infrastructure and can be used in conventional engines. Hexanol can also be used as a drop-in fuel substitute, and is

even more desirable due to its higher energy density than other alcohols (Fernández-Naveira, Veiga et al. 2017). The only other known species to produce hexanol are *Clostridium scatologenes*, *Clostridium butyricum* and *Clostridium kluyveri* (Tracy, Jones et al. 2012). Another interesting feature of this organism is its ability to grow on a wide range of synthesis gas including its ability to grow on 100% CO, which is not possible for all acetogens (Moersdorf, Frunzke et al. 1992). It also has been demonstrated to grow without the addition of yeast extract (defined media), which has been more difficult for other acetogens (Phillips, Atiyeh et al. 2015).
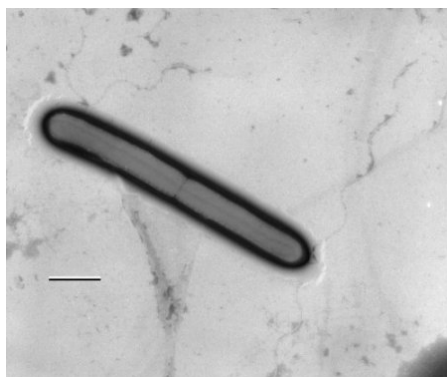
Figure 3.7. Clostridium carboxidivorans isolated from an agricultural settling lagoon in Oklahoma, USA in 2005. Image from (Liou, Balkwill et al. 2005).

3.8.1 Mixotrophic Behavior of *Clostridium carboxidivorans* in the Presence of 100% ^{13}CO

We hypothesize that the formation of the various products in *Clostridium carboxidivorans* are a complex interplay between electron and redox shuffling. This physiological behavior to external electrons is beneficial for employing anaerobic, non-photosynthetic (ANP) mixotrophy (Fast, Schmidt et al. 2015, Jones, Fast et al. 2016). Highly reduced products usually require more reducing power, and when

grown on gases alone, the limit in electrons is usually the bottleneck to achieving high product yields, in particular those with higher degrees of reduction such as alcohols. In order to establish a syngas enhanced mixotrophic fermentation profile behavior for *Clostridium carboxidivorans*, we grew *Clostridium carboxidivorans* in the presence of both syngas (100% CO) and hexose (6 g/L glucose). We labeled the carbon, allowing us to monitor the gas uptake rate as well as the CODH activity by observing ^{13}CO to $^{13}CO_2$ conversion. Actively growing cells were inoculated into fresh media, and within 24 hours the cells reached a maximum cell density of ~1.0 (optical density measured at 600nm). The maximum growth rate was an average of 0.091 hr^{-1}, which is consistent with literature values (Fernández-Naveira, Veiga et al. 2017) (when grown on CO alone). The pressure stayed fairly consistent until the later stages of fermentation when the pressure slowly dropped (about 8 psi) (Figure 3.8).
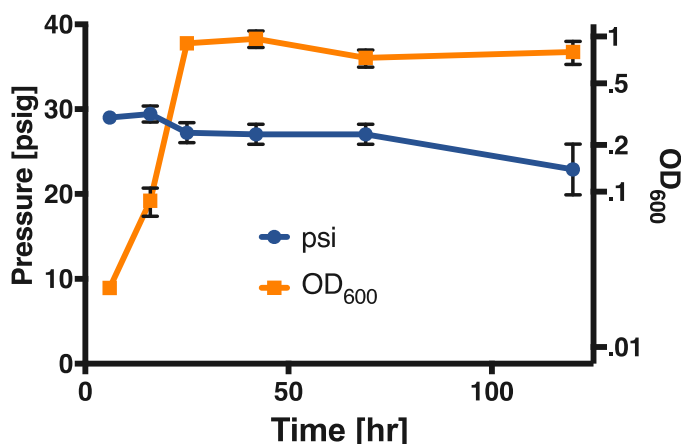
Figure 3.8. Growth profile and pressure increase for fermentation of *Clostridium carboxidivorans* with 6g/L glucose and 100% ^{13}CO headspace (30 psi).
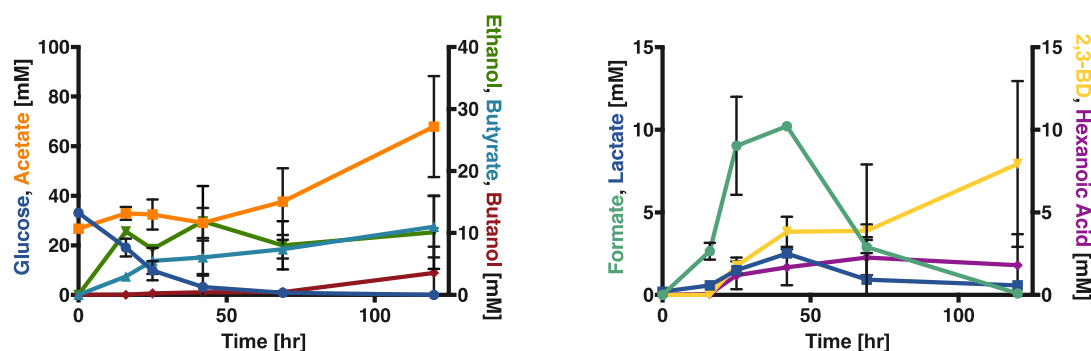
Figure 3.9. Metabolite profile for fermentation of *Clostridium carboxidivorans* on 10 g/L glucose and 100% CO headspace (30 psi). Left: glucose (blue), acetate (orange), ethanol (green) and butyrate (turquoise) and butanol (red), Right: lactate (blue), hexanoic acid (purple), 2,3-Butanediol (yellow) and formate (seafoam green).

Clostridium carboxidivorans was able to ferment all of the glucose present in the medium within 48 hours of fermentation (Figure 3.9). The rate of glucose consumption was 3 mmoles/hr/gDW during the first 24 hours (using a value of 0.45 gDW/L for 1.0 OD_{600} as measured for *M. thermoacetica* (Seifritz, Fröstl et al. 2002). Acetate, butyrate, ethanol, lactate, 2,3-butanediol (2,3BD) and hexanoic acid were some of the primary metabolites formed. Formate was formed at the same time as glucose was being consumed, but once all glucose was depleted, formate was consumed as well. The production of formate is either due to the formate dehydrogenase (fdh) enzyme that converts CO_2 into formate, or due to the pyruvate-formate lyase (pfl) enzyme, catalyzing the conversion of pyruvate and CoA to acetyl-CoA and formate. The labeling pattern in formate at 42 hours indicates 17% of formate is labeled. Since the percentage of labeling in CO_2 is much higher than that of formate (30% vs. ~17%) (Figure 3.10), some of the formate must be derived through the pyruvate-formate lyase enzymatic step, diluting the carbon labeling. This could

further be interrogated using labeling data of various pyruvate or C1-pool derived amino acids, such as alanine, serine or methionine requiring further ^{13}C analysis.
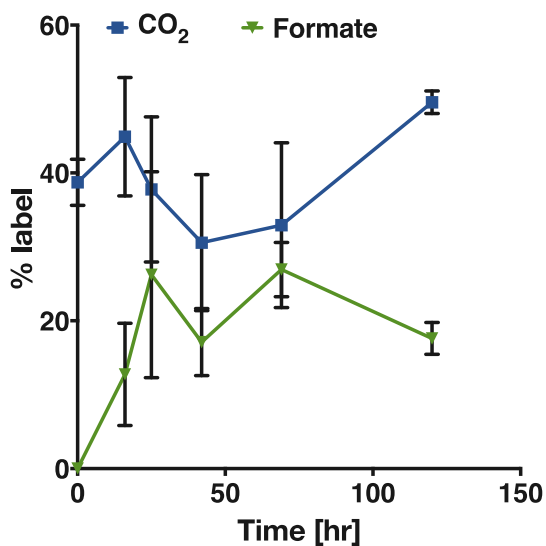
Figure 3.10. Percent of ^{13}C label in formate (green) compared to the labeling in CO_2 (blue). Because of the difference in labeling for the two compounds, formate is unlikely solely produced from the reduction of CO2 by the formate dehydrogenase, but is also produced from the pyruvate-lyase enzyme.

Just like formate, lactate was produced only when glucose was present, and later was converted into 2,3BD. However, once glucose was depleted, the 2,3BD concentration increased. The final average product titer of 2,3 butanediol was 8mM, with one replicate producing a modest 5mM and another up to 13mM. Comparable yields on fructose have been shown in *Clostridium autoethanogenum* (Liew, Henstra et al. 2016) in both mixotrophic and syngas enhanced mixotrophic conditions. When

comparing yields (2,3BD divided by fructose or glucose consumed), the *Clostridium carboxidivorans* strain had a yield of 2,3BD of 0.24, compared to a yield of 0.18 and 0.09 for *Clostridium autoethanogenum* grown on fructose + CO and fructose alone, respectively (Liew, Henstra et al. 2016). Even though small amounts of 2,3BD were formed, the yield was higher than previous published values. Besides the pyruvate-derived products such as lactate and 2,3BD, the cultures formed significant amounts of acetate once the glucose was depleted. Acetate levels increased to final titers of 68 mM, from the initial 30 mM at the start of the fermentation. There was a slight increase in acetate production in the beginning of the fermentation followed by a slight decrease, indicating a classic switch to solventogenesis as is observed in cultures of CAC (Papoutsakis 2008). After the glucose is depleted, there is a rapid increase in acetate production. The increase of acetate after glucose depletion is interesting. First, it indicates a preference for acetate production when grown autotrophically, as would be expected. Second, it also shows that acetate is not a primary product in the presence of glucose but rather a result of carbohydrate depletion and necessary gas consumption. The percent labeling in acetate was initially around 21% after 16 hours of the fermentation, which indicates that the gaseous uptake rate is not as fast as the carbohydrate uptake rate. The labeling in acetate does increase in the last 50 hours of fermentation (up to ~34% labeling) (Figure 3.11), either due to an increase in labeled CO and CO_2 uptake rate or due to the decrease in available carbohydrates. Acetate and ethanol exhibited similar amounts of labeling (~11-34%), but butyrate exhibited the highest percent labeling (up to ~40% labeling). However, the labeling in acetate, ethanol and butyrate is much lower than in the previous experiments for *Clostridium ljungdahlii*, *Clostridium autoethanogenum*, *Morealla thermoacetica* and *Eubacterium*

59

limosum. This could be due to the different culturing conditions (*Clostridium carboxidivorans* was grown on 100% CO) or this could be attributed to different regulatory mechanisms in this strain. In these experiments, the overall gas uptake was considerably lower and not all carbon monoxide was exhausted, as can be seen from Figure 3.12.
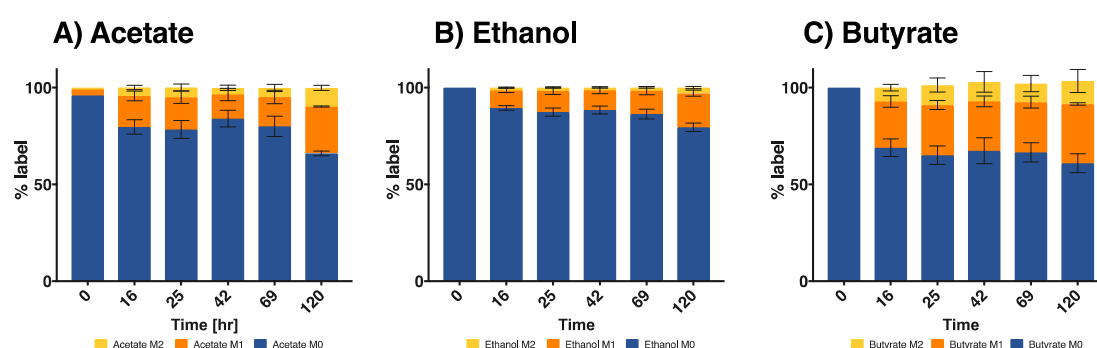
Figure 3.11. Percent of ^{13}C label from ^{13}CO in A) acetate, B) ethanol and C) butyrate. Unlabeled percentage is shown in blue, one labeled carbon is shown in orange, and two labeled carbons is shown in yellow. Labeling percentages are similar throughout the fermentation.

Carbon monoxide was consumed in the presence of glucose at a rate of 1.9 mmol/hr/gDW and at a rate slightly lower of 0.8 mmol/hr/gDW after glucose was exhausted. These values are much lower than what has been reported experimentally or calculated based on models for different strains of acetogens (20 mmol/hr/gDW and 34.4 mmol/hr/gDW, respectively) (Nagarajan, Sahin et al. 2013, Mohammadi, Mohamed et al. 2014). This indicates that the CO is not readily metabolized in this experiment utilizing *Clostridium carboxidivorans*. The slow gaseous uptake rate could

be due to the toxicity of CO. The toxicity of CO is a problem for many clostridia organisms, mainly due to the inhibition of the hydrogenase enzymes these bacteria employ to get rid of extra electrons and balance their internal redox balance. (Gray and Gest 1965, Meyer, Roos et al. 1986, Mohammadi, Mohamed et al. 2014). Mohammadi et al. demonstrated inhibition of CO for the acetogen *Clostridium ljungdahlii* at partial pressures well below this experiment (6.6 pisg vs. 30 psig in this study). The authors found an inhibitory effect of CO on the cell growth and substrate gas uptake at partial pressures above 4.4 psig. Even though *Clostridium carboxidivorans* is reportedly better equipped to deal with higher CO partial pressures, we see an almost 10-fold decrease in the gaseous uptake rate than what has been reported for *Clostridium ljungdahlii* experimentally growing on synthesis gas (mixture of CO, CO_2, H_2, and Ar (30/30/30/10). The authors also concluded that *Clostridium ljungdahlii* consumed H_2/CO_2 as the preferred substrate rather than CO. The Wood-Ljungdahl pathway can either convert CO directly into acetyl-CoA via the bifunctional carbon monoxide dehydrogenase/acetyl-CoA synthase enzyme (CODH/ACS), or it can undergo conversion to CO_2 using a monofunctional carbon monoxide dehydrogenase (CODH). We can observe the interchange of CO into CO_2 and H_2 by monitoring the increase in total $^{13}CO_2$ in the fermentation headspace. The conversion of ^{13}CO into $^{13}CO_2$ can be monitored by the change in ^{13}CO and increase in $^{13}CO_2$. The oxidation of CO increases 10-fold by the end of the fermentation, indicating an increase in the activity of one of the carbon-monoxide dehydrogenase enzymes or the bifunctional CODH/ACS enzyme. *Clostridium carboxidivorans* contains three monofunctional CODHs (Ccar_07140, Ccar_08590 and Ccar_23090) on the chromosome. Ccar_08590 has previously been shown to be upregulated during later stages of solventogenesis

(Ukpong, Atiyeh et al. 2012). In this study, we see that much of the consumed ^{13}CO is being converted into $^{13}CO_2$ during the later stages of fermentation rather than being taken up and directly converted into the cells for the production of metabolites.
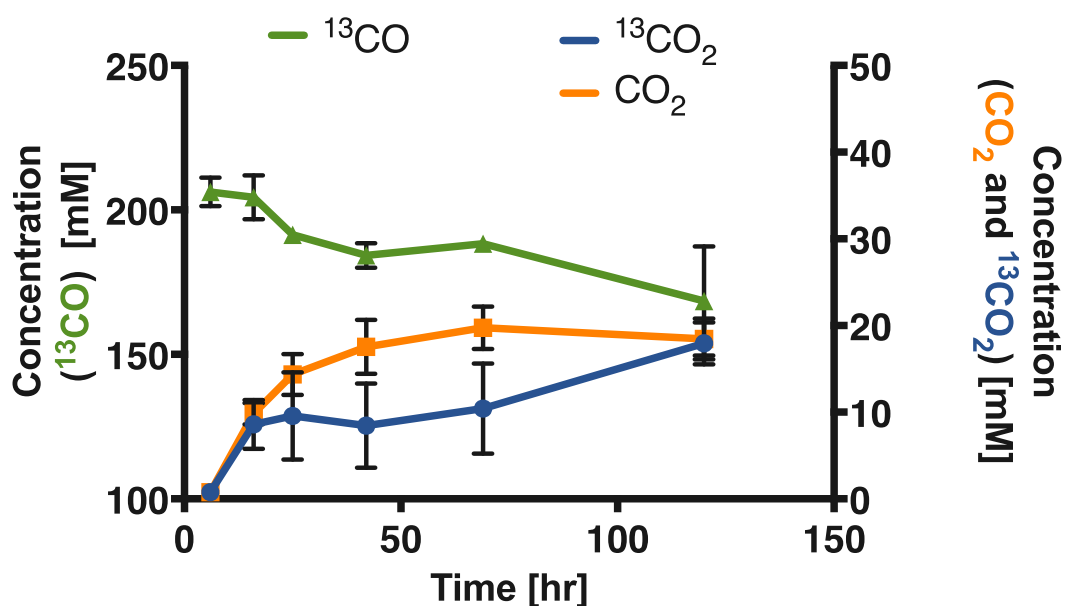
Figure 3.12. Gaseous concentrations in the headspace during the syngas enhanced mixotrophic fermentation of *Clostridium carboxidivorans* with 6 g/L glucose and 100% ^{13}CO headspace (30 psi). ^{13}CO (green), $^{13}CO_2$ (blue), CO_2 (orange).

To further interrogate the amount of gases converted into products, we set out to evaluate the total yield of products from glucose fermentation by *Clostridium carboxidivorans*. In Figure 3.13 we can see that the carbon balance for this fermentation starts out around 60%, which is consistent with heterotrophic metabolism of CAC cultures. During the next time points, however, the carbon balance decreases to 43% at t=69 hours. This indicates the possible formation of another product that is

currently not analyzed. The continued drop of the carbon balance is depicted in Figure 3.13, and is only seen to rapidly increase towards the later stages of fermentation. We observe that hexanoic acid is consumed between 69 hours and 120 hours (2.3 to 1.8 mM). One of the most obvious products missing in our analysis is hexanol, which is formed from the reduction of hexanoic acid. Unfortunately, the detection of hexanol requires more than 2-hour analysis time using current method employed for the detection of metabolites utilizing HPLC. It is possible that the presence of the hexanoic acid is only an intermediate, and that the production of hexanol is present even at 24 hours where we see the first decrease in the carbon balance. Towards the end of the fermentation, the carbon balance increases significantly and reaches 94%, which is much higher than the 66% theoretically possibly using heterotrophy alone, which indicates a significant amount of gas has been utilized in the production of metabolites. Including the production of hexanol for future experiments would greatly enhance the analysis of total product yields for mixotrophic fermentations of *Clostridium carboxidivorans*.
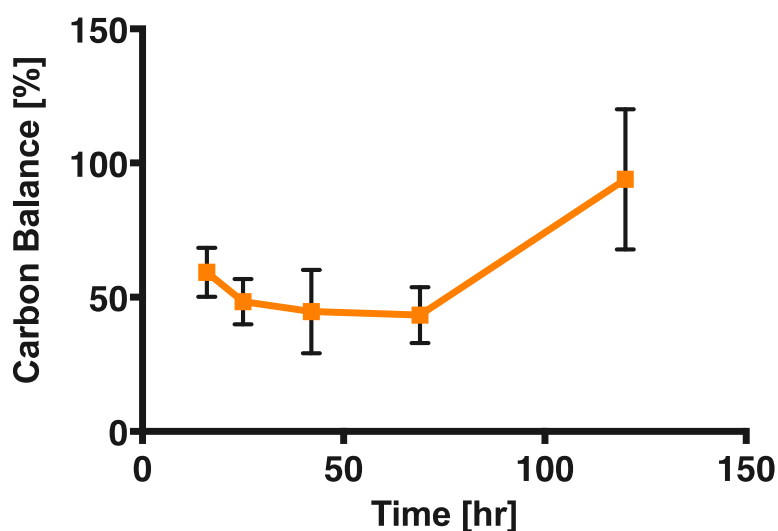
Figure 3.13. Carbon Balance for the metabolites of *Clostridium carboxidivorans* fermentation at given time points. Carbon balance (%) is defined as the total carbon moles of product divided by the total carbon moles of glucose consumed.

In conclusion, all though gas and sugar uptake were lower compared to literature values, the cultures of *Clostridium carboxidivorans* were able to ferment all of the glucose present and convert the feedstock into various metabolites, including 23BD and hexanoic acid. Gaseous feedstock was consumed simultaneously as the carbohydrate feedstock, as indicated by the labeling contained in many of the products. Much less gas was co-utilized alongside carbohydrates, potentially due to the high partial pressure of CO. Cultures of *Clostridium ljungdahlii*, for example, are unable to tolerate these high levels. The production of reduced metabolites was higher than what had previously been reported and indicate the potential of *Clostridium carboxidivorans* to serve as a microbial host utilizing mixotrophic fermentations.

3.8.2 Heterotrophic Behavior of *Clostridium carboxidivorans* with High Glucose Concentrations

Due to the rapid consumption of glucose in the previous experiment, we wanted to investigate the consumption of glucose in a media used routinely for the fermentation of *Clostridium acetobutylicum*. Clostridial Growth Medium (CGM) was supplemented with trace elements and vitamins of the standard, acetogenic medium (ATCC medium 1754). Actively growing cultures of *Clostridium carboxidivorans* were added to 30 ml of fresh media and the fermentation was started by the addition of either 10g/L or 40 g/L glucose. Samples were taken every 12 hours and metabolite concentrations were analyzed using HPLC. Strikingly, we see no difference in the amount of glucose up taken by cell between cultures supplemented with different amounts of glucose. Both cultures consumed ~4.7g/L glucose in this experiment. The rate of glucose uptake was similar in the first 32 hours (0.75mmoles/gDW/hr and 0.98mmoles/gDW/hr for 10g/L and 40 g/L, respectively). However, during late exponential phase the glucose uptake rate increased to 1.0 mmoles/gDW/hr and 1.96 mmoles/gDW/hr for 10g/L and 40 g/L, respectively. The glucose consumption ceased after 40 hours. The CGM media might not be buffered enough to allow the continuous consumption of glucose. The biomass yield was higher than that of the syngas enhanced mixotrophic experiment, which utilized an acetogenic media. One of the main differences between the acetogenic media and CGM is the amount of yeast extract (1 g/L versus 5 g/L). The higher yeast extract could attribute to the higher biomass yield for this experiment. The growth rate of 0.09 and 0.11 hr^{-1} for 10g/L and 40g/L respectively, indicates comparable rates to when grown on gases alone.
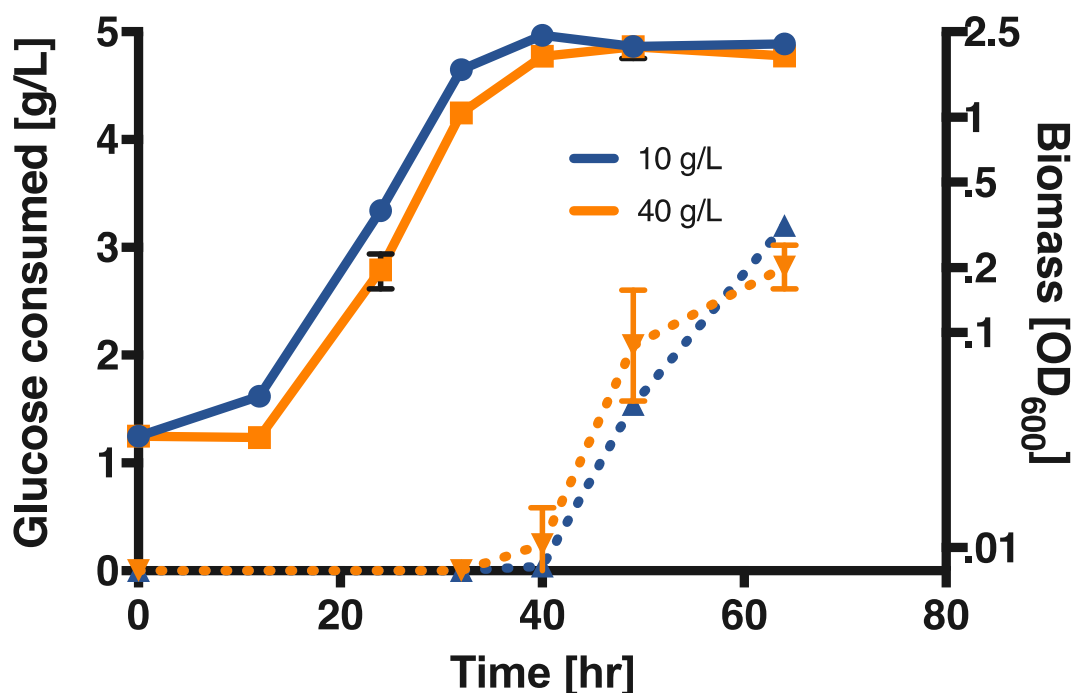
Figure 3.14. Total glucose consumed (dotted line) and biomass formed (solid line) for *Clostridium carboxidivorans* grown in clostridial growth medium supplemented with either 10g/L glucose (blue) or 40g/L glucose (orange). Glucose consumption is independent of glucose concentration.

The fermentation profiles exhibited similar trends between the two culture conditions. More formate was formed in the presence of 10 g/L than with 40 g/L. Initial lactate was present in the media and subsequently consumed in both conditions tested. The two conditions produced 3 and 2.4 mM of hexanoic acid (10 g/L and 40 g/L respectively). Total amounts of 2,3BD are similar to previously reported values (~8mM each). However, the yield is much higher than in the mixotrophic experiment (0.32 and 0.26 for 10 g/L and 40 g/L respectively, compared to 0.24 from the syngas enhanced mixotrophic experiment). Interestingly, 2,3BD production is usually associated with a redox imbalance, with increasing production of 2,3BD when the

cells are trying to get rid of excess reducing potentials (Liew, Henstra et al. 2016).

This is an interesting phenomenon given that the cells were solely grown on glucose

alone, and solventogenic clostridia such as CAC do not produce significant amounts of

lactate when grown on glucose. This indicates some inability of *Clostridium*

carboxidivorans to shuffle electrons derived through glycolysis into products. Besides

2,3BD, ethanol, butyrate and hexanoic acid are all products requiring electrons, and

therefore we would expect an increase in the production of these metabolites as well.

Ethanol concentrations reached up to 25mM (compared to 10mM in the syngas

enhanced mixotrophic experiment), and butyrate concentrations leveled out around

10mM. Interestingly, no significant amounts of butanol were detected in the

fermentation.
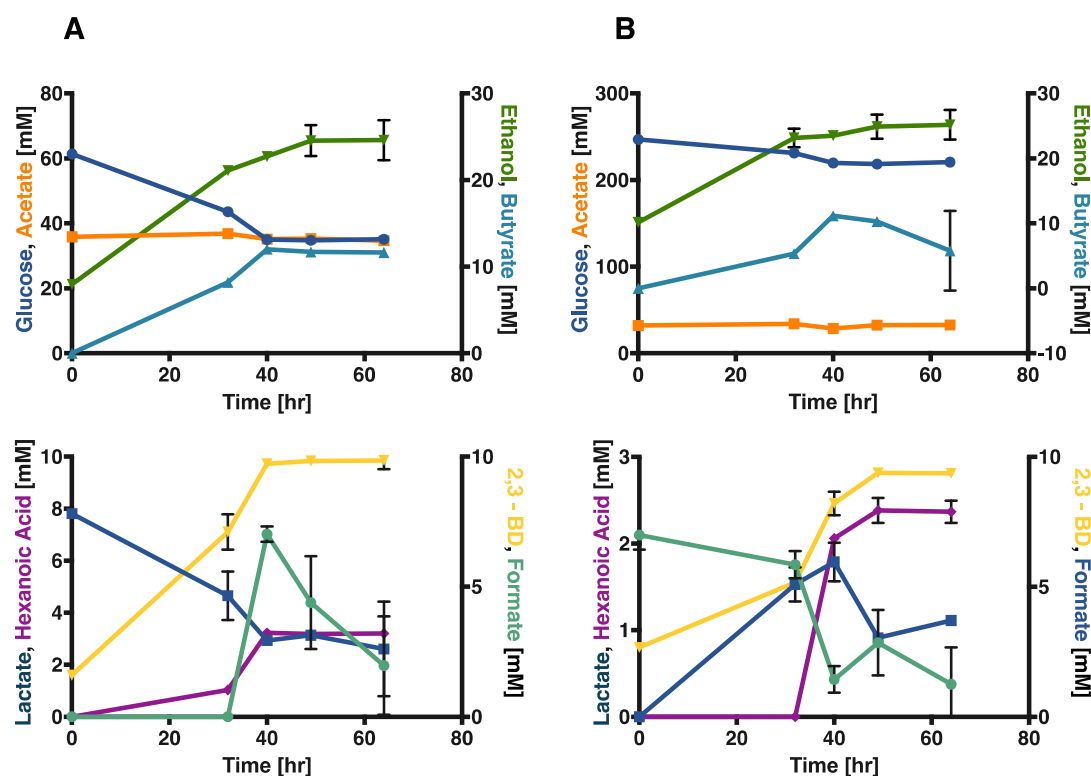
Figure 3.15. Fermentation profile during heterotrophic growth of *Clostridium carboxidivorans* with 10g/L(A) or 40g/L (B). Glucose (blue), acetate (orange), ethanol (green) and butyrate (turquoise) are shown in the top figures, lactate (blue), hexanoic acid (purple), 2,3-Butanediol (yellow) and formate (seafoam green) are shown in the bottom figures.

Even though the experiment utilizing the solventogenic growth medium routinely used for CAC increased total biomass yield, the rate of glucose uptake was not increased from the previous syngas enhanced mixotrophic experiment employing the acetogenic medium. This could indicate a bottleneck for *Clostridium carboxidivorans* when grown mixotrophically.

3.9   Conclusions

Mixotrophic fermentations enhanced the overall product yields by eliminating or reducing the amount of CO_2 that is evolved during glycolysis. This confirms the previous theoretical calculations that propose the coupling of glycolysis to the Wood-Ljungdahl pathway and the resulting product yield improvements. All acetogenic, syngas enhanced mixotrophic experiments indicated a simultaneous consumption of gases and carbohydrates, as suggested through ^{13}C carbon tracing experiments. The amount of gaseous uptake and subsequent conversion into metabolites was dependent upon species and culture conditions. This works further revealed the desired increase in reduced product profiles for fermentations in which an additional source of electrons (syngas or CO) is added to the fermentation (syngas enhanced mixotrophy). The product profile was species dependent and showed great potential for a variety of target products such as: ethanol, butyric acid, 23BD or hexanoic acid. Even though metabolic engineering strategies have been employed to shift product profiles towards more reduced products (for example, by Liew and colleges who knocked out the ACS enzyme and showed an increase in the production of 23BD for *Clostridium autoethanogenum* (Liew, Henstra et al. 2016)), it is clear that operational parameters and fermentation conditions can have a profound impact on product distributions as well. In a syngas-enhanced mixotrophic experiment utilizing CKK, the 23BD yield was 0.24, almost a 33% increase for previously published values for *Clostridium autoethanogenum*. With all recently discovered bacteria, much work needs to be done in order to establish practices to increase biomass yields and product yields to achieve comparable yields to what is routinely achieved in *Clostridium acetobutylicum* (up to 20g/L of products). Companies like White Dog Labs, Inc. and LanzaTech are further researching the application of acetogens for the industrial production of fuels and

chemicals, and one day these technologies might provide an alternative fuel or chemicals to us all.

3.10 Materials and Methods

Strains and Growth Conditions. *Clostridium ljungdahlii* DSM-13528 (CLJ), *Clostridium autoethanogenum* DSM-10061 (CAU), *Eubacterium limosum* DSM-20543 (ELM), *Moorella thermoacetica* DSM-521 (MTA) and *Clostridium carboxidivorans* DSMZ-15243 (CCK) were obtained from DSMZ (Braunschweig, Germany). All cultures were grown in sealed serum bottles in a shaking incubator (150 rpm) at 37°C, except for *Moorella thermoacetica* which was incubated at 55°C. They were cultivated anaerobically in American Type Culture Collection (ATCC) medium 1754 with 10 g/l of fructose, with the exception of *Eubacterium limosum* which was grown in a modified ATCC medium 1754 (supplemented with 10 g/L MES, pH 6.0) with 5 g/l of fructose. Growth was monitored by measuring the optical density at 600 nm (OD_{600nm}). A 5% inoculum of mid-exponential phase (OD_{600nm} of 0.8-1.5) was used to inoculate 160-ml serum bottles (Wheaton), with 50 ml of culture media and 110 ml of gas headspace. For autotrophic and syngas-enhanced mixotrophic cultures, the headspace was pressurized to 30 psig with syngas ($CO/CO_2/H_2/N_2$, 55:10:20:15), except for *Eubacterium limosum* which was pressurized to 20 psig. *M. thermoacetica* was grown in a mixture without CO (CO_2/H_2, 80:20). Heterotrophic and mixotrophic cultures were pressurized to 20 psig with N_2. The pH of the cultures was monitored and kept between 5.0-6.5 by adding

70

4M NH$_4$OH. *Clostridium carboxidivorans* was grown in ATCC medium 1754 and

100%CO (30 psig) for the enhanced mixotrophic experiment, and was grown in

clostridial growth media [CGM; 0.75 g/liter K$_2$HPO$_4$, 0.75 g/liter KH$_2$PO$_4$, 0.7 g/liter

MgSO$_4$·7H$_2$O, 0.017 g/liter MnSO$_4$·5H$_2$O, 0.01 g/liter FeSO$_4$·7H$_2$O, 2 g/liter

(NH$_4$)$_2$SO$_4$, 1 g/liter NaCl, 2 g/liter asparagine, 0.004 g/liter *p*-aminobenzoic acid, 5

g/liter yeast extract, 4.08 g/liter CH$_3$COONa·3H$_2$O] for heterotrophic experiments with

either 10g/l or 40 g/L glucose. Heterotrophic experiments were conducted with an

open headspace inside an anaerobic glove box.

^{13}C Metabolite Labeling. *Clostridium ljungdahlii* and *Clostridium*

autoethanogenum were grown as described above with 10 g/l of ^{12}C-fructose. The

syngas-enhanced mixotrophic and autotrophic cultures contained a mixture of syngas

(^{13}CO/^{13}CO$_2$/H$_2$/N$_2$, 55:10:20:15) with all carbons labeled. Samples were taken at

early, mid and late exponential phase and metabolites and biomass was analyzed for

^{13}C content, as described (Au, Choi et al. 2014). In addition, samples were taken for

qRT-PCR and Western blot analysis.

Detection of Metabolites. Culture supernatant samples were quantified using

an Agilent HPLC instrument (Agilent 1260 series, Agilent Technologies, Santa

Clara, CA, USA) equipped with an automatic sampler/injector and a refractive index

detector (RID) using an Aminex HPX-87H column (Bio-Rad, Hercules, CA, USA).

Gas samples were analyzed using an Agilent GC instrument with a Supelco 60/80

Carboxen-1000 column, used according to the manufacturer's recommendation. Acids and alcohols from 3.1 were quantified at their respective elution times. ^{13}C content of metabolites for *C. carboxidivorans* study was quantified using a Shimadzu QP-2010 Ultra gas chromatograph-mass spectrometer and a X column.

RNA Isolation and qRT-PCR. RNA was extracted using RNEasy Kit (Qiagen) with a modified protocol as follows: Cells were thawed on ice and washed and resuspended in 220 µl RNase-free SET Buffer + 20 µl Proteinase K. Samples were sonicated for 10 minutes using 15 seconds pulse on/off at 40% amplitude in a Fisher Scientific Sonic Dismembrator. 1 ml of Trizol was added to each sample, split in two and another 400 µl Trizol was added to have the final volume of ~1 ml. 200 µl of ice-cold chloroform were added to sample and mixed for 15 seconds, then incubated at room temperature for 3 minutes. Samples were spun at <12000 rpm for 15 minutes at 4°C. Upper aqueous phase was mixed with 500 µl of 70% ethanol and RNEasy protocol was followed per manual. Sample concentration was determined using a nanodrop. Concentrations ranged from ~50 ng/µl – 600 ng/µl depending on sample.
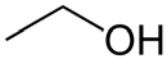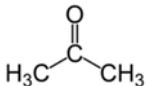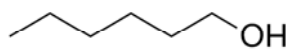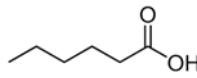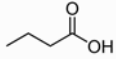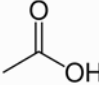
cDNA was synthesized using high capacity cDNA reverse transcription kit (Applied Biosystems). 1 µl of cDNA was used in qRT-PCR experiments using the SYBR green kit (BioRad) following the manufactures protocol. Primers are listed in Table S2. Each sample was tested with three technical replicates and three biological replicates. All technical replicates were averaged. The housekeeping gene was CLJ_c12520 (*gp*k, guanylate kinase)(Köpke, Mihalcea et al. 2011). Fold changes were

calculated using the autotrophic condition as the control case and either mixotrophy or syngas-enhanced mixotrophy as the experimental condition. All calculations were done using Graph Pad PRISM® software with statistical analysis using two-way ANOVA of the ΔCT between the three conditions (autotrophy, mixotrophy and syngas-enhanced mixotrophy).

Primer name	Sequence	Purpose
c37550 RT F	GGACTTGACCTCAGGGTTATTC	qRT-PCR for ACS Alpha
c37550 RT R	TGCACCTGCTGAAACTACAA	qRT-PCR for ACS Alpha
c37670 RT F	GGGTCGAAACAGTTTGGGATAG	qRT-PCR for ACS Beta
c37670 RT R	GTACCTGCTGCAACCATTCT	qRT-PCR for ACS Beta
c37570 RT F	TGCAAGAGCACTTCCTCTTTAT	qRT-PCR for CFeSP Alpha
c37570 RT R	CCTGCATCTGGTATAACCATCC	qRT-PCR for CFeSP Alpha
c37580 RT F	GTAGGAGCTGCAGGTGTAATG	qRT-PCR for CFeSP Beta
c37580 RT R	GCTGCAAGCTTTACTCTGTCTA	qRT-PCR for CFeSP Beta
c12520 RT F	AGGTACAGTTTGCAAGGCA	qRT-PCR housekeeping gene
c12520 RT R	ACTTGAGACTTAGGTGTACCATAATAG	qRT-PCR housekeeping gene

Western Blots. Cells were harvested by centrifugation at 4°C for 10 minutes at 7000xg. The cell pellets were frozen at -82°C. The cell pellets were then resuspended in 500μl of 100mM Tris-HCl (pH 7.0) (Buffer A). The samples were sonicated using a Fisher Scientific Sonic Dismembrator for 15 seconds pulse on/off at

50% amplitude for 10 minutes. The samples were spun down for 10 min at 16000 rpm.

The supernatant was collected and the cell debris was resuspended in same amount of

Buffer A. The samples were mixed in a 1:5 dilution with 5x loading Buffer (0.2 M

Tris-HCl (pH 6.8), 10% SDS, 1.43M 2-Mercaptoethanol, 0.05% bromophenol blue,

50% glycerol) and boiled at 95°C for 10 minutes. 30-50µl of aliquots were loaded onto

the Genscript ExpressPlus PAGE Gel, 4-20% gradient and run at 120V for 2 hours.

The gels were transferred using the BioRad mini-trans blot system. The polyclonal

antibodies against the CODH subunit were designed through ProteinTech and

obtained from rabbit serum. The AP colorimetric kit (BioRad) was used to visualize

the bands using a 1:10000 dilution of the polyclonal antibodies, following the

supplier's recommendations.

Name	Structure	Retention time	Organism
Ethanol		24	CAC, CLJ, CAU, MTA, CKL, ELM
Acetone		28	CAC,
Butanol		42	CAC, CCK
Hexanol			CCK, CKL, CSK, CBUT
Hexanoic Acid		68	CCK, CKL, CSK, CBUT
Butyric Acid		27	CAC, MTA, CKL, ELM
Acetic Acid		18	CAC, CLJ, CAU, MTA, CKL, ELM
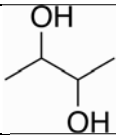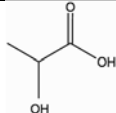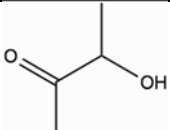
2,3 Butanediol		21	CLJ, CAU, MTA, ELM
Lactate		15	CCK, CKL, CSK, CBUT
Acetoin		22	CAC, CCK, CKL, CSK, CBUT

Table 3.1. Metabolites produced by various Clostridia. All these products are included in the product yield calculations. Included is the retention time on HPLC along with the organisms known to produce given metabolite. CAC: *Clostridium acetobutylicum*, CLJ: *Clostridium ljungdahlii, Clostridium autoethanogenum* (CAU); *Clostridium carboxidivorans* (CCK), *Eubacterium limosum* (ELM), *Moorella thermoacetica* (MTA), *Clostridium kluyveri* (CKL), *Clostridium butyricum* (CBUT), *Clostridium scatologenes* (CSK)

Chapter 4

HETEROLOGOUS EXPRESSION OF THE *CLOSTRIDIUM CARBOXIDIVORANS* CO DEHYDROGENASE ALONE OR TOGETHER WITH THE ACETYL COENZYME A SYNTHASE ENABLES BOTH REDUCTION OF CO_2 AND OXIDATION OF CO BY *CLOSTRIDIUM ACETOBUTYLICUM*

4.1 Preface

This chapter has been published as a paper in Applied Environmental Biology under the same title with the following DOI number: 10.1128/AEM.00829-17.

4.2 Abstract

With recent advances in synthetic biology, CO_2 could be utilized as a carbon feedstock by native or engineered organisms, assuming the availability of electrons. Two key enzymes used in autotrophic CO_2 fixation are the CO dehydrogenase (CODH) and acetyl coenzyme A (acetyl-CoA) synthase (ACS), which form a bi-functional heterotetrameric complex. The CODH-ACS complex can reversibly catalyze CO_2 to CO, effectively enabling a biological water-gas shift reaction at ambient temperatures and pressures. The CODH-ACS complex is part of the Wood-Ljungdahl pathway (WLP) used by acetogens to fix CO_2, and it has been well characterized in native hosts. So far, only a few recombinant CODH-ACS complexes have been expressed in heterologous hosts, none of which demonstrated *in vivo* CO_2 reduction. Here, functional expression of the *Clostridium carboxidivorans* CODH-ACS complex is demonstrated in the solventogen *Clostridium acetobutylicum*, which was engineered to express CODH alone or together with the ACS. Both strains

exhibited CO_2 reduction and CO oxidation activities. The CODH reactions were interrogated using isotopic labeling, thus verifying that CO was a direct product of CO_2 reduction, and vice versa. CODH apparently uses a native *Clostridium acetobutylicum* ferredoxin as an electron carrier for CO_2 reduction. Heterologous CODH activity depended on actively growing cells and required the addition of nickel, which is inserted into CODH without the need to express the native Ni insertase protein. Increasing CO concentrations in the gas phase inhibited CODH activity and altered the metabolite profile of the CODH- expressing cells. This work provides the foundation for engineering a complete and functional WLP in nonnative host organisms.

4.3 Importance

Functional expression of CO dehydrogenase (CODH) from *Clostridium carboxidivorans* was demonstrated in *C. acetobutylicum*, which is natively incapable of CO_2 fixation. Expression of CODH, alone or together with the *C. carboxidivorans* acetyl-CoA synthase (ACS), enabled *C. acetobutylicum* to catalyze both CO_2 reduction and CO oxidation. Importantly, CODH exhibited activity both in the presence and absence of ACS. ^{13}C-tracer studies confirmed that the engineered *C. acetobutylicum* strains can reduce CO_2 to CO and oxidize CO, during growth on glucose.

4.4 Keywords

CO_2 fixation, CO_2 reduction, CO oxidation, metabolic engineering, synthetic biology, the Wood-Ljungdahl pathway, acetogens

4.5 Introduction

The Wood-Ljungdahl pathway (WLP) is the most efficient pathway for CO_2 fixation, whereby two molecules of CO_2 are reduced to form one molecule of acetyl coenzyme A (acetyl-CoA), a primordial biological building block for cellular components (Fast and Papoutsakis 2012). The WLP is composed of two linear branches: the so-called eastern, or methyl, branch reduces CO_2 to formate via formate dehydrogenase and transfers the carbon molecule to the C1 carrier tetrahydrofolate, while the second western, or carbonyl, branch reduces CO_2 to CO (Bar-Even, Noor et al. 2012). The final carbonylation step for acetyl-CoA synthesis combines CO with the activated methyl group from the Eastern branch and the CoA moiety and is catalyzed by the bifunctional enzyme complex of carbon monoxide dehydrogenase (CODH)/acetyl-CoA synthase (ACS). The native CODH/ACS complex used by acetogens is characterized by a $\alpha_2\beta_2$ tetrameric structure containing a central core of two CODH subunits that are associated on either side by two ACS subunits (Can, Armstrong et al. 2014). Each subunit contains an active site; the β site is responsible for CO oxidation and CO_2 reduction (C-cluster), and the α site is responsible for acetyl-CoA synthesis (A-cluster). CODH reversibly oxidizes CO to CO_2 and allows many bacteria to grow on CO as a sole carbon source (Genthner and Bryant 1987, Abrini, Naveau et al. 1994 , Köpke, Mihalcea et al. 2011, Can, Armstrong et al. 2014). In addition, reduction of CO_2 allows acetogens to grow on CO_2 and H_2, as well. In the chemical industry, the interconversion of CO and CO_2 is an important process known as the water-gas shift reaction for the generation of H_2, in which CO is oxidized under high temperature and pressure. In contrast, the biological reaction occurs at atmospheric pressure and temperatures between 37 and 60°C.

The first study to examine the biological oxidation of CO to CO_2 was performed with methanogenic bacteria (Daniels, Fuchs et al. 1977) and later with *Clostridium formicoaceticum* and *Moorella thermoacetica* (formerly *Clostridium thermoaceticum*) (Diekert and Thauer 1978). All strains were able to oxidize CO to CO_2, grow on CO_2 and H_2 and have been shown to contain a WLP and the necessary CODH/ACS proteins/genes. The most extensively studied bifunctional CODH/ACS is from *M. thermoacetica*, which has been purified (Drake, Hu et al. 1980), characterized (Shanmugasundaram and Wood 1992) and its crystal structure elucidated (Doukov, Iverson et al. 2002). There exists evidence that the two subunits are connected to enable substrate channeling thus enhancing the substrate flux between the two active sites thereby lowering the internal thermodynamic barrier for CO_2 reduction (Maynard and Lindahl 1999, Maynard and Lindahl 2001, Volbeda and Fontecilla-Camps 2004, Tan, Loke et al. 2005, Tan and Lindahl 2008). CO_2 is reduced to CO at the active site of the CODH (C-cluster) and can migrate to the active site of the ACS, the A-cluster, without leaving the hydrophobic pockets of the enzyme. Even though these enzymes have been well studied, much remains to be understood regarding the exact catalytic mechanisms and redox states for the multifaceted process of fixing CO_2. Traditionally, CO oxidation is monitored *in vitro* with an artificial electron carrier such as methyl viologen; in other cases, ferredoxin isolated from anaerobic bacteria is used (Shanmugasundaram and Wood 1992). The *in vitro* assay for the ACS involves the "carbon exchange reaction" between CO and the carbonyl group of acetyl-CoA, monitored using ^{14}C radioactive tracers. Although *in vitro* analysis is a convenient measure of enzyme activity, it cannot simulate physiological conditions involved in *in vivo* CO_2 reduction.

CO$_2$ is the most oxidized form of carbon and is therefore a stable and highly inert compound. Since CO$_2$ reduction and subsequent acetyl-CoA synthesis provide acetogens the sole means for growth on gases alone, reduction of CO$_2$ occurs under physiological conditions. However, under standard conditions, reduction of CO$_2$ to CO has a ΔG of +32 kJ/mol (Bar-Even, Noor et al. 2012). Clearly, acetogenic bacteria create an intracellular environment and/or low redox potential that allows this reaction to proceed to reduce CO$_2$ to form CO. The CODH/ACS subunits from *M. thermoacetica* have been expressed in *Escherichia coli* JM109, but did not exhibit the native tetrameric structure and were thus found inactive (Roberts, James-Hagstrom et al. 1989). More recently, however, Loke *et al.* demonstrated that expression of the two subunits in the same *E. coli* host produced a protein complex that migrated as a single band through non-denaturing electrophoretic gels (Loke, Bennett et al. 2000). The purified complex exhibited CO oxidation activity *in vitro*, but the *in vitro* acetyl-CoA "carbon exchange reaction" required incubation with nickel after purification.

We hypothesized that expression of the bifunctional CODH/ACS complex would benefit from a host more closely related to native acetogens. *E. coli* is a Gram-negative prokaryote and does not contain electron carriers, such as ferredoxin, the necessary electron carrier for acetogenic CODHs (Ragsdale, Clark et al. 1983, Shanmugasundaram and Wood 1992). In contrast, the Gram-positive *Clostridium acetobutylicum* is an excellent host for expressing the CODH/ACS complex since it is more closely related phylogenetically to acetogens (Bruant, Lévesque et al. 2010), is strictly anaerobic, and it contains the co-factor (ferredoxin) required for the *in vivo* function of the CODH/ACS complex (Shanmugasundaram and Wood 1992). In this study, we sought to express and demonstrate *in vivo* activities of the CODH/ACS

proteins from the acetogen *Clostridium carboxidivorans*, aiming to engineer CO_2

reduction in *C. acetobutylicum*. With the ultimate goal of engineering a functional

WLP in *C. acetobutylicum*, here, we sought to demonstrate the functional expression

of the CODH/ACS complex, an essential first goal, hitherto not accomplished. We

demonstrate functional CODH activity expressed in tandem with ACS and alone, and

we show that the reduction of CO_2 does not require the ACS subunit. *In vivo* CO_2

reduction by the engineered *C. acetobutylicum* suggests that *C. acetobutylicum*

possesses electron carriers that have a low enough redox potential to overcome the

thermodynamic challenge of CO_2 reduction. This was achieved in a nonnative host.

While there is no known *in vivo* functional assay for the ACS activity, we also

attempted to establish one that would be analogous to the aforementioned carbon

exchange reaction between CO and the carbonyl group of acetyl-CoA, but using ^{13}C-

tracers.

4.6   Results

4.6.1   Expression and purification of recombinant CODH/ACS demonstrates correct assembly of the heterotetrameric protein complex.

To test the functional expression of the CODH/ACS complex in the

heterologous host *C. acetobutylicum*, we expressed both proteins, CODH and ACS,

from the acetogen *C. carboxidivorans* (Liou, Balkwill et al. 2005), and investigated

their expression as a proper tetrameric structure through his-tag purification and

Western-blot identification (Figure 4.1). The plasmid-borne construct contained the

genes for the two subunits of the complex, CODH and ACS, and a His-tag following

the ACS coding region prior to the stop codon (Figure 4.1C). The operon was under

control of the strong native *C. acetobutylicum* P_{ptb} promoter (Tummala, Welker et al.

81

1999). Recombinant *C. acetobutylicum* cells harboring the plasmid vector for expressing the CODH/ACS complex were grown under anaerobic conditions to mid-exponential phase. Harvested cells were lysed and the supernatant was purified using a Ni-NTA affinity column under native conditions so that the heterotetrameric structure is preserved and the four subunits stay tightly associated. After purification, the eluent was subjected to a denaturing gel to verify the presence of the CODH and ACS subunits. Western blots utilizing polyclonal antibodies raised in rabbit against each subunit were used to visualize the two components of the tetramer. The data show that the eluent contained both ACS and CODH subunits, which moved independently on the denaturing SDS-PAGE gel according to their size (Figure 4.1 A& B). Next, we applied whole-cell lysates to a native PAGE gel, and observed the movement of a large protein complex of approximate size of 300 kDA not found in control cells (Figure 4.1 D). The expected mass of the *C. carboxidivorans* heterotetramer is 289 kDA, and a little larger with the His-tag. Western blots using antibodies against the His-tag confirmed that the large protein complex contained the ACS subunit tightly bound to the CODH subunit (Figure 4.1 E). We reached this conclusion because the native complex, upon purification, contained the CODH and ACS units (Figure 4.1 A&B). Taken together, these data suggest a correct assembly of the heterologously-expressed CODH/ACS heterotetrameric protein complex in *C. acetobutylicum*. We noted that the CODH/ACS complex is in the soluble fraction of the cell extracts, as little or none was detected in the insoluble fraction.
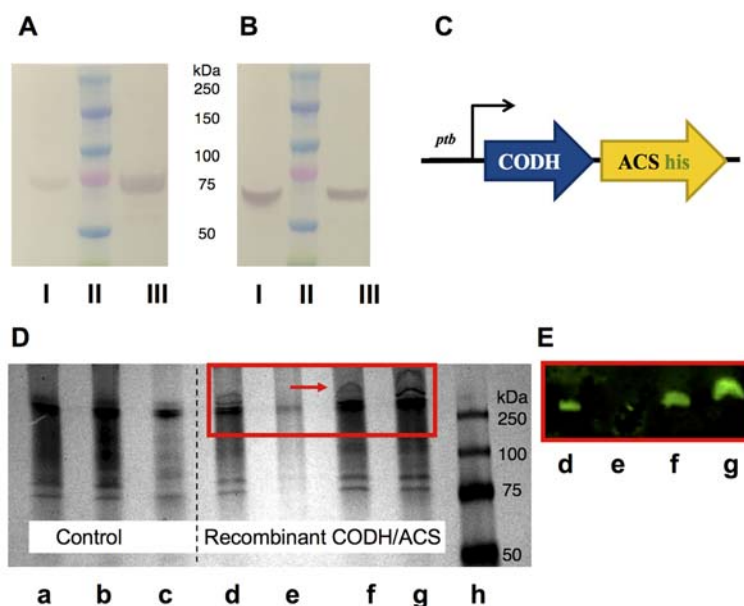
Figure 4.1. Protein expression analysis of the heterologously expressed CODH/ACS enzyme complex in *C. acetobutylicum* using his-tag purification, SDS-PAGE and native PAGE. **A,B)** Cell lysates were purified on a Ni-NTA column under native conditions. The purified fraction was loaded onto a SDS-PAGE gel and transferred onto a nitrocellulose membrane. Two blots were probed against **A)** the ACS subunit (~77.5 kDA) or against **B)** the CODH subunit (~67.6 kDA) using polyclonal antibodies. I) Whole cell lysates from *C. carboxidivorans* (positive control); II) protein ladder, III) His-tag purified CODH/ACS protein from *C. acetobutylicum* under native conditions. **C)** Schematic representation of the CODH/ACS expression cassette. Both subunits are under the control of the P_{ptb} promoter and the ACS subunit contains a His-tag prior to the stop codon. **D)** Native PAGE gel of WT *C. acetobutylicum* (control) and *C. acetobutylicum* expressing CODH/ACS. a) Whole-cell extract control, b) insoluble cell-extract fraction of control, and c) soluble cell-extract fraction of control; d) whole -cell extract of strain expressing CODH/ACS, e) insoluble cell-extract fraction of strain expressing CODH/ACS, f,g) soluble cell-extract fraction of strain expressing CODH/ACS (early and late stage of growth), and h) protein ladder. **E)** Western blot of native gel shown in D (d-g) whereby blot was probed with Anti-6X His-tag® and Alexa Fluor® 647 to show that the high molecular band seen on native PAGE-gel is that of the CODH/ACS tetrameric complex.

83

4.6.2 In vivo reduction of CO_2 by *C. acetobutylicum* expressing the CODH/ACS complex.

To test the activity of the CODH/ACS protein complex, the *C. acetobutylicum* strain expressing CODH/ACS was tested for its ability to reduce CO_2. The strain was grown on 40 g/L glucose in defined medium in sealed serum bottles with 10 psi CO_2 and H_2 (20/80) in the headspace. CO formation over 24 hours was confirmed using gas chromatography (Figure 4.2 C). To verify that the CO was a direct product of CO_2 reduction, we added 30 mM [^{13}C]sodium bicarbonate to actively growing cells to achieve a ~18% ^{13}C-labeling in CO_2, as the headspace already contained $^{12}CO_2$ from decarboxylation reactions due to the glucose fermentation. The percentage of ^{13}C-label in CO, as measured by gas chromatography coupled to mass spectrometry (GC-MS; Figure 4.2 B), increased with time. This confirmed that the CO is produced due to reduction of CO_2 in the headspace. Control cells carrying an empty plasmid failed in all experiments to produce CO, that is, no CO could be detected on the chromatogram (Figure 4.2 C). Since the CODH natively employs a reduced ferredoxin (Fd_{red}) to reduce CO_2 to CO (Figure 4.2 D) (Drake, Hu et al. 1980, Shanmugasundaram and Wood 1992), it is clear that the recombinant CODH used a *C. acetobutylicum*-native Fd_{red} to carry out this reaction.
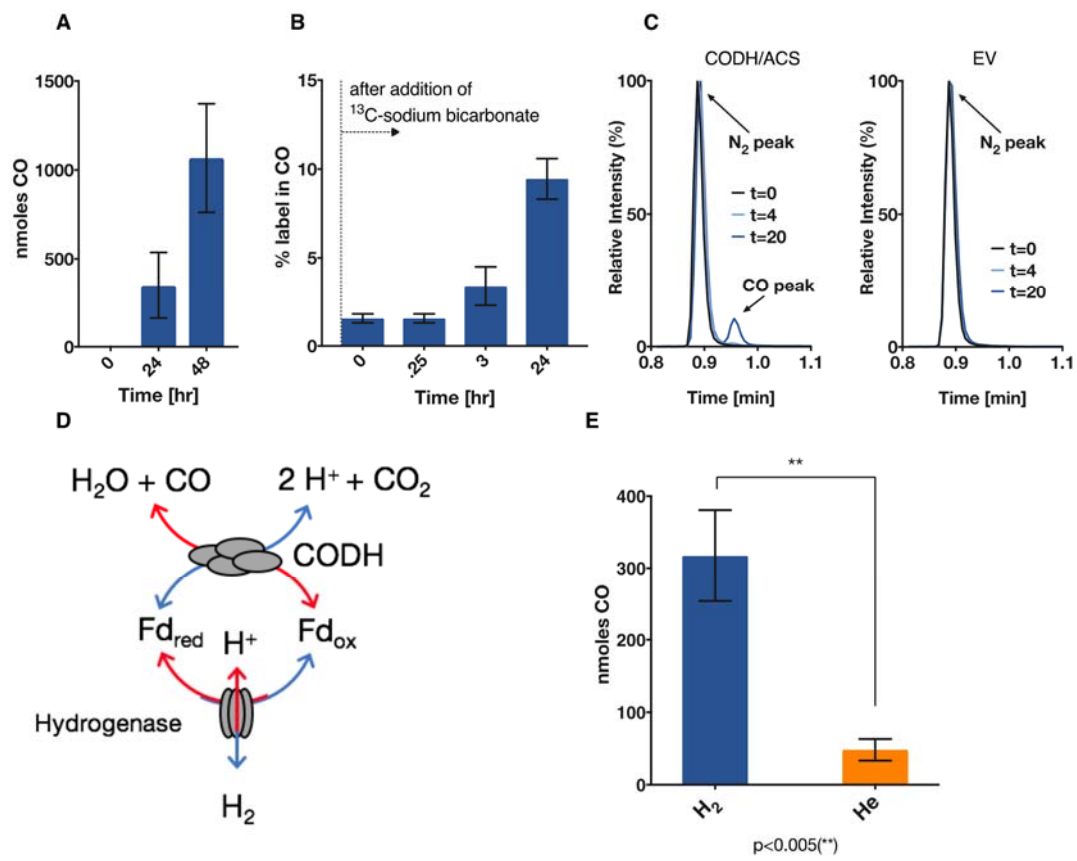
Figure 4.2. *In vivo r*eduction of CO_2 by *C. acetobutylicum* expressing the CODH/ACS complex. CO is a product of CO_2 reduction as shown by ^{13}C-tracing. *C. acetobutylicum* expressing CODH/ACS enzyme grown on glucose in defined medium in sealed serum bottles with 10 psi CO_2 and H_2 (20/80) in the headspace. A) CO concentration in headspace at 0, 12 and 24 hours. Empty vector (EV) control never produced any CO. B) Percent of [13]CO in CO after addition of ^{13}C-bicarbonate to actively growing and CO producing cells. C) GC-MS spectra of headspace gas samples from *C. acetobutylicum* expressing CODH/ACS (left) and empty vector control (right). The CODH/ACS strain exhibits a CO peak at 0.98 minutes after 20 hours. Gas analysis from the control strain (EV) shows only the N_2 peak at 0.9 minutes but no CO peak. D) Schematic depicting the interaction of ferredoxin with the hydrogenase and the CODH. E) *C. acetobutylicum* expressing CODH/ACS enzyme grown on glucose in defined media in sealed serum bottles with 20% CO_2 and H_2 or He balance in the headspace (10 psi). More CO is produced in the presence of hydrogen than in the absence of hydrogen. The amount of CO (in nanomoles) produced per culture after 24 hours was statistically significant (**, $p < 0.005$). Error bars indicate the standard error of at least two biological replicates, and statistical significance was tested with a two-sample t-test.

4.6.3 Externally added H_2 enhances the CODH-catalyzed CO formation from CO_2 reduction.

Here we wanted to further support the logical conclusion that a *C. acetobutylicum* native ferredoxin is involved in the CODH reaction in this host. Hydrogenases of *C. acetobutylicum* utilize a reduced ferredoxin (Fd_{red}) as the electron donor (Papoutsakis 2008). Cells can dispose of excess electrons through the production of H_2 (Figure 4.2 D) or to produce reduced products such as butanol and ethanol (Papoutsakis 1984). Exogenously added H_2 to fermentations of *C. acetobutylicum* has been shown to result in higher concentrations of reduced metabolites (Yerushalmi, Volesky et al. 1985), suggesting a larger internal Fd_{red} pool that can be used to increase the NADH pool and enable the production of more reduced metabolites (Papoutsakis 1984, Meyer and Papoutsakis 1989, Papoutsakis

2008). Furthermore, it has been shown that, during the solventogenic fermentation phase, where the cells produce alcohols, cultures of *C. acetobutylicum* can consume H_2 (Kim and Zeikus 1992), which would produce more Fd_{red} to be used again for alcohol formation through increased NADH concentrations. Based on these data, we hypothesized that in the presence of H_2, the hydrogenase reaction to form H_2 will be operating at reduced rates, thus oxidizing the Fd_{red} (produced by the pyruvate decarboxylation reaction) at reduced rates and resulting in a higher intracellular Fd_{red} pool. This in turn could drive the reduction of CO_2 more efficiently. The *C. acetobutylicum* strain expressing CODH/ACS was tested for CO_2 reduction both in the presence or absence of H_2, where helium (He) was used in place of H_2. Cells were grown in the presence of 20% CO_2 and either 80% H_2 or 80% He. CO formation was measured after 24 hours (Figure 4.2 E). Cells grown in the presence of H_2 produced significantly more ($p<0.005$) CO than the cells grown in the presence of He.

To further pursue the importance of the ferredoxin intracellular pool, we tested the formation of CO under both growing conditions and non-growing (stationary) conditions. Cells were washed and used to inoculate media with glucose to an initial OD at 600nm (OD_{600}) of ~ 0.1 or without glucose to an initial OD_{600} ~ 3. Both conditions were subject to a headspace composition of 20% CO_2 - 80% H_2. Incubation of the cells without glucose failed to produce CO (data not shown). Fd_{red} is produced during glycolysis, namely, by the decarboxylation of pyruvate to acetyl-CoA (Papoutsakis 2008). When glucose is absent, oxidized ferredoxin is not reduced, resulting in a low intracellular Fd_{red} pool. H_2 cannot replenish the Fd_{red} pool in the absence of glycolytic activity. This is likely due to the low cellular energy charge that prevents the maintenance of the cellular membrane potential and ΔpH, which are

87

essential for these complex electron exchange reactions. Taken together, these data further support the conclusion that the recombinant CODH interacts with a native *C. acetobutylicum* ferredoxin as it would in native acetogens.

4.6.4   CO$_2$ is reduced to CO by *C. acetobutylicum* expressing the CODH subunit alone.

The CODH/ACS protein complex in acetogens couples the reduction of CO$_2$ to CO with the subsequent condensation with a methyl group to form acetyl-CoA (Hadj-Saïd, Pandelia et al. 2015). The CO which is generated at the C-cluster of the CODH travels through the internal channel to the ACS subunit and catalytic active site, relying on a tight association between the two subunits. Monomeric CODHs such as those from *Carboxydothermus hydrogenoformans* and *Rodhospirillum rubrum* have been characterized but have only been shown to operate in the energetically favored direction of CO oxidation, and CO$_2$ reduction has not been reported. We pondered whether the *C. carboxidivorans* CODH alone (i.e., without the presence of its cognate ACS partner) could reduce CO$_2$ to CO. To test this possibility, we expressed the CODH subunit alone in *C. acetobutylicum*, and as before, we grew the cells on glucose in the presence of 20% CO$_2$/80% H$_2$ and CO production was monitored using gas chromatography. We also added 50 mM ^{13}C-sodium-bicarbonate to label the CO$_2$ pool resulting in roughly ~20% initial ^{13}C labeling. CO was produced by both the *C. acetobutylicum* strains expressing the CODH only or both the CODH and ACS. (Figure 4.3 A). The ^{13}C-labeling of CO was significantly higher than the natural abundance ($p < 0.0001$) in both the CODH and the CODH/ACS expressing strains compared to the control (Figure 4.3 B). These results are somewhat surprising in that the CODH enzyme is found to be functioning on its own to reduce CO$_2$. In addition,

there seems to be no statistically significant difference between to two strains, indicating the ACS subunit does not play a role in the CO_2 reduction to CO. This is a novel and hitherto unexpected conclusion.
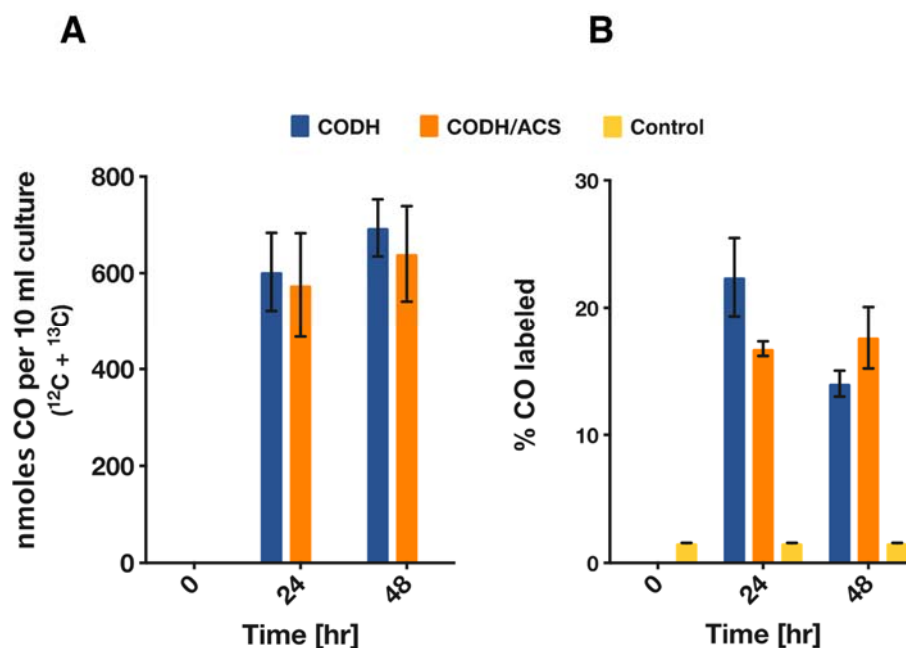
Figure 4.3. *In vivo* reduction of CO_2 by *C. acetobutylicum* expressing the CODH/ACS complex or the CODH enzyme alone**.** Cells of *C. acetobutylicum* expressing the CODH/ACS complex or the CODH enzyme alone were grown on glucose (40 g/L) in defined media in sealed serum bottles with 10 psi CO_2 and H_2 (20/80) in the headspace. 50 mM ^{13}C-bicarbonate was added to the sealed bottles. **A)** Total nanomoles of CO (^{12}CO and ^{13}CO) in each serum bottle (10 ml of liquid culture). **B)** % of ^{13}CO in produced CO. There was no statistically significant difference in either the amount of CO produced or the % of ^{13}C labelling in CO (n=4). Error bars indicate the standard error of four biological replicates.

4.6.5 Reversibility shown in oxidation of CO by *C. acetobutylicum* expressing either the CODH/ACS complex or the CODH subunit alone.

CODH reversibly catalyzes the oxidation of CO to CO_2 in native acetogens. Here, we set out to examine if this is the case when expressed in *C. acetobutylicum* by characterizing the *in vivo* function of the enzyme in the direction of CO oxidation. *C. acetobutylicum* expressing the genes for the CODH/ACS complex or the gene for the CODH enzyme by itself were grown in the presence of 5% ^{13}CO with the balance being helium. Only the two strains expressing the CODH enzyme were able to oxidize CO, whereas the empty vector control was unable to oxidize any CO (Figure 4.4 A). The decrease in ^{13}CO was monitored throughout the fermentation and it was inversely proportional to the increase in $^{13}CO_2$. The increase in $^{13}CO_2$ resulted in higher than natural abundance (~1%) labeling in the CO_2 peak on the chromatogram (Figure 4.4 B). The CO peak on the chromatogram spectrum did not decrease for the empty vector control (data not shown), but did completely disappear for the CODH/ACS strain and the CODH strain after about 72 hours (Figure 4.4 C). These results show the CODH is capable of both CO oxidation and CO_2 reduction.
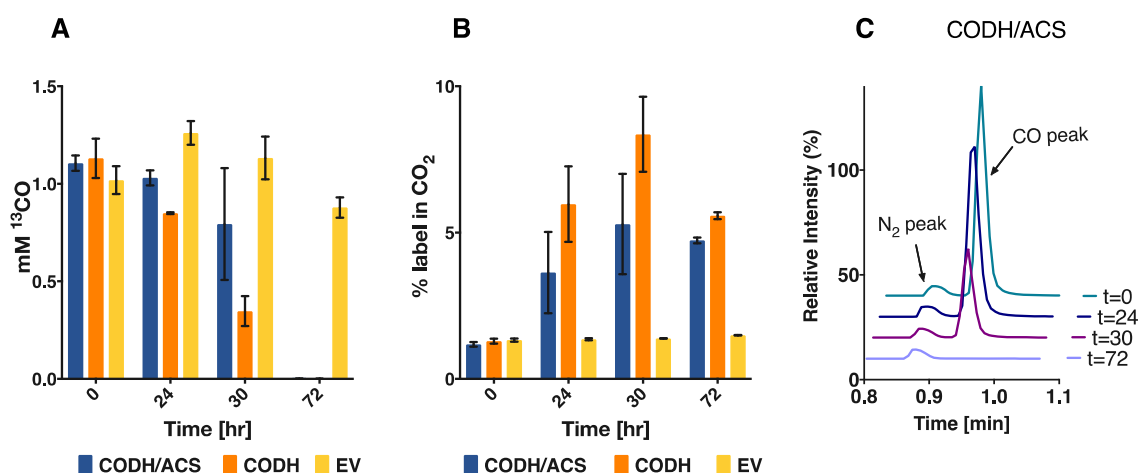
Figure 4.4. *In vivo* CO oxidation by *C. acetobutylicum expressing* either the CODH/ACS complex or the CODH subunit alone. A) *C. acetobutylicum* strains grown on defined medium in the presence of 5% ^{13}CO (balance N_2) in the headspace (5 psi). CO concentration was measured for the CODH/ACS, the CODH and an empty vector strain (n=2). The empty vector control strain did not oxidize CO during the 72 hours of monitoring. B) ^{13}C labeling in CO_2 as a function of time. **C)** GC-MS analysis of the headspace demonstrating CO oxidization by the *C. acetobutylicum* strain expressing CODH/ACS. Error bars indicate the standard error of two biological replicates.

4.6.6 CO concentration affects CO oxidation and metabolite distribution in cultures of *C. acetobutylicum* expressing the CODH subunit.

We then set out to investigate the impact of initial CO concentration on CO oxidation. Because CO is known to affect the growth rate of *C. acetobutylicum* (Kim, Bellows et al. 1984, Datta and Zeikus 1985, Meyer, Papoutsakis et al. 1985, Meyer, Roos et al. 1986), we resorted to a stationary (no growth) experiment with a high initial cell density ($OD_{600} \sim 3.5$) while varying the amount of ^{13}CO (balance was He) in the headspace with 20 psi total pressure. Small amounts of glucose (ca. 5 g/l [30 mM]) were added to maintain low metabolic activity. There were small amounts of metabolites present at the setup; all below 4 mM, except for acetate (ca. 43 mM),

which is used as pH buffer, and ethanol (ca. 49 mM), which is used to dissolve the antibiotic for plasmid maintenance. Cultures were sampled 24 hours after setup. The specific rate of CO_2 formation by the CODH was calculated by the change of $^{13}CO_2$ per min per gram of dry cell weight. As the concentration of CO increased, the rate of CO oxidation decreased (Figure 4.5 A). At higher than 10% ^{13}CO, we observed a drastic decrease in the production of $^{13}CO_2$, indicating inhibition of CO oxidation and thus inhibition of the CODH. At 5% CO, the highest rate of $^{13}CO_2$ formation (which is equal to the rate of ^{13}CO oxidation) was an average of 2.4 μmoles per min per mg of dry cell weight (Figure 4.5 A). Literature values for CO oxidation have been reported as 0.2- 0.4 μmol per min per mg of wet cell weight (Diekert and Thauer 1978). For all CO concentrations, glucose was completely consumed in 24 hours in the cultures of the CODH expressing *C. acetobutylicum*. In contrast, in two cultures of the plasmid control strain at 19% CO, glucose was not utilized, and only small amounts of butyric acid were taken up, thus indicating severe inhibition of cell metabolism at this high CO concentration.

CO inhibition of *C. acetobutylicum* growth derives from the inhibition of the hydrogenase, which contains an active site (H-cluster) containing a novel [4Fe4S] subcluster (Cornish, Gärtner et al. 2011), which can bind CO and inhibit function, similar to the inhibition of hemoglobin by CO. As a result, H_2 formation is severely inhibited or totally abolished (Meyer, Papoutsakis et al. 1985, Meyer, Roos et al. 1986), and cell metabolism, in batch systems, shifts towards metabolites (ethanol, butanol) (Kim, Bellows et al. 1984, Meyer, Papoutsakis et al. 1985) whose formation requires electrons. This is further accompanied by reduced acetone, butyrate and acetate formation. In one report from our lab, where CO was introduced in continuous

culture of *C. acetobutylicum*, lactate and acetoin were also induced by CO gassing (Meyer, Roos et al. 1986). While the changes in metabolite concentrations were low due to low glucose concentrations (29 mM at t = 0; at such low glucose, wild-type *C. acetobutylicum* produces only acids), the patterns of metabolite formation were quite informative (Figure 4.5 B). For all conditions tested, the cells exposed to CO produced less to no acetone and drastically lower butyrate concentrations than cells not exposed to CO (Figure 4.5 B). Acetate was consumed at 14% and 19% CO, whereas acetate was produced at the other conditions tested. Butanol and ethanol formation was enhanced by the presence of CO as previously reported. Lactate and acetoin were produced for all conditions with CO, but virtually none was formed in the absence of CO (Figure 4.5 B). Overall, the changes in metabolite formation due to CO were not predictable or proportional. For example, lactate production increased as CO concentration increased, but butanol and acetoin production remained largely unchanged after an initial increase by the addition of CO. We note that lactate and acetoin production in response to CO presence has been reported only by us for continuous cultures (Meyer, Roos et al. 1986), but not for batch systems. The mechanism by which the inability to produce H_2 alters the cell's biosynthetic machinery to produce metabolites requiring electrons is not well understood. It likely involves the sensing of the altered redox environment (due to accumulation of reduced ferredoxin, NADH and other electron carriers) by the redox sensor Rex, which regulates the expression of several product formation genes and pathways (Wietzke M 2012, Papoutsakis, Wu et al. 2013). As stated above, inhibition of the H_2-producing hydrogenase would increase the Fd_{red} pool and NADH pool derived from Fd_{red}. The cells apparently use two mechanisms to deal with the increased NADH and/or Fd_{red}

pools. First, they use NADH to produce products (butanol, ethanol) that utilize NADH, and suppress the formation of products (acetone, butyrate, acetate) that use less or no NADH (Papoutsakis 1984). They also apparently slow down the production of Fd_{red} by reducing the rate of pyruvate decarboxylation that produces Fd_{red}; instead they direct the carbon flux from the pyruvate pool to acetoin. Lactate production serves both mechanisms: increased NADH utilization by the lactate dehydrogenase, and reduction of Fd_{red} formation by reducing pyruvate decarboxylation. Taken together, these data when compared to the plasmid-control data and prior literature suggest that CODH modulates the response of the cells to CO presence.
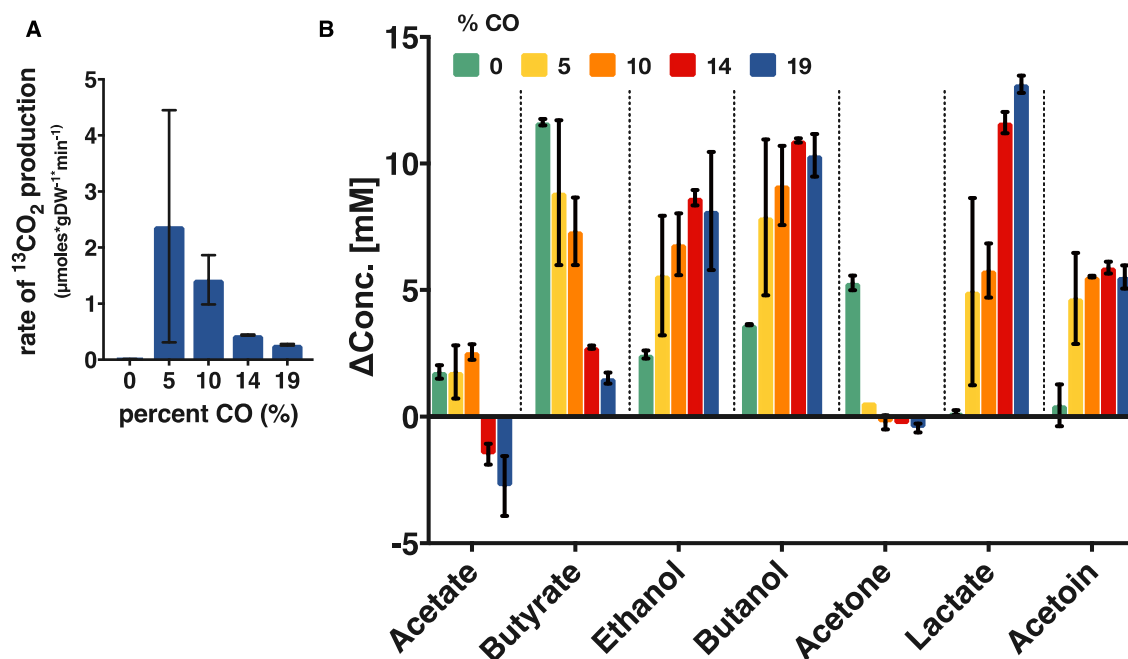
Figure 4.5. CO concentration affects CO oxidation and metabolite distribution. *C. acetobutylicum* expressing the CODH enzyme was grown on defined medium in the presence of varying amounts of ^{13}CO (balance He) in the headspace (20 psi total) during high cell density, low glucose concentration experiments (5 g/L glucose). A) Micromoles of $^{13}CO_2$ formed per gram dry weight of cells (n=2). The large error bar for the experiments with 5% CO is largely due to the difficulty of precisely charging the gas phase with low partial pressures of CO. This combined with the gas mixing and solubility and the biological variability creates the large error bars. B) Metabolite profile (shown as change in metabolite concentration from 0 to 24 hours) of cultures in the presence of varying CO concentrations. The ethanol data have been corrected for the evaporation of ethanol upon charging the culture with gas. The initial ethanol was ca. 49 mM, since ethanol is used to dissolve the antibiotic for plasmid maintenance. Error bars indicate the standard error of two biological replicates.

4.6.7 Nickel enhances the activity of the recombinant CODH expressed in *C. acetobutylicum*.

Nickel is an important element found in the active site of oxygen sensitive, acetogenic CODHs. It had been previously shown that cells of *C. formicoaceticum* grown in the absence of nickel had reduced CODH activity, but adding 1 μM $NiCl_2$ to the medium during growth restored CODH activity (Diekert and Thauer 1980). We assume that this would be the case of CODHs in other acetogens. Given that the intracellular environment of *C. acetobutylicum* is different than that of *C. carboxidivorans*, we wanted to test if nickel had an effect on the activity of the recombinant CODH expressed in *C. acetobutylicum.* To do so, the CODH/ACS expressing strain was grown in the absence of nickel in a defined medium to mid-exponential phase. Cells were concentrated and used to inoculate serum bottles containing varying amounts of nickel. The activity was almost completely absent without nickel present, but CO production increased with increasing nickel concentration (Fig. 6A). This indicates the nickel is inserted *in vivo* into the active site of the CODH expressed in *C. acetobutylicum*, despite the absence of a known Ni-inserting accessory protein. This is pursued further in the next section.

4.6.8 The Ni-inserting accessory protein CooC enhances *in vivo* CODH activity at lower nickel amounts.

The CODH/ACS gene cluster of native acetogens contains two small subunits, CooC and AcsF, which are believed to be involved in active-site maturation, namely they are responsible for nickel insertion (Bender, Pierce et al. 2011). Tests in *Rhodospirillum rubrum*, known to contain a Ni-CODH, bearing CooC mutations required circa 1000 fold higher nickel concentrations to sustain CO-dependent growth and restore wild-type levels of growth on CO (Kerby, Ludden et al. 1997). Our data

(Figure 4.6 A) show that nickel supplementation is sufficient for the assembly of the active, nickel containing C-cluster of the recombinant CODH, thus suggesting that Ni insertion takes place without the presence of a Ni insertase. Nevertheless, we wanted to test the hypothesis that co-expression of the CODH maturation protein CooC (encoded by Ccar_18840) found in the WLP gene cluster of *C. carboxidivorans* would decrease the amount of nickel required for CO production and result in higher CODH activity. To this effect, we constructed a plasmid bearing the CODH/ACS genes followed by the genes coding for the CooC maturation protein, and repeated the experiment of the previous section with varying Ni concentrations in the media. CooC co-expression did not increase CO production significantly over the range of nickel tested. However, in the absence of added nickel, the accessory protein increased the production of CO, even though the significance was at the 90% confidence level (n=4, $p < 0.1$) (Figure 4.6 B). This could indicate that the accessory protein can facilitate nickel insertion into the active site at trace (residual) Ni concentrations in the media (from impurities of salts used in media preparation) and therefore requires less added Ni for higher activity.
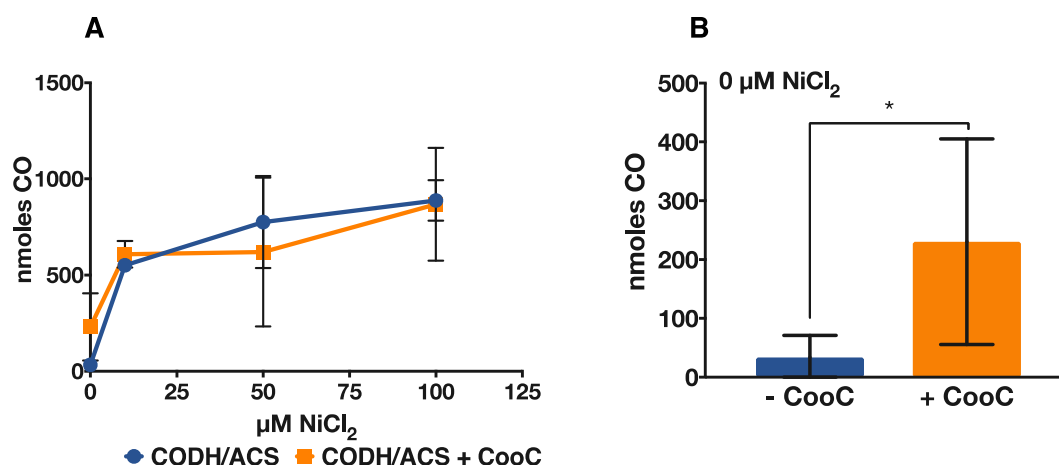
Figure 4.6. Impact of added Ni on CO production by *C. acetobutylicum* expressing the CODH/ACS complex without or with co-expression of the Ni-inserting CooC protein. A) CO concentration was measured in the headspace for concentrated *C. acetobutylicum* expressing the CODH/ACS complex alone (blue circles/line) or with the accessory protein CooC (orange squares/line) after 24 hours of growth in defined medium with varying amounts of Ni. B) Total CO produced in the absence of nickel for the CODH/ACS expressing strain (blue) and the CODH/ACS+CooC expressing strain (orange). There is a significant difference at the 90% confidence level between the two strains ($p < 0.1$, n=4), indicating that the accessory protein can facilitate nickel insertion into the active site in the trace of trace levels (residual) of Ni.

4.6.9   An *in vivo* assay for the ACS exchange activity?

The ACS protein has been studied extensively (Loke, Tan et al. 2002 , Tan, Loke et al. 2005 , Tan and Lindahl 2008) and its structure and active-site have been determined (Doukov, Iverson et al. 2002). As discussed above, ACS activity is tested *in vitro* by the carbon exchange reaction between CO and the carbonyl group of acetyl-CoA, using ^{14}C-radioactive tracers. This reaction has been reported only for purified ACS, and has been shown to be feasible with the ACS subunit alone (Tan, Loke et al. 2005, Tan and Lindahl 2008). We set out to investigate if this exchange

activity could be explored in the *in vivo* setting using ^{13}C-tracers and whole cell catalysts. In native acetogens, CO release by the cells has not been reported. We hypothesized that ^{13}C-labeling of the acetate carbonyl group could label the carbonyl group of the intracellular acetyl-CoA pool. The ACS enzyme could then bind the acetyl-CoA and exchange the carbon from CO with the carbon from the carbonyl group of acetyl-CoA. If functioning as in *in vitro* experiments, ACS could bind to ^{13}C-acetyl-CoA, and exchange the ^{13}C with the ^{12}C from CO. An increase in the percentage of labeling of CO could then be observed. To test this, *C. acetobutylicum* strains expressing either the CODH/ACS, or the CODH or the ACS alone were grown in the presence of Ni in a defined medium with the addition of 30 mM sodium [1-^{13}C]acetate. The strain expressing the CODH/ACS enzymes showed an increase in the labeling of CO, but so did the strain containing only the CODH, indicating the increase was not due to the exchange reaction of the ACS. We concluded that through the production of acetone, some of the label from acetate is released as CO_2, which resulted in ~3% labeling in CO_2. Conversion of labeled CO_2 into labeled CO due to the activity of the CODH could explain the slightly higher labeling in CO in those strains containing the CODH (Figure S4.1). To confirm this, we grew the *C. acetobutylicum* strain containing the ACS protein alone (incapable of reducing the partially labeled CO_2 to CO, but still capable of the exchange reaction, if such reaction can take place *in vivo*), and showed that this strain did not exhibit an increase in the labeling in CO, which showed the labeling of the ^{13}C natural abundance (~1 %). Since the active site of the ACS, the A-cluster, also requires a special Ni-containing center, we set out to investigate the necessity of a Ni-accessory protein, AcsF, found in the WLP gene cluster (Ccar_18805). Recently, the Ni-insertion accessory protein AcsF

from *Carboxydothermus hydrogenoformans* was shown to be necessary for the ACS active site to fully develop (Gregg, Goetzl et al. 2016). The *C. acetobutylicum* strain expressing the ACS and the AcsF from *C. carboxidivorans* did not increase the labeling in CO either. Last, a positive control consisting of *C. carboxidivorans* cells used under the same experimental set-up did not lead to an increase in labeling of CO. Taken together, the data from these experiments suggest that the *in vitro* exchange activity may not function under *in vivo* conditions, at least for the strains of this study.

4.7 Discussion

This is the first report of a recombinant, engineered system capable of reducing CO_2 utilizing an acetogenic CODH/ACS expressed in a non-acetogenic host. The CODH/ACS has been studied in several acetogens such as *M. thermoacetica, C. formicoaceticum,* and *Acetobacterium woodii,* as well as *Desulfovibrio vulgaris* and *Carboxydothermus hydrogenoformans* (Diekert and Thauer 1980, Drake, Hu et al. 1980, Wang, Ragsdale et al. 2013, Bertsch and Müller 2015, Hadj-Saïd, Pandelia et al. 2015)*.* In these organisms, a reduced, anaerobic environment provides the conditions for CO_2 fixation (Müller 2003). The CODH/ACS enzyme has been expressed in a non-native host (*E. coli*) before, however, the enzyme was shown to be active only in the direction of CO oxidation *in vitro* (Loke, Bennett et al. 2000). Never before has this enzyme been shown to function *in vivo* in a non-native host. To reduce CO_2, a suitable, low-potential electron carrier is required. The CO_2/CO redox couple has a standard redox potential of -520 mV (standard redox potential calculated at 1 M for all reactants at pH 7 by (Schuchmann and Müller 2014)), and only reduced ferredoxin has a low enough redox potential to provide electrons for this reaction. The CODH/ACS enzymes of *M. thermoacetica* and *A. woodii* have been shown to interact *in vitro* with

a ferredoxin derived from *C. pasteurianum* (Shanmugasundaram and Wood 1992, Schuchmann and Müller 2013). *C. acetobutylicum* contains several native ferredoxins, which serve as electron carriers in several reactions, and notably in conserving high energy electrons from the pyruvate decarboxylation reaction to form acetyl-CoA as well the reactions leading to butyryl-CoA synthesis. Reduced ferredoxin(s) serve(s) as electron donors for H_2 formation but also NADH generation used for alcohol production. Here, our data support the hypothesis that a native *C. acetobutylicum* Fd_{red} apparently interacts with the heterologous CODH/ACS. Indeed, we showed that CO_2 reduction was effected by the H_2 pressure, and exhibited dependence on growth-associated glucose utilization. Since ferredoxin is produced in the cells during active glycolysis from the conversion of pyruvate to acetyl-CoA or the formation of butyryl-CoA, growing cells contain higher concentrations of Fd_{red}.

Surprisingly, CO_2 reduction did not depend on the presence of the ACS protein subunit of the CODH/ACS enzyme complex, and functionality in both oxidation and reduction directions was enabled by the CODH subunit alone. Although the function of the ACS subunit has been studied *in vitro* (Tan and Lindahl 2008) and *in vivo* (Liew, Henstra et al. 2016) before, the CODH subunit from the bifunctional CODH/ACS complex has not been studied by itself before, and it was not known if it can reduce CO_2 to CO on its own.

CO oxidation by an engineered *C. acetobutylicum* strain is the first step towards growth on CO, which could be both a carbon and electron source. CO is quite toxic and only few anaerobes grow in the presence of 100% (v/v) CO (Moersdorf, Frunzke et al. 1992). Previous studies have engineered the archaeon *Pyrococcus furiosus* to heterologously express a CODH operon from *Thermococcus onnurineus*,

making the engineered organism capable of CO oxidation and able to generate energy via the generation of an ion gradient using the electrons from CO oxidation (Schut, Lipscomb et al. 2016). Here, we have shown that at gaseous concentrations of 5% (v/v) CO, the engineered *C. acetobutylicum* strain is capable of complete CO oxidation using the acetogenic, bifunctional CODH/ACS. Developing tolerance to higher amounts of CO by engineering a superior CODH exhibiting higher activity could provide a source of additional electrons from CO and thereby alter the fermentation behavior. Previous studies of heterologous CODH expression reported that incubation with nickel after purification was necessary to restore activity (Loke, Bennett et al. 2000 , Maynard and Lindahl 2001 , Loke, Tan et al. 2002), and that chelating agents such as 1,10-phenanthroline abolish CODH activity, indicating the need for Ni in the active site (Shin and Lindahl 1992). Here, we found that the culture medium required nickel supplementation (ca. 50-100 µM) for maximizing CODH activity (Fig. 6). Many CODH loci code for a nickel-insertion accessory protein, which is believed to facilitate the insertion of nickel into the CODH active site (Gregg, Goetzl et al. 2016). Here, expression of the nickel-accessory protein CooC from *C. carboxidivorans* did increase activity, but only in the in the case of no nickel supplementation. Interestingly, the highest activity achieved required nickel at much higher concentrations than what is required in media of acetogens (~100 µM versus 1.2 µM in DSMZ141 medium). This might suggest that Ni-insertion proteins are essential for CODH activity in low Ni media.

As stated, in all studies examining the ACS activity, highly purified amounts were needed to achieve an carbon exchange reaction between CO and the carbonyl-carbon from acetyl-CoA (Ragsdale, Clark et al. 1983, Loke, Bennett et al. 2000,

Svetlitchnyi, Dobbek et al. 2004, Gregg, Goetzl et al. 2016). The *in vitro* ACS activity based on this "carbon exchange reaction" is typically much slower than the *in vivo* reaction that supports the growth of acetogens. This could indicate that the *in vitro* reaction uses a different mechanism than the *in vivo* reaction. The *in vitro* experiment requires hyper-anoxic conditions, extensive ACS purification, and high protein concentrations. Furthermore, it is necessary to insert nickel through *in vitro* incubation of the purified enzyme with nickel chloride to restore activity and achieve the nickel insertion into the active site. Recently, Gregg *et al.* showed the necessity of a nickel accessory protein, AcsF, to facilitate the insertion of nickel into the active site in *Carboxydothermus hydrogenoformans* (Gregg, Goetzl et al. 2016). Even though we tested our system with the additional expression of the AcsF accessory protein, the *in vivo* carbon exchange reaction could not be detected. The native acetogen *C. carboxidivorans* was also incapable of demonstrating the exchange activity *in vivo*, but this could be due the presence of a functional WLP that prevents CO accumulation.

The tetrameric CODH/ACS plays an important role as the acetyl-CoA synthase in the WLP, in which the reaction of CO_2 reduction is coupled with the formation of acetyl-CoA from a methyl-group and CO. The first step of CO_2 reduction is an important step for achieving synthetic CO_2 fixation in an organism that does not fix CO_2. We have shown that the reduction of CO_2 is feasible without any additional codon optimization or protein engineering. The enzymes were expressed and active in a closely related *Clostridium* host. *C. acetobutylicum* presents a great platform organism due to its native production of butanol and acetone, but also because of the availability of an extensive set of metabolic engineering tools (Papoutsakis 2008,

Tracy, Jones et al. 2012). Here we have shown that the organism can be engineered to reduce CO_2. Further engineering efforts towards the reduction and incorporation of CO_2 holds great promise to achieve synthetic CO_2 fixation in *C. acetobutylicum* using a functional WLP.

4.8   Materials and Methods

Chemicals. Stable isotope gases and all chemicals were purchased from Sigma Aldrich.

Strains, culture conditions and medium.

C. acetobutylicum ATCC824 was grown anaerobically at 37°C in either 2xYTG medium (16 g/liter Bacto tryptone, 10 g/liter yeast extract, 4 g/liter NaCl, and 5 g/liter glucose; pH 5.8) or defined clostridial growth medium (dCGM; 0.75 g/liter K_2HPO_4, 0.75 g/liter KH_2PO_4, 0.7 g/liter $MgSO_4 \cdot 7H_2O$, 0.01 g/liter $MnSO_4 \cdot H_2O$, 0.01 g/liter $FeSO_4 \cdot 7H_2O$, 1 g/liter NaCl, 0.004 g/liter p-aminobenzoic acid, 10 µg/L biotin, 3.3 g/liter $C_2H_3O_2NH_4$ and 40 g/liter glucose; pH 6.8). Recombinant strains were grown on solid 2xYTG media supplemented with 40 µg/ml erythromycin, and single colonies were picked and grown anaerobically in 10ml dCGM as pre-culture. *In vivo* experiments were conducted as described below. Transformations into *C. acetobutylicum* were performed as previously described (Mermelstein, Welker et al. 1992). All molecular cloning steps were completed in *E. coli*, and strains were grown aerobically at 37°C and 220 rpm in liquid LB medium with shaking at 220 rpm, or on LB with 1.5% agar supplemented with 50 µg/ml ampicillin. *C. carboxidivorans* DSM 15243 was grown anaerobically in American Type Culture Collection (ATCC) medium 1754 with 10 g/l of glucose at 37°C.

Vector and strain construction.

All plasmid vectors were constructed in either *E. coli* (NEB Turbo) or *E. coli* (NEB 5-alpha). All primers are listed in Table 4.1. Plasmid vector p94_CODH/ACS was designed for expression of the CODH/ACS enzyme complex in *C. acetobutylicum*. It contained both the *codh* (Ccar_18845) and the *acs* (Ccar_18785) genes from *C. carboxidivorans* in an operon arrangement under the control of the strong P_{ptb} promoter native to *C. acetobutylicum* (Tummala, Welker et al. 1999). The *codh* gene was amplified from *C. carboxidivorans* gDNA using primers CODH_F and CODH_R. Similarly, the *acs* gene was amplified from the same gDNA using primers ACS_F and ACS_R. Vector pSOS94_MCS was digested with BamHI, and the CODH and *acs* genes were cloned into the vector using Gibson Assembly (New England Biolabs), resulting in p94_CODH/ACS. The His-tag was added using p94_CODH/ACS digested with SbfI and KspI and primers p94_sbfI_f and CODH/ACS_his_R. The CODH subunit by itself was constructed using primers that flanked the *acs* gene to be deleted (CODHonly_f & CODHonly_r) using p94_CODH/ACS as the template. The Q5® Site-Directed Mutagenesis Kit from NEB Biolabs was used for easy plasmid isolation. The resulting vector (p94_CODH) has the same promoter configuration as p94_CODH/ACS (described above). The strain containing the *codh*, *cooC* (Ccar_18840), and *acs* genes was constructed by amplifying two fragments from *C. carboxidivorans* gDNA using primers p94_CODH/CooC_f&p94_CODH/CooC _r and p94_ACS_f&p94_ACS_r. The pSOS94_MCS vector was digested with BamHI and XbaI and the three fragments were assembled using Gibson Assembly (New England Biolabs). For the strain containing the *acs* gene alone, the gene was amplified from *C. carboxidivorans* gDNA

using primers (ACS_BamHI_f and ACS_XbaI_r) and inserted into the digested

pSOS95_MCS vector (BamHI and XbaI) using Gibson Assembly (New England

Biolabs). The resulting vector p95_ACS contained the *acs* gene under the thiolase

promoter (P_{thl}). The gene for the AcsF accessory protein (Ccar_18805) was amplified

using primers p95_AcsF_f and p95_AcsF_r using *C. carboxidivorans* gDNA as

template, and ligated into the digested p95_ACS (digested with SphI and MluI) using

Gibson Assembly (New England Biolabs).

Vector transformations. Vectors were transformed into *E. coli* (NEB Turbo)

and isolated using the Qiaprep Spin Kit (Qiagen). Before transformation into *C.*

acetobutylicum, vectors were transformed into electrocompetent *E. coli*

ER2275(pAN3) (Al-Hinai, Fast et al. 2012) for the *in vivo* methylation by the Φ3T I

methyl transferase contained on the pAN3 vector as described (Mermelstein and

Papoutsakis 1993). Methylated vectors were isolated using the Qiaprep Spin Kit

(Qiagen) and transformed into *C. acetobutylicum* ATCC824 using a well-established

protocol (Mermelstein, Welker et al. 1992).

Culture conditions and harvesting of recombinant *C. acetobutylicum*.

Recombinant *C. acetobutylicum* strain expressing the CODH/ACS enzyme complex

were grown in 2xYTG to an OD_{600} around 0.7. The cultures were harvested by

centrifugation at 4°C for 10 min at 7000xg, and cell pellets were frozen at -82°C. Cells

of the *C. acetobutylicum* empty vector control strain and wild-type *C. carboxidivorans*

were collected in the same manner.

Native His-tag purification. The his-tagged proteins were purified with a Ni-

NTA spin column kit (Qiagen) following the protocol for purification under native

conditions. First, the frozen cell pellets were thawed, washed once, and re-suspended

in lysis buffer followed by sonication for 5 min at 50% power with intervals of 15 s sonication followed by 15 s of rest using a Fisher Scientific Sonic Dismembrator and a cup horn. The samples were clarified by centrifugation for 10 min at 16000 rpm and 4°C, and the remainder of the protocol was followed per manufacturer recommendations. Eluates were quantified using a protein assay (Bio-Rad RC DC™ Protein Assay).

Sodium dodecyl sulfate polyacrylamide gel electrophoresis (SDS-PAGE).
The cell pellets were re-suspended in 500 μl of 100 mM Tris-HCl, pH 7.0, and sonicated as described above. The samples were clarified by centrifugation for 10 min at 16000 rpm and 4°C. Supernatants were collected and the cell debris was re-suspended in the same amount of Tris-HCl buffer. Samples were mixed in a 1:5 dilution with 5x loading buffer (0.2 M Tris-HCl (pH 6.8), 10% SDS, 0.05% bromophenol blue, 50% glycerol) and boiled at 95°C for 10 min. Aliquots of 30-50 μl were loaded onto an SDS-PAGE gel (Genscript ExpressPlus, 4-20% gradient) and proteins were separated at 120V for 2 hours. The gels were either stained with Coomassie blue or transferred onto 0.2 μm nitrocellulose membranes (Bio-Rad) using the Bio-Rad mini-Trans Blot®. Purified polyclonal antibodies against the CODH and ACS subunit were custom produced by ProteinTech (Rosemont, IL) and obtained from rabbit serum. The CODH subunit was raised against the peptide sequence PEVVDILTNKMEDWVGAKFF and the ACS subunit against the peptide sequence of VVAFLEEKGHPALTMDPIM. Polyclonal antibodies were used at a 1:10000 dilution. An AP colorimetric kit (Bio-Rad) was used to visualize the bands on the Western blot.

Non-denaturing PAGE. Cell pellets were re-suspended and sonicated as above except that the samples were mixed in a 1:5 dilution with 5x non-denaturing loading buffer and loaded onto an PAGE gel (Genscript ExpressPlus, 4-20% gradient) following the manufacturer's protocol for native gels. All subsequent steps, including Western blotting were followed as described earlier. The tetrameric band was visualized on the Western blot using 6x-His-Tag Monoclonal Antibody (Invitrogen) and Alexa Fluor® 647 anti-mouse on a Typhoon™ FLA 9000 laser scanner.

Gas chromatography and mass spectrometry (GC-MS). All gas composition measurements were done with a Shimadzu QP-2010 Ultra gas chromatograph-mass spectrometer. Headspace samples of 50 μl were manually collected and injected using an airtight syringe. Gas separation was performed on a Carboxen®-1006 PLOT column (30 m × 0.32 mm, df of 15 μm, Supelco) with injector temperature of 150°C, split ratio of 5, and carrier gas flow of 15.4 psi He (~3ml/min). The oven temperature was initially held at 30°C for 2.5 min, with ramping at 40°C/min to 120°C. CO separated from N_2 on the column around 0.9 minutes. The mass spectrometer was set as a scan speed of ~450 and scanning from 4.00 to 60.00 m/z. Additional single ion monitoring (SIM) was performed for N_2 (28.00 and 29) and CO_2 (44.00 and 45.00).

Detection of metabolites. High-performance liquid chromatography was used to measure metabolite concentrations in fermentation media. Metabolites were detected using an Agilent HPLC instrument with a Bio-Rad Aminex HPX 87H column using a 5 mM H_2SO_4 mobile phase and a flow rate of 0.5 ml/min (Jones, Fast et al. 2016).

CO₂ reduction using growing cells. *C. acetobutylicum* cells expressing either the CODH/ACS complex or CODH as well as empty vector control were grown to mid-exponential phase and collected by centrifugation. Cell pellets were re-suspended in fresh dCGM with 40 g/L glucose and 200 µM $NiCl_2$. The final OD_{600} of the cultures was 0.1. 10 ml of the cell suspension was added to 26 ml serum bottles (Wheaton®) and sealed with aluminum crimp caps. The headspace was pressurized to ~10 psig using a 20/80 mixture of CO_2/H_2. The headspace was monitored with GC/MS as previously described. For the Ni experiments, cells were grown in absence of Ni to mid-exponential phase and collected by centrifugation. The cells were resuspended in fresh media (dCGM with 40 g/L glucose) and various amounts of Ni were added. 10 ml were transferred and grown in 110 ml serum bottles (Wheaton®). The headspace was monitored using GC-MS.

CO oxidation using growing cells. All experiments were performed in 26 ml serum bottles (Wheaton®). *C. acetobutylicum* cells expressing either the CODH/ACS complex or CODH as well as empty vector control were grown to mid-exponential phase and collected by centrifugation. Cell pellets were re-suspended in fresh dCGM with 40 g/L glucose. 200 µM $NiCl_2$ and 5 ml were dispensed into the bottles secured with a thick butyl rubber stopper and crimped with aluminum seals. The headspace was pressurized to 3 psig using a 20/80 mixture of CO_2/H_2. 100% ^{13}CO was added into the headspace via a syringe. The headspace was monitored using GC. Metabolites were detected using HPLC.

CO oxidation using resting cells. All experiments were performed in 26 ml serum bottles (Wheaton®). *C. acetobutylicum* cells expressing the CODH as well as empty vector control were grown to mid-exponential phase and collected by

centrifugation. Cell pellets were concentrated in fresh dCGM with 5 g/L glucose supplemented with 200 mM $NiCl_2$ to an OD of ~3.5. 5 ml of cell suspensions were dispensed into 26 ml bottles secured with a thick butyl rubber stopper and crimped with aluminum seals. The headspace was pressurized with varying amounts of ^{13}CO (the balance was He) to a total pressure of 20 psig. The headspace was monitored using GC. Metabolites were detected using HPLC.

ACS exchange activity. All experiments were performed in 26 ml serum bottles (Wheaton®). *C. acetobutylicum* cells expressing either the CODH/ACS complex or CODH as well as empty vector control were grown to mid-exponential phase and collected by centrifugation. Cell pellets were re-suspended in fresh dCGM prepared with ^{13}C-sodium acetate and 40 g/L glucose and 200 µM $NiCl_2$. 5 ml were dispensed into each bottle and secured with a thick butyl rubber stopper and crimped with aluminum seals. The headspace was pressurized to 3 psig using a 20/80 mixture of CO_2/H_2. A small amount (1 ml) of 100% CO was added into the headspace. The headspace was monitored using GC for the increase in the ^{13}CO peak using a SIM for 28.00 and 29.00.

Table 4.1. Primers for construction of strains used in this work.

Primer	Sequence (5' --> 3')
CODH_F	tcatttaacatagataattggatccGTAATTCAGCAAGGAGGG
CODH_R	atttatataaaaTTTATATTCCTAATTTTTTACGTTTTTCATTG
ACS_F	taggaatataaaTTTTATATAAATTTTAATTTTAGGGAGGG
ACS_R	gcggattctagattggATTACATTATTGGATCCATAGTTAATG
CODH/ACS_his_R	accgcggattctagattggattaatgatgatgatgatgatgCATTATTGGATCCATAGT
p94_sbfI_f	AAAGCTCCTGCAGGTCGACTGTGGATGG
CODHonly_f	GTAAAAGAGATTGTTTCTAGCTC
CODHonly_r	TAAAATTTATATTCCTAATTTTTTACGTTTTTC

ACS_BamHI_f	ggtttatctgttaccccgtaggatccTAGGGAGGGGCAAAAAAA
ACS_XbaI_r	gatgcatgctaccgcggattctagaTGTCGTATTATAAGTTTTATTACATTATTG
p95_AcsF_f	ctagaatccgcggtagcatgcTGCATGACAATAGGAGGAG
p95_AcsF_r	atcattaagtggcgcctttacgcgtAGGAAGAACACTTTCTCC
p94_CODH/CooC_f	gttaatcatttaacatagataattggatccAGGAGGGAATTTATTAAAATGG
p94_CODH/CooC _r	gttaatcatttaacatagataattggatccAGGAGGGAATTTATTAAAATGG
p94_ACS_f	gggggtattttaaAGGGAGGGGCAAAAAAATG
p94_ACS_r	gggggtattttaaAGGGAGGGGCAAAAAAATG

4.9 Acknowledgements

4.10 Supplemental: The Effect of Hydrogen on CO Production in C. acetobutylicum Heterologously Expressing the Carbon Monoxide Dehydrogenase from *C. carboxidivorans*

4.10.1 Abstract

Hydrogen has been found to influence the metabolite profile of *C. acetobutylicum*, and more recently, has shown to increase the production of CO from CO_2 utilizing a heterologously expressed carbon monoxide dehydrogenase from *C. carboxidivorans* in the of *C. acetobutylicum* host. Previous experiments did not set out to characterize the effect of hydrogen production in the presence of hydrogen, and did not evaluate the change in metabolism of the engineered strains. Here, we set out to compare the strain expressing the CODH/ACS complex and the nickel insertase accessory protein to the control strain in terms of hydrogen generation in the presence or absence of hydrogen. Interestingly, the control strain in the presence and absence of

hydrogen produced the same amount of hydrogen (total change in hydrogen). The control strain in the presence of initial hydrogen therefore reached higher partial pressures of hydrogen. The CODH strain produced more hydrogen (total change in hydrogen) in the presence of hydrogen than in the absence of hydrogen. In the absence of hydrogen, the change in hydrogen was lower than the two control strains.

As in our previous experiments, more CO is produced in the presence of hydrogen. The total amounts of butanol or acetone produced were not changed by the expression of the CODH/ACS enzyme or by the presence of hydrogen. There was, however, a difference in glucose consumption. The control in the presence of hydrogen consumed only 21 g/l glucose, whereas the control in the presence of helium consumed 30 g/L glucose.

Because of the difference in glucose consumption, the total carbon yield of butanol was higher for the strain expressing the CODH/ACS enzyme in the presence of hydrogen than for the control strain. The difference was significant ($p<0.005$). The strain expressing the CODH/ACS enzyme directed 0.31 mol/mol glucose towards butanol, the control strain only 0.27 mol/mol. Expression of the CODH/ACS complex together with the nickel insertase in the absence of hydrogen did not have any effect on the butanol carbon yield. By dividing the product by the amount of glucose consumed (Cmol/Cmol) the direction of carbon flow becomes more apparent.

4.10.2 Introduction

Hydrogenases in *C. acetobutylicum* are part of the complex regulation of redox potential by providing the cells with a way to dispose of extra electrons (Gray and Gest 1965). During anaerobic fermentation of carbohydrates, the oxidation of substrates result in the accumulation of NAD(P)H or reduced ferredoxin which is

utilized by the cells for the formation of reduced products. Any electrons not utilized for metabolites are used by the hydrogenase(s) to form H_2 thus preventing the accumulation of electrons. Two [FeFe]-hydrogenases are found within the genome of *C. acetobutylicum*, HydA1 (gene CAC0028, also known as HydA) and HydA2 (gene CAC3230, also known as HydB). There also exists a nickel iron [NiFe]-hydrogenase (HupSL), which unlike the other two, is found on the pSOL1 megaplasmid (encoded by CA_P0141-CA_P0142) (Demuez, Cournac et al. 2007). Roos, McLaughlin and Papoutsakis have measured hydrogen activity, and found that hydrogen production slowed down at the onset of solvent production, but that in acid only producing fermentations, hydrogen production peaked at the same time as CO_2 production (Roos, McLaughlin et al. 1985). The authors calculated the ratio of CO_2/H_2 and found it to be less than 1 for cultures producing solvents (Papoutsakis 1984, Roos, McLaughlin et al. 1985). Demuez et al. characterized the HydA1 gene of *C. acetobutylicum* through *in vitro* characterization of the redox partners. The authors identified the ferredoxin encoded by CA_C0303 to play a major role in this hydrogenase (Demuez, Cournac et al. 2007). Activity measurements of the purified hydrogenase (HydA) indicated high catalytic efficiencies for both H_2 uptake and H_2 evolution (Demuez, Cournac et al. 2007). However, to our knowledge, *in vivo* hydrogen uptake has not been reported. Hydrogen evolution has been reported to be highest during the early stages of fermentation (acidogenenesis) when cells are producing mainly acetate and butyrate, and slows down towards later stages (solventogenesis) in which the electron flow is directed more towards the production of reduced products such as butanol and ethanol (Papoutsakis 1984, Roos, McLaughlin et al. 1985, Kim and Zeikus 1992). By testing the hydrogen evolution and uptake rates of acidogenic and solventogenic cultures,

Kim and Zeikus hypothesized that two hydrogenases are utilized during each stage, and that they appear to utilize different electron carriers (ferredoxin during acidogenesis, unknown carrier during solventogenesis). They only observed this by noticing that the solventogenic culture had a higher hydrogenase activity coupled with neutral red than the acidogenic culture (Kim and Zeikus 1992). However, later Yoo et al. found that only one hydrogenase, *hydA*, is expressed during fermentation, which was confirmed through transcriptomics and proteomics. The expression was highest during acidogenesis and expression was decreased 3-fold during solventogenic conditions. The *hydB* or *HupSL* were not found to be expressed and no protein was detected throughout the fermentation (Yoo, Bestel-Corre et al. 2015). The authors did note that the expression of the ferredoxin protein partner (*fdx1* , CA_C0303) was reduced during alcohologenic culutres, and another potential redox partner (CA_C3486), which encodes a multimeric flavodoxin was upregulated 6-fold (Yoo, Bestel-Corre et al. 2015). In comparison, an earlier DNA-microarray study also found that the *hydA* gene was expressed highest in the beginning of fermentation, and expression was decrease 4-fold later in the fermentation. However, the authors did find the *HupSL* gene to be upregulated during late stages of fermentation (Jones, Paredes et al. 2008). Besides these findings, there have been very few reports dealing with the measurements of hydrogenases in *C. acetobutylicum*.

Because of the complex interplay of the hydrogenases and the acid and solvent production in *C. acetobutylicum*, researchers have focused on inhibiting, or knocking out hydrogenases to increase the production of reduced metabolites or overexpressing hydrogenases for the increased production of hydrogen. Besides modulating hydrogenase activity with increased partial pressure of hydrogen or the addition of

various electron carriers (Yerushalmi, Volesky et al. 1985, Kim and Zeikus 1992), CO has also been investigated as a potential modulator/inhibitor of hydrogenase activity (Datta and Zeikus 1985, Meyer, Papoutsakis et al. 1985, Meyer, Roos et al. 1986). Klein et al. overexpressed two different clostridial hydrogenases in *C. acetobutylicum* but showed no increase in hydrogen production compared to wild-type, indicating that there is no bottleneck in terms of sufficient hydA activity (Klein, Ansorge-Schumacher et al. 2010). Jang et al. developed a high butyric acid producing strain by knocking out HydA1 (Jang, Im et al. 2014). However, others have attempted to knock out this gene but have been unable to achieve it (Cooksley, Zhang et al. 2012). Jan *et al.* argue that the HydA1 KO was achieved in a mutant strain (pta-buk-ctfB-adhE1 deficient) rather than in WT. Our lab has been unable to obtain a WT HydA1 mutant either (personal communication).

Throughout all these experiments, it has become clear that the hydrogenases of *C. acetobutylicum* are important for regulation of metabolites, but still more research needs to be done to elucidate the mechanisms of H_2 production and its influence on the metabolic profile.

4.10.3 Presence of Hydrogen Increases CO Production

We had previously shown that an increase in H_2 partial pressure in the gas phase of *C. acetobutylicum* heterologously expressing the *C. carboxidivorans* CODH leads to increased CO formation. We presumed the reason for this to be the increase in the internal reduced ferredoxin pool, leading to an increase in the reduction of CO_2 to CO. To further investigate this phenomenon, we interrogated H_2 production and consumption throughout the experiment. In addition, a richer, more commonly used medium (CGM) was used to characterize the typical fermentation behavior of *C.*

acetobutylicum when expressing the CODH in the presence or absence of H_2. We tested *C. acetobutylicum* expressing the CODH/ACS complex along with a nickel-insertion protein that had previously shown to slightly enhance activity without nickel supplementation. All genes were present as mRNA (Figure 4.8). The additional gene at the end of the CODH/ACS operon did not change expression of the *acsA* or *acsB* gene (Figure 4.7), so we continued all experiments utilizing the three-gene plasmid. Pre-cultures grown to mid-exponential phase were subjected to a headspace of either 80% He or H_2, the balance being CO_2. Fermentations were monitored for CO, CO_2, and H_2 partial pressures using GC-MS. Liquid samples were drawn for metabolite analysis using HPLC.
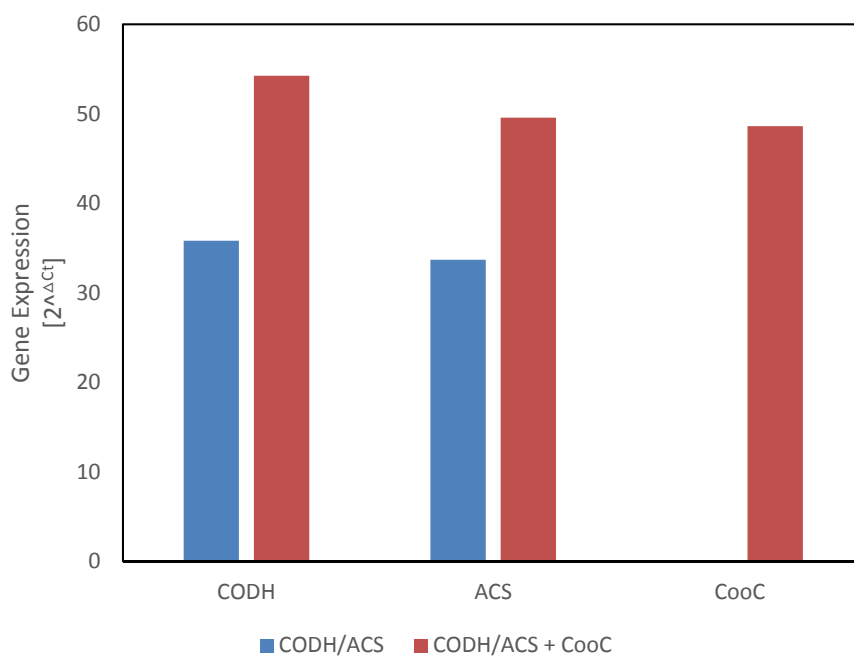
Figure 4.7. Gene expression for construct containing CODH/ACS and construct containing CODH/ACS and accessory protein CooC. Q-RT-PCR was performed on cDNA for both samples.
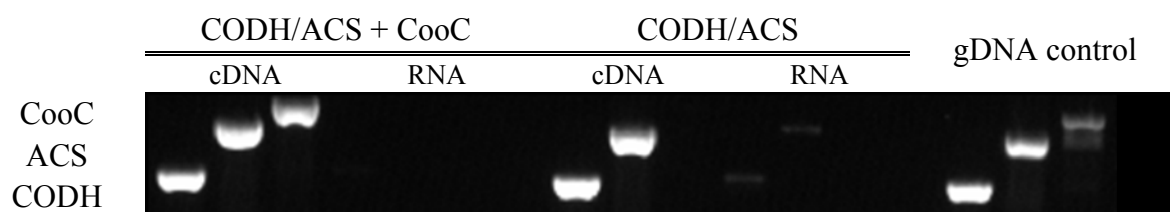
Figure 4.8. mRNA transcripts for CODH/ACS complex and accessory gene. The RNA
control indicates no gDNA contamination present in RNA samples.

4.10.4 All Strains and Conditions Tested Showed Similar Growth Behavior

All strains exhibited similar biomass formation as can be seen by the
measurements of the optical density of the cultures during the fermentation (4.10, F).
The pressure for all strains increased consistently throughout the experiment (4.10, C).
Measurements of CO_2 and H_2 partial pressure showed similar behavior for all strains
(4.10, D,E). When converting partial pressures to mmoles of gases, we can relate the
measured values to those calculated. Using a stoichiometric model based on
Papoutsakis *et al.,* a total of ~1.5 mmoles of CO_2 was released, which was also
confirmed by our measurements (4.9, (Papoutsakis 1984)).
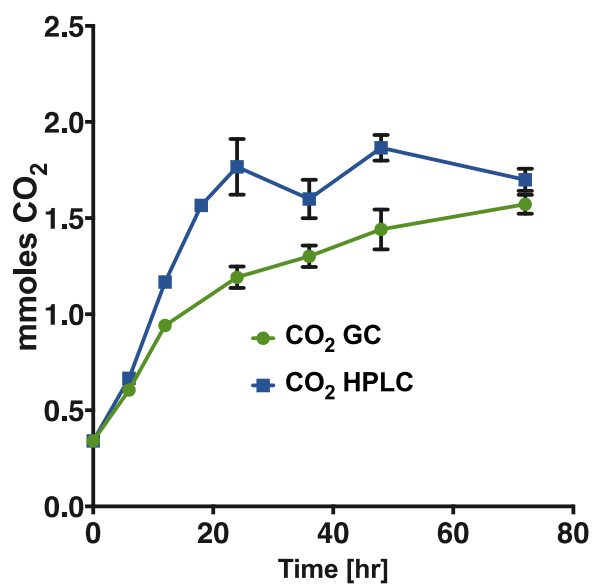
Figure 4.9. Amount of CO_2 produced during fermentation as measured by GC (green) or calculated through metabolites formed from HPLC data (blue). The amount of CO_2 estimated through both methods is in agreement, indicating good calibration on the GC and HPLC.
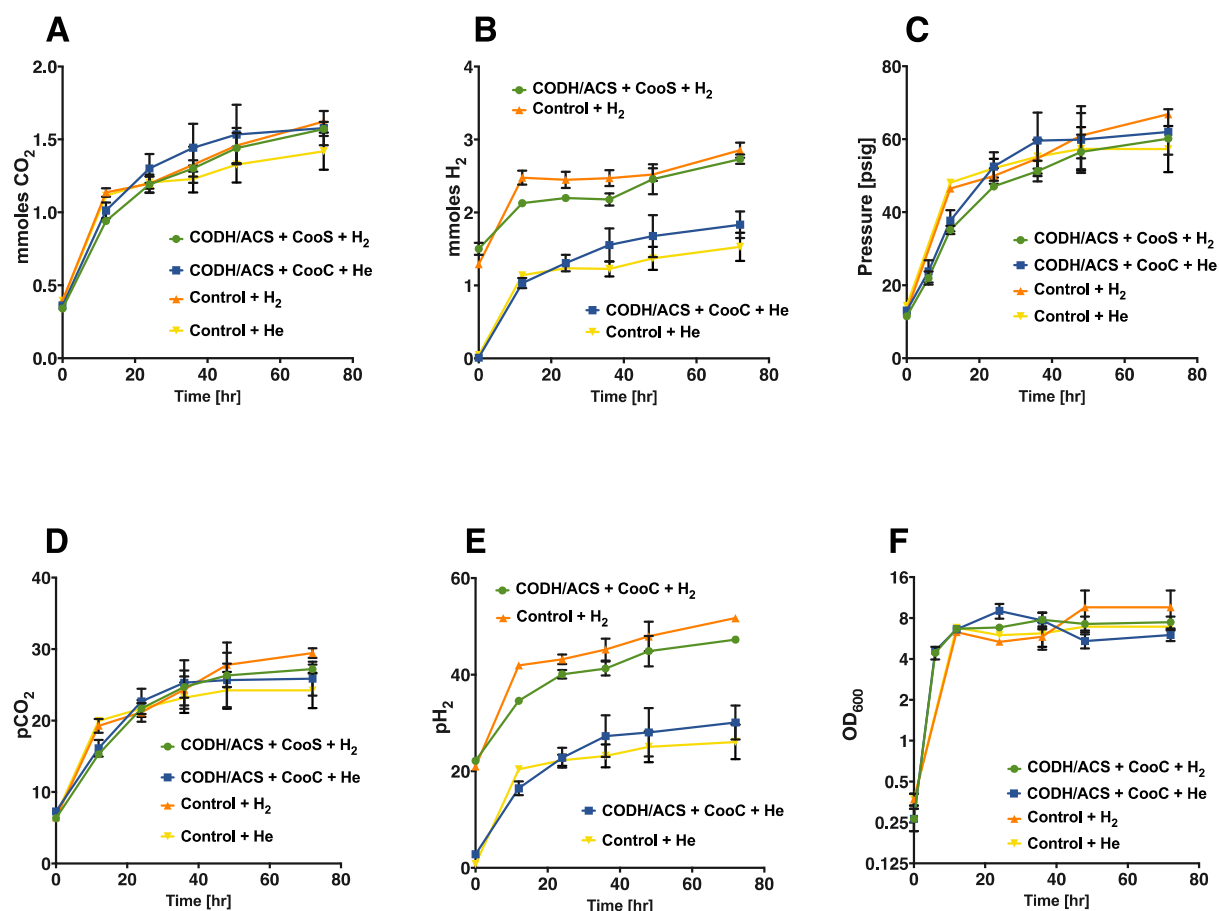
Figure 4.10. Amount of CO_2 produced during fermentation (A) and H_2 produced during fermentation (B). Total pressure increase during fermentation (C). All strains and culture conditions exhibited the same amount of CO_2 released, indicating comparable rates of glycolysis. No statistical difference in the amount of H_2 production was seen between the CODH/ACS and the control strain in the presence of Helium or Hydrogen. D) Partial pressure of CO_2 produced over time. E) partial pressure of hydrogen produced over time. F) Measurements of biomass (OD_{600}) over time. The pressure profile of all four types of experiments (n=3) exhibited similar trends, indicating good biological reproducibility.

4.10.5 Less H_2 Is Produced when H_2 Is Added to the Gas Phase

The rate of H_2 production was highest in the first 24 hours of fermentation, slowing down later in the fermentation. To further investigate the H_2 production, the

initial H_2 concentration (at t=0 as measured by GC) was subtracted from subsequent time points (ΔH_2) (Figure 4.11). The control strain had the same increase of H_2 in the presence or absence of initial H_2. Interestingly, the strain expressing the CODH/ACS enzyme complex exhibited different behavior in the presence of absence of H_2. The CODH/ACS strain in the absence of initial H_2 produced significantly more H_2 after 24 hours of the fermentation. At t=24, H_2 production was increased almost by 82% compared to the strain that was grown initially in the presence of H_2. By the end of fermentation, the CODH/ACS strain in the absence of initial H_2 produced 48% more total H_2. The production of H_2 in *C. acetobutylicum* is associated with the oxidation of reduced ferredoxin, and serves as a way to modulate electron imbalances/remove excess reducing equivalents within the cells (Papoutsakis 1984, Demuez, Cournac et al. 2007). Reduced ferredoxin interacts with the CODH and becomes oxidized during the conversion of CO_2 to CO (Shanmugasundaram and Wood 1992). Therefore, reduced H_2 production should result in higher CO_2 reduction activity. When comparing the CODH/ACS strain in the two culture conditions with and without initial H_2, there was a statistically significant ($p<0.05$) difference in the amount of CO produced. The strain in the presence of H_2 produced an average of 3.2 micromoles of CO and the strain in the absence of H_2 produced only 2.2 micromoles of CO.
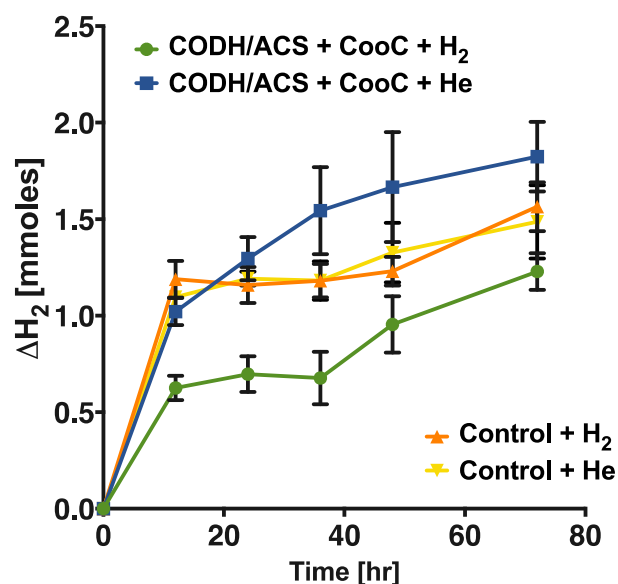
Figure 4.11. Change in total H_2 produced during these fermentation experiments. The CODH/ACS strain in the presence of H_2 (green) produced significantly less H_2 than the CODH/ACS strain in the absence of H_2 (blue). The control strains (orange and yellow, with and without H_2, respectively) produced the same amount of total hydrogen.

TWO-WAY ANOVA COMPARISON BETWEEN TOTAL H_2 PRODUCED BY THE CODH/ACS+COOC STRAIN IN THE PRESENCE AND ABSENCE OF HYDROGEN

TIME	Mean Diff.	95.00% CI of diff.	Significant?	Summary	Adjusted P Value
0	0	-0.5771 to 0.5771	No	ns	>0.9999
12	-0.3957	-0.9728 to 0.1814	No	ns	0.3149
24	-0.5987	-1.176 to -0.02158	Yes	*	0.039
36	-0.8667	-1.444 to -0.2896	Yes	**	0.0015
48	-0.712	-1.289 to -0.1349	Yes	*	0.0101
72	-0.5943	-1.171 to -0.01725	Yes	*	0.041

121

Table 4.2. Two-way ANOVA comparison between total H_2 produced by the CODH/ACS+CooC strain in the presence and absence of hydrogen. Calculations were done using PRISM 7 (Graphpad Software, Inc.). (Statistical significance shown as *= $p<0.05$ and **=$p<0.005$).

The previous study done by us found the strain in the presence of H_2 produced significantly more CO in the first 24 hours ($p<0.005$) compared to the strain in the presence of He. The previous study was done with a larger headspace and the significance was reported after 24 hours. In this experiment, the difference in CO was only significant by the end of the experiment ($p<0.05$, calculated by student's t-test, assuming equal standard deviation between time points and samples). It is possible that the cultures of the previous experiment and this experiment did not have the same growth rate and therefore produced different results. It is also possible that the different media (in this case a more complex media than a defined medium) produced a different effect in the presence of H_2. Further studies need to be conducted to elucidate the complex mechanism by which the production of H_2 influences the activity of the CODH and vice-versa.
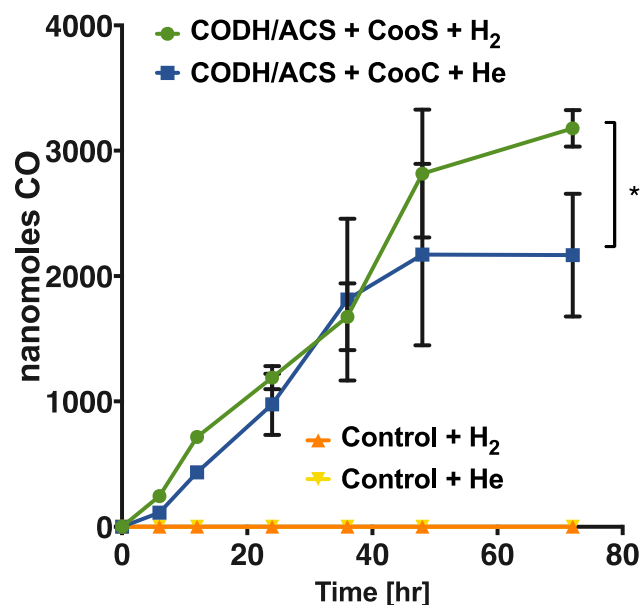
Figure 4.12. Amount of CO produced during fermentation. The CODH/ACS strain in the presence of H_2 (green) produced significantly more CO towards the later stages of fermentation than the CODH/ACS strain without H_2 (blue). The control strains did not produce any CO (orange and yellow, with and without H_2, respectively).

4.10.6 Primary-Metabolite Profiles Are not Influenced by Increased Starting H_2 partial pressure

The metabolite profile of all strains exhibited similar trends indicating the expression of the CODH and the production of CO had no effect on the metabolism in this study. The fermentation profiles can be seen in Figure 4.14. Even though a prior study found an increase in the production of more reduced products (Yerushalmi, Volesky et al. 1985), this study did not observe this trend. However, the H_2 partial pressures in the experiment by Yerulshalmi were significantly higher than in this experiment (40 psi vs. 24.7 psi) so it is possible the effect could be not seen at these moderately low pressures. Most strikingly, however, was that the amount of glucose consumed in these experiments was significantly different between the two strains and

123

the two conditions tested. There was no trend for the observed difference, as the CODH/ACS strain in the presence of H_2 consumed the most glucose and the control strain in the presence of hydrogen produced the least amount of glucose. Therefore, the carbon yield of metabolites was quite different although the strains achieved similar total titers. The CODH/ACS strain produced significantly more butanol than the control strain in the presence of hydrogen. The control strain in the presence of hydrogen also produced less acetone than without the presence of hydrogen, a trend seen also with the inhibition of the hydrogenase through CO (Meyer, Roos et al. 1986). Taken together, these results indicate a slight effect of the presence of the CODH/ACS enzyme and the hydrogen during the initial stages of fermentation.
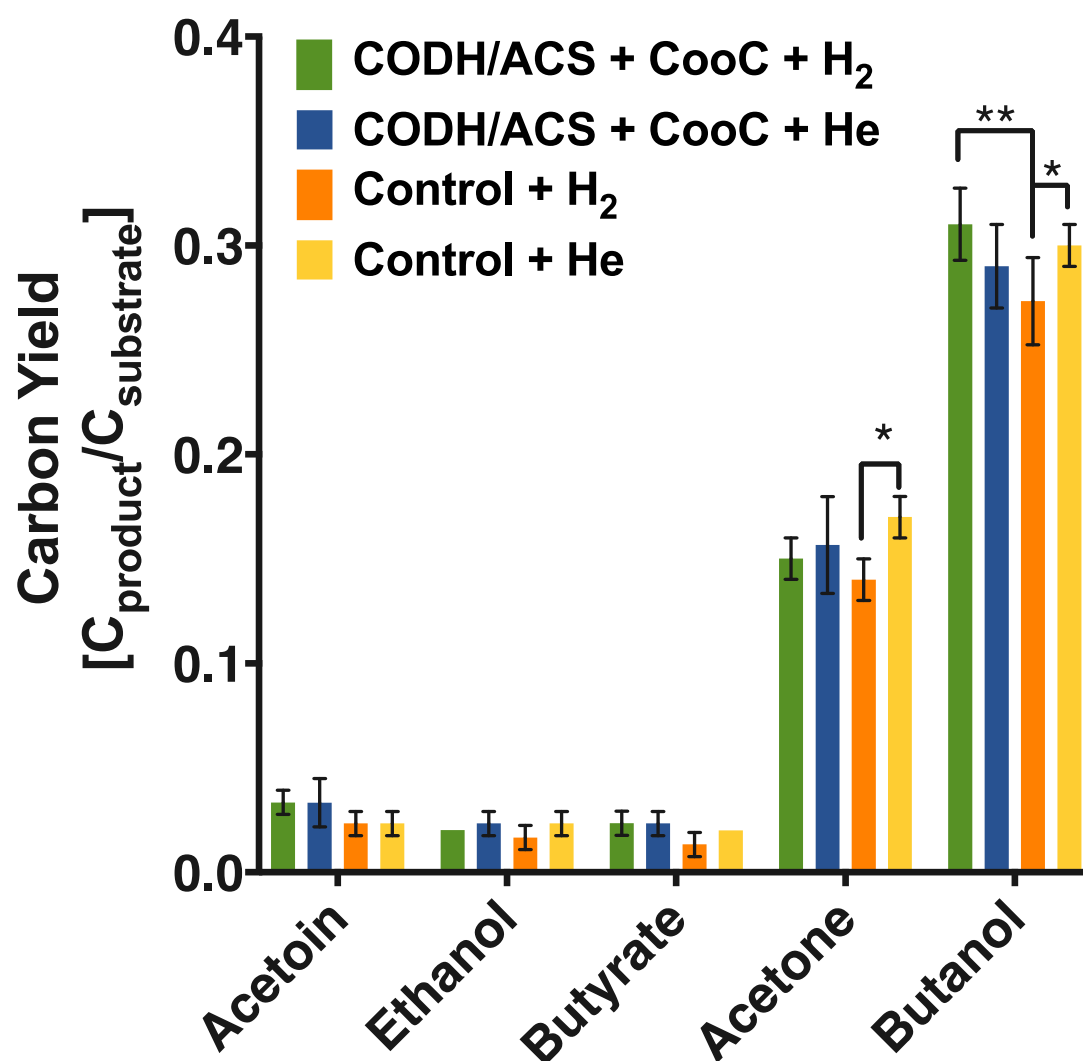
Figure 4.13. Carbon Yields (carbon moles product divided by carbon moles glucose consumed) at the end of the fermentation by the two strains (CODH/ACS+CooC and control) for the two culture conditions (+/- H_2). Up to 10g/L of butanol were produced by all strains. Calculations were done using PRISM 7 (Graphpad Software, Inc.). (Statistical significance shown as *= $p<0.05$ and **=$p<0.005$).
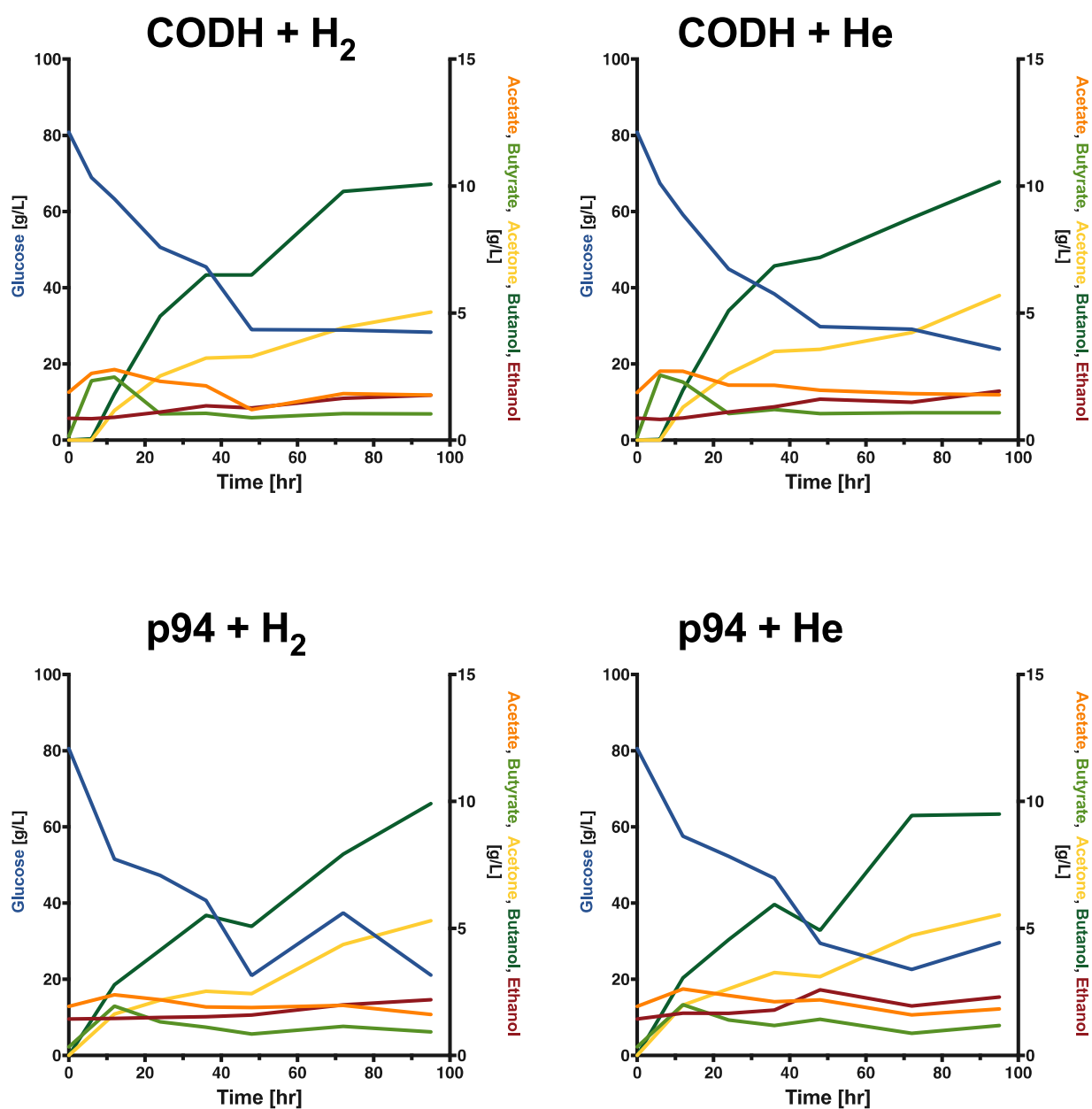
Figure 4.14. Fermentation profiles of the two strains (CODH/ACS+CooC and control) for the two culture conditions (+/- H2). Up to 10g/L of butanol were produced by all strains. Shown are the averages for the three replicates.

4.10.7 Conclusions

The presence or absence had a positive effect on the total amount of CO produced during the fermentation of *C. acetobutylicum* when expressing the CODH/ACS (+CooC) enzyme (Figure 4.12). Less hydrogen was produced, which results in a larger internal pool of reduced ferredoxin, leading to the increase in CO production. The *C. acetobutylicum* strain expressing the CODH/ACS (+CooC) enzyme produced 0.59 mmoles less hydrogen, which resulted in 1 micromole of an increase in CO. This could indicate some inefficiencies in utilizing the ferredoxin for the production of CO. The carbon yield of butanol was increased for the strain expressing the CODH/ACS enzyme compared to the control. The production of butanol probably served as a sink for the additional electrons that were not oxidized towards hydrogen. Even though there were some significant findings, more experiments need to conducted to further explain the behavior of *C. acetobutylicum* strain expressing the CODH/ACS (+CooC) enzyme complex.

4.10.8 Experimental Methods

Growth and Culture Conditions

C. acetobutylicum (ATTC824) was transformed with a plasmid that contained both the *codh* (Ccar_18845) and the *acs* (Ccar_18785) genes from *C. carboxidivorans* in an operon arrangement under the control of the strong P_{ptb} promoter native to *C. acetobutylicum* (Tummala, Welker et al. 1999). The two subunits were followed by a nickel insertion gene, *cooC* (Ccar_18840).

Single *C. acetobutylicum* colonies were grown anaerobically on solid 2× YTG medium (16 g/liter Bacto tryptone, 10 g/liter yeast extract, 4 g/liter NaCl, and 5 g/liter glucose; pH 5.8) and transferred to 10 ml of liquid clostridial growth media [CGM;

0.75 g/liter K$_2$HPO$_4$, 0.75 g/liter KH$_2$PO$_4$, 0.7 g/liter MgSO$_4$·7H$_2$O, 0.017 g/liter

MnSO$_4$·5H$_2$O, 0.01 g/liter FeSO$_4$·7H$_2$O, 2 g/liter (NH$_4$)$_2$SO$_4$, 1 g/liter NaCl, 2 g/liter

asparagine, 0.004 g/liter *p*-aminobenzoic acid, 5 g/liter yeast extract, 4.08 g/liter

CH$_3$COONa·3H$_2$O, and 80 g/liter glucose] until mid-exponential phase. The media

was supplemented with erythromycin (Em) (100 μg/ml) and 200uM NiCl$_2$ for active

expression of CODH/ACS enzyme. 5 ml of actively growing cells were added into a

sterile, helium flushed serum bottle (26ml). 20% CO$_2$ balance helium or 20% CO$_2$

balance hydrogen was used to first flush and then pressurize the headspace to 10psi.

Samples were drawn every 12 hours to monitor growth and product formation. Gas

chromatography was used to measure the headspace gas composition.

Table 4.3. Primers for band visualization of cDNA:

NB_CODH_F	GTATTTGTGGTGCTGACGCA
NB_CODH_R	GTTCAGCATCTGCCATACAGC
67ºC	Length: 408
NB_ACS_F	GTTGCATTTGCAGCAGCATTC
NB_ACS_R	TGGTACTGCTTGACATGGTCC
67ºC	Length: 699
NB_CooC_F	ATAAGGACTTTAAATAACTAGTGAG
NB_CooC_R	TTAAACTAACTGACCTTCTAACTTTTC
58ºC	Length: 824

Table 4.4. Primers for Q-RT-PCR:

qRTAcsB_F	TTGTGGTGCAGTTTCATGGC

qRTAcsB_R	TGGTACTGCTTGACATGGTCC
qRTAcsA_F	TGGTGTGGAAACAGCTTGGG
qRTAcsA_R	CAGCAAACACCTGCTGAACC
CooC	
qRTCooC_F	ATAACGGGAAAAGGTGGCGT
qRTCooC_R	TCTGGATCTGCATCTACAGCC

RNA Isolation and Reverse Transcription

Recombinant *C. acetobutylicum* strain expressing the CODH/ACS enzyme complex and the strain expressing CODH/ACS and CooC were grown in CGM to an OD_{600} around 1.0. The cultures were harvested by centrifugation at 4°C for 10 min at 7000xg, and cell pellets were frozen at -82°C. Cells of the *C. acetobutylicum* empty plasmid control strain and wild-type *C. carboxidivorans* were collected in the same manner. The frozen cell pellets were thawed, resuspended in TE buffer (30 mM Tris•Cl, 1 mM EDTA, pH 8.0) containing 15 mg/ml lysozyme following the **RNAprotect (Qiagen) protocol.**

Samples were additionally disrupted by sonication for 5 min at 50% power with intervals of 15 s sonication followed by 15 s of rest using a Fisher Scientific Sonic Dismembrator and a cup horn. The protocol for the RNeasy® Mini Kit (Qiagen) was performed with an additional DNase treatment step (Qiagen) to obtain purified RNA. High-Capacity cDNA Reverse Transcription Kit (Applied Biosystems™) was used for cDNA synthesis. Primers listed in Table 4.3 were used to amplify from cDNA or RNA (control) to ensure proper digestion of genomic DNA.

Calculation for evolved CO_2

Since initial CO_2 concentration was unknown at t=0, GC estimates were used to describe initial concentrations. CO_2 concentrations at later time points were calculated with the following equation:

$$CO_2 = initialCO_2 + 3 * \Delta Acetone + 2 * \Delta(Butyrate + Butanol) + 1$$

$$* \Delta(Acetate + Ethanol) + 1 * \Delta Acetoin$$

Where $\Delta(Metabolite) = Metabolite_{final} - Metabolite_{initial}$

Chapter 5

CARBON MONOXIDE OXIDATION USING A HETEROLOGOUSLY EXPRESSED CARBON MONOXIDE DEHYDROGENASE IN *CLOSTRIDIUM ACETOBUTYLICUM* TO MODULATE FERMENTATION PROFILE

5.1   Abstract

Toxic effects of CO are well known, but many bacteria and archaea participate in the detoxification and remediation of CO. Many of these organisms utilize CO for growth or as a source of carbons or electrons. Through the heterologous expression of the carbon monoxide dehydrogenase from *Clostridium carboxidivorans* in *Clostridium acetobutylicum,* we have successfully engineered a *C. acetobutylicum* strain capable of detoxification of CO. Previous studies have shown CO to influence metabolite profiles, by increasing the production of butanol, acetoin and ethanol, and decreasing the production of acetone. In this work, we demonstrate that the engineered strain lacks these characteristics when grown in the presence of low partial pressures of CO. The metabolites where unchanged in the presence or absence of CO. We investigated two partial pressures of CO (0.2 and 0.34 atm), and demonstrate the higher partial pressure of CO leading to a faster rate of CO oxidation. The engineered strain is capable of producing butanol/acetone ratios much lower than what has previously been demonstrated. Further work could elucidate the complex mechanism by which acetone, butanol, acetoin and ethanol are regulated and how expression of heterologous genes influences the metabolite distribution.

5.2   Introduction

The CODH enzyme catalyzes the interchange between CO and CO_2, an important reaction for the detoxification, remediation and growth on CO (Moersdorf,

131

Frunzke et al. 1992). Microbes containing the CODH enzyme help to remove and oxidize 108 tons of CO from earth's lower atmosphere every year, which in turn helps to maintain low ambient CO levels (Ragsdale 2009). The oxidation of CO to CO_2 is known as the water gas shift reaction, an important industrial reaction that utilizes the electrons of CO to produce H_2 from water. Hydrogen is of industrial importance, and is used for the Haber-Bosch process which generates ammonia from nitrogen, one of the most important inventions of the 20th century, as it provides fertilizers to increase crop yields across the globe. The water-gas shift reaction usually uses heterogeneous catalysts and occurs at temperatures between 200-350°C and relatively high pressures. The CODH enzyme completely converts CO to CO_2 at biological relevant temperatures (between 30-60°C) and low pressures (1-2 atmosphere). CO oxidation usually occurs with two half reactions as displayed in Figure 5.1, with an electron acceptor accepting the electron exchange between the enzyme and CO and water being the oxygen donor.

$$CO + H_2O + acceptor_{ox} = CO_2 + 2H^+ + acceptor_{red} \qquad \text{Equation 3}$$
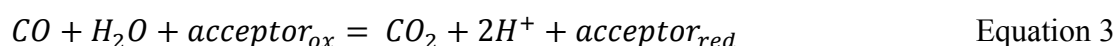
The two half reactions of CO oxidation are (i) first the oxidation of CO to CO_2 generating the two-electron reduced enzyme, followed by (ii) the oxidation of the enzyme by the oxidized electron acceptor (Can, Armstrong et al. 2014). The CO oxidation occurs through an active site transition metal center formed by a bridge between Ni and the Fe-S cluster, termed the C-cluster, undergoing a total of three different oxidation states differing by one electron (Jeoung and Dobbek 2007). The C-

cluster contains a H_2O/OH^- ligand and a Ni^{2+} ion to which the CO binds and further

reacts with the Fe ion-bound OH group (Jeoung and Dobbek 2007).

The CODH enzyme can use a variety of electron acceptors, such as

ferredoxins, flavodoxins, rubredoxins, cofactors (FAD and FMN, but not NAD(P)),

redox enzymes (such as hydrogenases), or artificial electron acceptors (viologen dyes)

(Can, Armstrong et al. 2014). Many acetogenic isolated CODH's have been shown to

function with ferredoxin, a ubiquitous electron carrier found in many clostridia whose

redox potential is near -450 mV, the only biochemical relevant electron carrier low

enough to overcome the very low standard redox potential of the CO/CO_2 couple (E'_o=

-520 mV) (Schuchmann and Müller 2014).
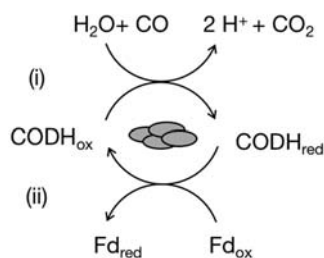
Figure 5.1. The two half reactions depicting the electron shuffling during the oxidation
of CO by the carbon monoxide dehydrogenase. Adapted from (Ragsdale
and Kumar 1996).

5.3 Carbon Monoxide Oxidation in Bacteria and Archaea

Biological oxidation of CO to CO_2 was first reported in 1959 in sulfate-

reducing bacteria (Yagi 1958, Ragsdale and Kumar 1996), but since then it has been

shown in methanogens and in acetogens as either a CO detoxification process or as

means for cells to grow on CO and other gas mixtures as sole substrates (Fuchs,

Schnitker et al. 1974, Daniels, Fuchs et al. 1977, Diekert and Thauer 1978). In methanogenic bacteria, the oxidation of CO is coupled with the reduction of CO_2 to methane, and in acetogenic bacteria, with the incorporation of CO_2 into acetyl-CoA. Other bacteria and archaea utilize CO oxidation as means to create energy by generating a proton motive force through the coupling of CO oxidation to H_2 evolution. Many Carboxidotrophs and Phototrophs are capable of using CO as a sole energy and carbon source. In *Rhodospirillum rubrum*, for example, a Ni and Fe containing CODH was isolated which coupled the CO oxidation to hydrogen evolution and energy generation via a membrane-bound hydrogenase (Kerby, Ludden et al. 1997). A similar CODH complex from the hyperthermophilic archaeon *Thermococcus onnurineus* consists of a 12-subunit hydrogenase-antiporter complex (Mrp- Mbh) together with the two subunits of CODH, which allows the host to create an ion gradient to generate ATP. This CODH complex has been heterologously expressed in *Pyrococcus furiosus*, and the engineered strain was able to oxidize CO and utilize the resulting electrons to establish a proton gradient (Schut, Lipscomb et al. 2016). From the many examples of the CODHs in nature, it is clear that there are many ways in which the oxidation of CO benefits the host, whether it is for energy generation or for carbon fixation. In all these instances, CODH interacts with a protein partner to carry out specialized functions, such as hydrogen generation or incorporation of carbon into cell biomass and products.

5.3.1 Carbon Monoxide Oxidation by Clostridia

The first isolation of a clostridial and anaerobic CODH enzyme, from the same organisms (*Moorella thermoacetica*), was published by two research groups in 1983 (Diekert and Ritter 1983, Ragsdale, Clark et al. 1983). Both studies demonstrated

nickel as part of the active form of the enzyme. The first detailed CODH study was with the CODH from *Clostridium pasteurianum*, which was found to oxidize CO to CO_2 at a rate of 15 nmol/min/mg protein (Fuchs, Schnitker et al. 1974), and later researchers discovered the requirement of nickel in media for the function of the CODH (Diekert, Graf et al. 1979). Another study in Clostridia was done by Diekert *et al.* and showed the oxidation of CO by growing cultures of *Clostridium formicoaceticum* in the presence of 5 g/l fructose (Diekert and Thauer 1978). Concentrated cell suspensions were able to oxidize ~50 μmoles of CO. Even when CO was labeled with a ^{14}C radioactive tracer, very little labeling was observed in biomass or metabolites due to the large unlabeled CO_2 pool that resulted from the decarboxylation of pyruvate (Diekert and Thauer 1978).

5.3.2   Carbon Monoxide Inhibits Cell Growth of *Clostridium* Organisms

There exist many organisms or biological systems that are unable to oxidize CO, and instead, CO causes severe toxicity to the cells. Even some acetogenic bacteria, which contain a CODH, suffer from high CO partial pressure inhibition (Mohammadi, Mohamed et al. 2014). The toxic effects of CO on biological systems are well known (Gray and Gest 1965) and have been shown in *Clostridium acetobutylicum* before (Kim, Bellows et al. 1984, Meyer, Papoutsakis et al. 1985, Meyer, Roos et al. 1986, Moersdorf, Frunzke et al. 1992). Both Meyer *et al.* and Kim *et al.* showed the reduction of growth in the presence of CO in the headspace of *Clostridium acetobutylicum* fermentations. Kim and coworkers described the effect on growth rate of low partial pressures of CO (2-10%) in batch cultures of *Clostridium acetobutylicum* and showed that even at 5% the growth rate was reduced by 66%. They showed that more butanol and ethanol and less acetone are produced in batch

culture. No other metabolic changes were reported. Meyer et al. (Meyer, Papoutsakis et al. 1985, Meyer, Roos et al. 1986) showed the reduced growth in both batch and continuous fermentation sparged with CO. Meyer et al. (Meyer, Papoutsakis et al. 1985, Meyer, Roos et al. 1986) found that production of butanol and ethanol are enhanced or induced ab initio, acetone production was reduced or abolished, acetoin and lactate production induced ab initio, H_2 production reduced or abolished, and that CO inhibition was reversible. CO inhibits the Fe-Ni production hydrogenase (11) of *C. acetobutylicum* by binding to the novel Fe-S cluster (H-cluster) (Demuez, Cournac et al. 2007). The inhibition of the hydrogenase leads to an increased pool of reducing carriers (electron carriers Fd_{red} and NADH), which has a profound effect on the metabolism by shifting the redox balance. Previous fermentation studies have recognized the importance of the electron balance and flux and its ability to influence product profiles (Roos, McLaughlin et al. 1985, Meyer, Roos et al. 1986). Other methods to influence metabolism have been the use of artificial electron carriers such as methyl viologen (Hönicke, Janssen et al. 2012) and neutral red or increasing the hydrogen partial pressure (Yerushalmi, Volesky et al. 1985). Even though some major players involved in regulation have been identified, such as the redox-sensing protein Rex, which regulates transcription of some of the key solventogenic genes, much remains to be elucidated about his complex mechanism.

We set out to investigate a newly constructed strain of *C. acetobutylicum* heterologously expressing the CODH from *C. carboxidivorans* and this strains ability to oxidize CO, making the hypothesis that the organism would utilize the available electrons in CO to shift its metabolism to more reduced products like alcohols. We anticipated the recombinant strain to be able to (i) detoxify the carbon monoxide to

alleviate the inhibition of the hydrogenase by CO, and (ii) utilize the resulting reduced electron carriers for the production of more reduced products such as butanol. In this experiment, an effect on the redox balance should be noticed when CO is oxidized to CO_2.

5.4 CO oxidation at Partial Pressures of 0.2 and 0.35 atm of CO of *Clostridium acetobutylicum* expressing CODH

We embarked on determining the effects of ~8-10% CO headspace on the fermentation behavior of *Clostridium acetobutylicum* containing the heterologous expressed CODH enzyme from the closely-related acetogen *Clostridium carboxidivorans*. The CO was labeled using ^{13}C-carbon tracers to monitor the CO oxidation. The headspace composition was measured using GC/MS. Previous experiments had demonstrated the inhibition of CO at partial pressures between 0.1 to 0.3 atm CO. We wanted to determine if the *C. acetobutylicum* strain expressing the CODH would outperform the *C. acetobutylicum* control in terms of biomass formation (growth) and CO_2 partial pressures (glucose consumption). As can be seen from 5.2, at 0.2 atm of CO, there was no statistical significance between the *C. acetobutylicum* strain expressing the CODH or the control for both biomass formation and CO_2 partial pressure. At 0.35 atm CO, however, the *C. acetobutylicum* strain expressing the CODH had higher biomass formation than the control strain ($p<0.0001$). However, there was no statistical significance in the partial pressure of CO_2 between the two strains. This indicates that at 0.35 atm of CO, the control strain's growth was inhibited but the inhibition did not affect glucose consumption. The results are rather curious, but previous research has shown that glucose uptake was increased 300% in continuous cultures of *C. acetobutylicum* sparged with CO (Meyer, Roos et al. 1986).

A similar effect could be observed here. A detailed gas consumption and evolution report for the experiment at 0.2 atm can be found in the appendix (Figure **Error! Reference source not found.**1). In addition, a summary of the set up of the two experiments is given in detail in 5.1.

Table 5.1. Summary of Experimental Set-Up for *Clostridium acetobutylicum* expressing CODH

	0.2 atm CO	**0.35 atm CO**
Headspace Volume	150 ml	21 ml
Liquid Volume	10 ml	5 ml
^{13}CO	1.2 mmoles	0.28 mmoles
e⁻ from CO	1.2 mmoles	0.28 mmoles
Glucose	40 g/L	80 g/L
e- from glucose	8.8 mmoles	8.8 mmoles
% e⁻ (e⁻CO divided by e⁻ glucose)	13%	3%
Pressure (initial)	20 psig	20 psig
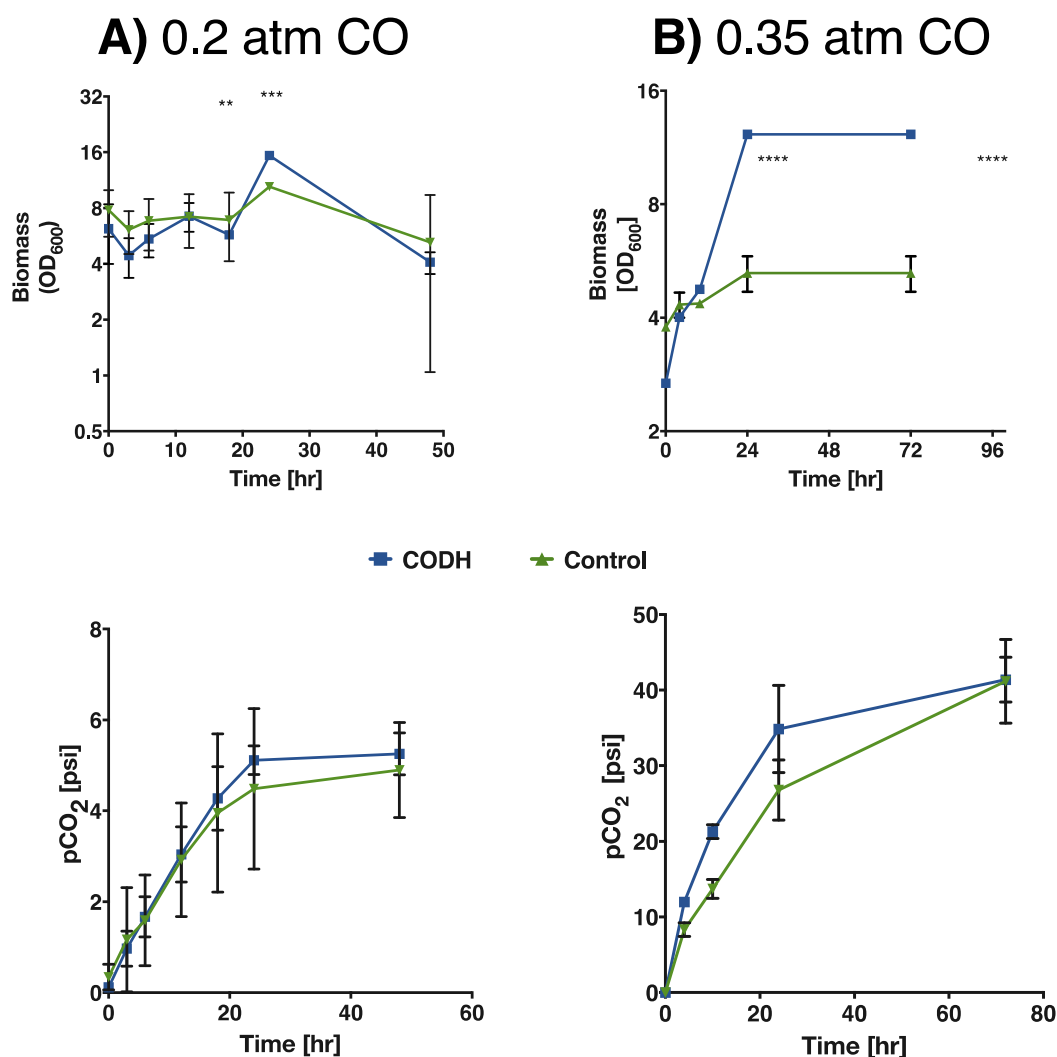
Figure 5.2. Biomass (top) and partial pressure of CO_2 (psig) of two experiments at various CO partial pressures (0.2 atm left, 0.35 atm right). *C. acetobutylicum* expressing CODH (blue) or the control (green) were grown in the presence of CO (three biological replicates each). The experiment with 0.2 atm of CO was grown with 40 g/L glucose in 10 ml liquid media and in a 150 ml headspace, the experiment with 0.35 atm of CO was grown with 80 g/L glucose in 5 ml liquid media and in a 21 ml headspace. There was no statistical significance between the CODH and the control experiment in the presence of 0.2 atm CO. At 0.35 atm CO, the CODH strain formed significantly more biomass than the control strain ($p<0.0001$). The partial pressure of CO_2 was not significant between the two strains.

139

Gas chromatography was utilized to measure the headspace composition for both strains tested in the two experiments. With the coupling of mass spectrometry, CO concentrations were measured by the peak at 0.9 minutes using single ion monitoring of 29.00 m/z. The decrease in the peak in Figure 5.3 indicates a reduction in total CO. The CO consumption, defined as the amount CO at any given time point divided by the initial amount of CO, indicated that CO was oxidized. The CO was consumed only by the *C. acetobutylicum* strain expressing the CODH enzyme at both partial pressures of CO (Figure 5.4). The control was unable to oxidize the CO in any of the experiments. At 0.2 atm CO, by the end of the fermentation, 64% of the initial CO was consumed. At 0.35 atm CO, more than 88% of the initial CO had been converted by the end of the fermentation. Because of the diffences in headspace volume of the two experiments, the total amount of CO oxidized was different between the two experiments. The *C. acetobutylicum* strain expressing the CODH enzyme exposed to 0.2 atm consumed 0.96 mmoles of CO, the highest amount of CO consumed by this engineered strain so far. The other experiment employed a smaller headspace (21 ml versus 150 ml), so at 0.35 atm only 0.25 mmoles of CO were consumed. The rate of CO oxidation was ~3.8 times higher in the experiment employing a larger partial pressure of CO. At 0.2 atm CO, the rate of CO oxidation was 805 nmoles/min/gDW and at 0.35 atm CO, the rate of CO oxidation was 3080 nmoles/min/gDW. The higher rate is due to the higher dissolved CO concentration in the liquid media (4.43 versus 7.8 mg of CO per liter in lower (0.2 atm) and higher (0.35 atm) CO partial pressure experiments). This was calculated using Henry's law, and a constant of solubility for CO of 0.023g/L/atm (Fernández-Naveira, Veiga et al. 2017).
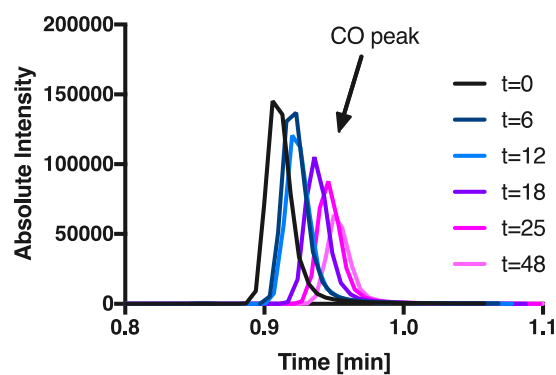
Figure 5.3. Chromatograph of the CO peak with time. The CO peak is measured at 29.00 m/z using single ion monitoring. *Clostridium acetobutylicum* expressing CODH is able to oxidize CO, as can be seen by the decrease in the CO peak. The chromatograph is from the experiment at 0.2 atm CO. Time points are slightly shifted for better visualization.
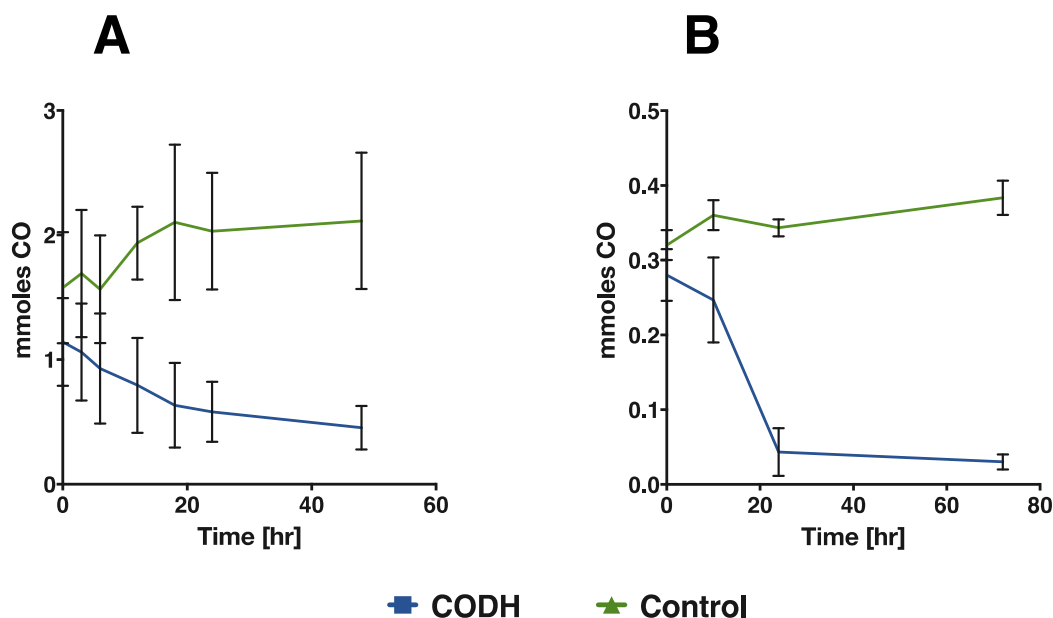
Figure 5.4. Amount of CO consumed at 0.2 atm of CO (A) or 0.35 atm of CO (B) for strains of *Clostridium acetobutylicum* expressing CODH (blue) or the control (green) (three biological replicates each). Only the *Clostridium acetobutylicum* strain expressing CODH was able to oxidize CO. The control was unable to oxidize CO in both experiments. The rate of CO oxidation was highest in the experiment with 0.35 atm of CO.

5.4.1 ^{13}C-carbon Tracing Identifies that CO is Oxidized to CO_2

In order to demonstrate that CO is oxidized to CO_2, the CO contained in the headspace of the experiments was labeled using ^{13}C-tracers. Gas chromatography coupled to mass spectrometry was used to monitor the labeled gases. If the [13]CO is oxidized to [13]CO_2, the percent labeling in CO_2 should increase. Indeed, 5.5 demonstrates the percent labeling increases for both experiments for the *C. acetobutylicum* strain expressing the CODH enzyme only. At 0.2 atm [13]CO, the labeling in CO_2 increases to about 11% in the first 12 hours of the fermentation, and

then decreases to ~9% ^{13}C-labeling at the later time points. For the experiment exposed to 0.35 atm ^{13}CO, the labeling in CO_2 was consistently around ~8% ^{13}C-labeling. The observation that the labeling in CO_2 is consistent throughout the fermentations indicate that the rate of CO oxidation is proportional to the rate of CO_2 production or glycolysis. This was further interrogated by plotting the rate of CO oxidation and the rate of CO_2 production for the experiment exposed to 0.2 atm ^{13}CO (Figure 5.6). The rate of CO oxidation was highest at the same time as the rate of CO_2 production (6 hours after initiation of the experiment). Both glycolysis and CO oxidation slowed down in later stages of the fermentation. Both the correlation between the rates and the consistent CO_2 labeling show a direct link between CO oxidation and glycolysis.
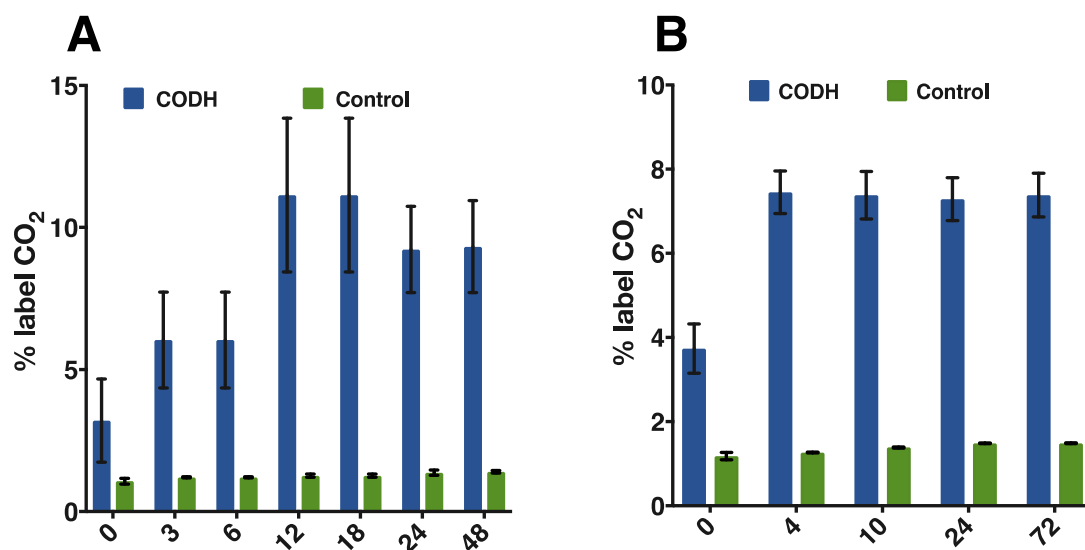
Figure 5.5. Percent labeled CO_2 throughout fermentations of *C. acetobutylicum* expressing CODH (blue) or the control (green) (three biological replicates each). Cells were exposed to 0.2 atm ^{13}CO (150 ml headspace) (A) and 0.35 atm ^{13}CO (21 ml headspace) (B). After about 4 hours, the percent labeling in CO_2 stays consistent, indicating that the rate of CO oxidation is proportional to the rate of CO_2 production through glycolysis.
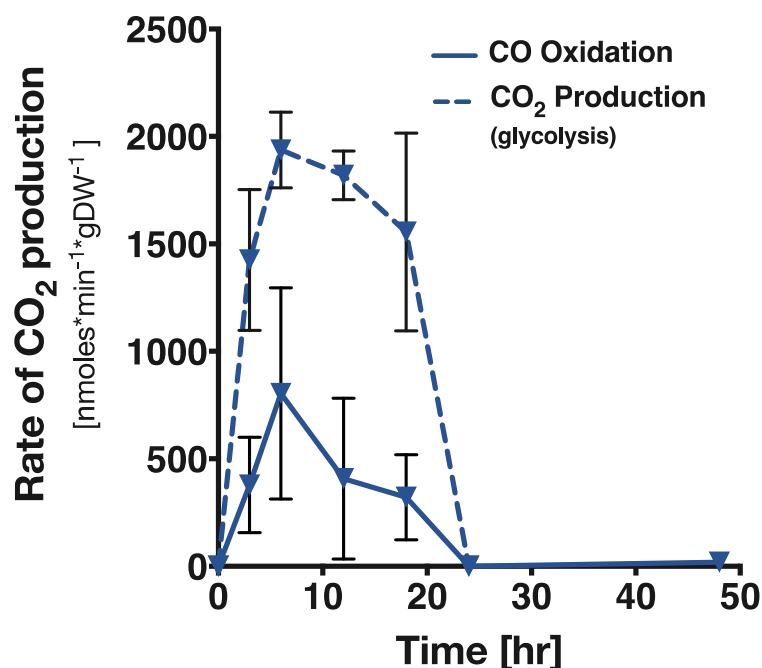
Figure 5.6. Rate of CO oxidation (solid) and CO_2 production (dashed) resulting from glycolysis ($^{12}CO_2$). The rate of CO oxidation is highest when the rate of glycolysis is highest as well, suggesting the need for metabolically active cells to oxidize CO. These calculations were done for the experiment of *C. acetobutylicum* expressing CODH at 0.2 atm CO (150 ml headspace). Error bars are plotted as standard deviations of three biological replicates). The rate of CO oxidation and CO_2 production are statistically significant between 3 and 18 hours (*t*-test).

5.4.2 ^{13}CO Labeling Decreases Due to Isotopic Exchange Between $^{12}CO_2$ and ^{13}CO

From the previous findings, it is clear that CO is consumed and oxidized to CO_2, as demonstrated using carbon tracing i.e. the labeled CO is converted into labeled CO_2. Because the CO is 99.6% labeled initially, it is interesting to note that the percent labeling in CO decreases with time. As can be seen from Figure 5.7, the label in CO decreases to about 94% by the end of fermentation for the experiment at 0.2 atm. For the experiment at the higher partial pressure, the CO decreased even further

to ~80% at 24 hours and finished at 65% labeling by the end of the experiment. This reduction in the labeling of CO is an indication of the isotopic exchange between $^{12}CO_2$ and ^{13}CO using the active site of the CODH enzyme. The isotopic exchange indicated the ability of the CODH enzyme to break the C-O bond and exchange the carbons. ^{12}CO is formed from $^{12}CO_2$. Even though the net reaction is towards CO synthesis, it is interesting to note the differences in labeling for the two experiments. The extend of the isotopic exchange is dominated by the partial pressures of $^{12}CO_2$ in the experiments. The higher the partial pressure of $^{12}CO_2$, the higher the isotopic exchange between $^{12}CO_2$ and ^{13}CO.
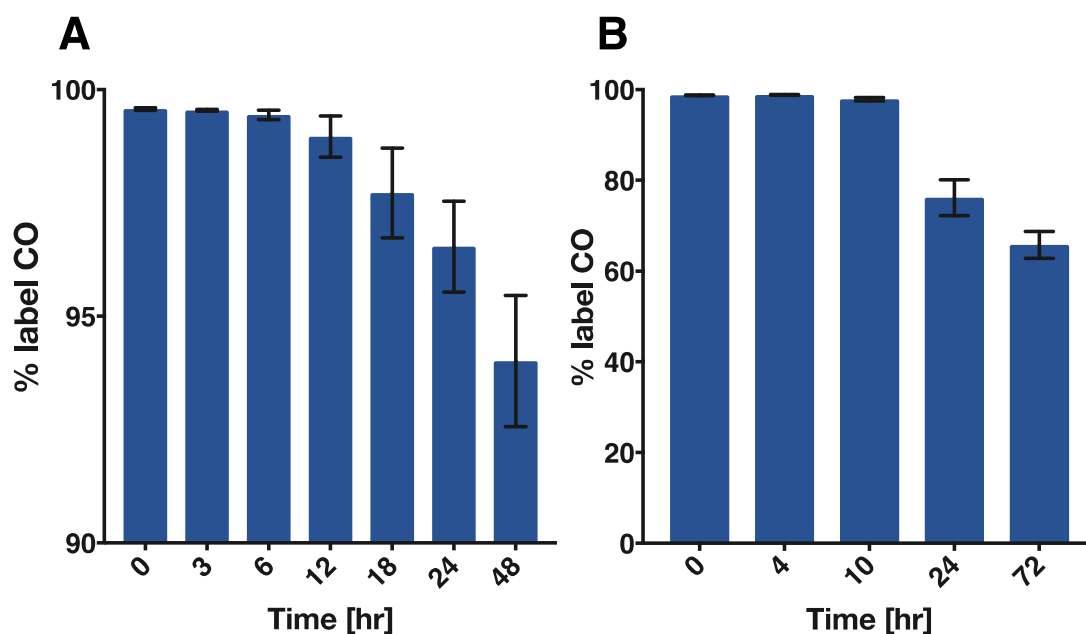
Figure 5.7. Percent labeled CO throughout fermentations of *C. acetobutylicum* expressing the CODH enzyme (three biological replicates each). Experiments were exposed to 0.2 atm CO (150 ml headspace) (A) and 0.35 atm CO (21 ml headspace) (B). The percent label of CO decreases with time, indicating an isotopic exchange reaction between ^{13}CO and $^{12}CO_2$.

5.4.3   The Metabolism is Influenced by the Presence of CO

The change in metabolite concentrations for both experiments are depicted in Figure 5.8. The change in metabolites was calculated by taking the difference between t=0 and t=72 hours of the fermentation. At the lower (0.2 atm CO partial pressure), the control strain produced significantly ($p<0.0001$) less acetone than the strain expressing the CODH enzyme. The control strain produces slightly more butanol than the CODH strain ($p<0.05$) (Figure 5.8A). The reduction of acetone production is a hallmark of CO inhibition (Datta and Zeikus 1985, Meyer, Papoutsakis et al. 1985, Meyer, Roos et al. 1986). Allthough butanol production was hypothesized to increase in the strain expressing the CODH, there appears to be no evidence of this. On the contrary, the butanol to acetone ratio, an indication of alchologenesis versus acidogenesis, for the strain expressing the CODH was 1.3 compared to 2.1 for the control strain. Figure 5.8 B depicts the metabolite changes for the experiment at 0.35 atm CO partial pressure. Most notably, butanol, ethanol and acetoin were significantly enhanced in the control strain than the CODH strain. This has previously been shown (Meyer, Roos et al. 1986). Again the CODH strain produced significantly more acetone, and at ratios unusual for *C. acetobutylicum* fermentations. Generally speaking, a butanol to acetone ratio of 2 is "normal" during the ABE fermentation, indicating that butanol generally is found at concentrations twice that of acetone. In these fermentations, however, for the strains containing the CODH the butanol to acetone ratio was 1.3 - 1.35. How the expression of the CODH affects this unusual fermentation behavior is currently unclear, it is most likely caused by an imbalance in co-factor regeneration, which could be the result of an increased Fd_{red} pool. It could also be that the control strain exhibits "normal" behavior since the CO partial pressure is quite low, and the CODH strain exhibits abnormal behavior.
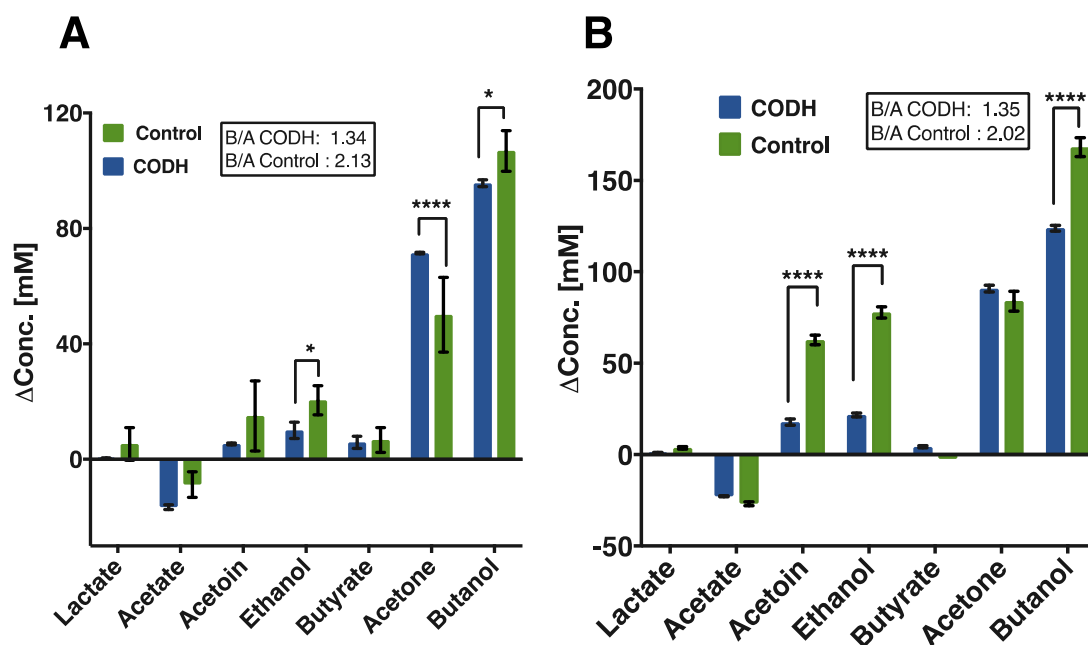
Figure 5.8. Metabolite profile (shown as change in metabolite concentration from 0 to 72 hours) of *C. acetobutylicum* expressing CODH in the presence of CO (blue) *C. acetobutylicum* expressing a control plasmid in the presence of CO (green). A) Metabolite profile for partial pressures of 0.2 atm CO. B) Metabolite profile for partial pressures of 0.35 atm CO. The ratio of butanol to acetone was ~2 for the control in both experiments, and ~1.3 for the CODH strain. Error bars are the standard deviation of 3 biological replicates. Significance was calculated using two-way Anova (Prism 7, Graphpad). Statistical significance is indicated with * ($p < 0.05$) or **** ($p > 0.0001$).

5.4.4 *C. acetobutylicum* Expressing the CODH Enzyme is Unaffected by 0.2 atm CO

Because we observed a difference in the metabolites for the *C. acetobutylicum* strain expressing the enzyme CODH or expressing a control plasmid when in the presence of CO, we wanted to investigate the metabolic profile of the *C. acetobutylicum* strain expressing CODH in the presence and in the absence of CO. If there was no significant difference, it would indicate that the difference seen in the

previous experiment between the CODH strain and the control strain is due to the CO affecting the metabolism of the two strains differently. Figure 5.9 shows the total change in metabolites for the experiment of *C. acetobutylicum* strain expressing the CODH enzyme in the presence and in the absence of CO. As can be seen from the figure, there is no difference in the metabolites produced. The butanol to acetone ratio for both experiments (with and without CO) was 1.3. This indicates that the CO had no effect on the increased acetone production. Generally speaking, this ratio is closer 2. Nevertheless, the experiment showed that the presence of 0.2 atm CO had no effect on the metabolism of *C. acetobutylicum* strain expressing the CODH enzyme, contrary to the effect of CO that had been observed on the metabolism of *C. acetobutylicum* expressing a control plasmid in the previous experiments. The detailed fermentation profiles are depicted in Figure C.2.
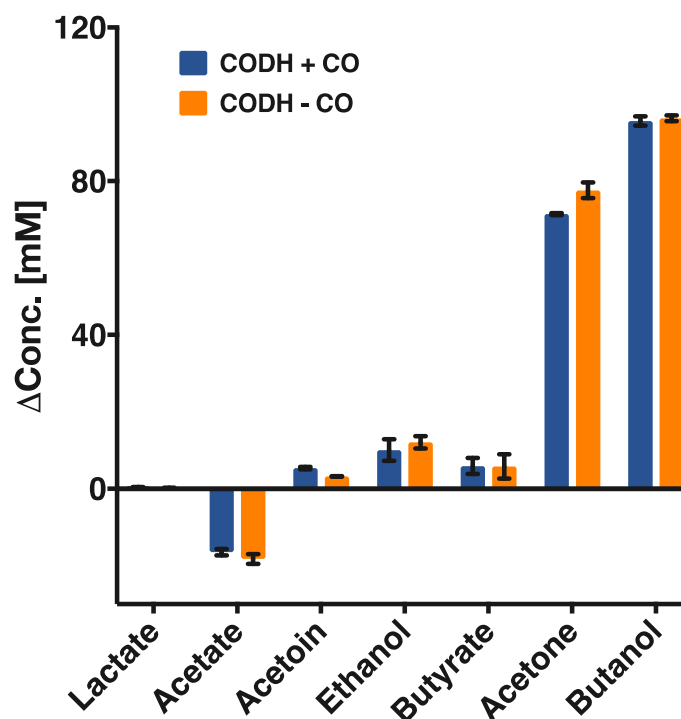
Figure 5.9. Metabolite profile (shown as change in metabolite concentration from 0 to 72 hours) of *C. acetobutylicum* expressing CODH in the presence (blue) or absence (orange) of 0.2 atm CO. There is no statistical significance between the experiment in the presence or the absence of CO. The ratio of butanol to acetone was ~1.3 for the CODH strain. Error bars are the standard deviation of 3 biological replicates.

5.4.5 Defined Media Could Cause Lower than Usual Butanol to Acetone Ratios

One explanation for the lower butanol to acetone ratio could be that the expression of the CODH enzyme enhanced acetone production, the other explanation could be the use of defined media in this experiment. We tested the defined clostridial growth medium (dCGM) used in this experiment and compared it to clostridial growth medium (CGM). The two media are different in containing yeast extract (5 g/L) (only CGM), and using different buffer systems (sodium acetate versus ammonium acetate, CGM and dCGM, respectively). Figure 5.10 show the difference in metabolites

obtained when *C. acetobutylicum* strain expressing the CODH enzyme is grown in a closed headspace. Even though the acetone to butanol ratio when grown with CGM is still slightly lower than 2, it is significantly higher than the 1.3-1.5 ratio obtained when grown in dCGM. All future experiments should be conducted in CGM media to ensure a more accurate representation of the butanol to acetone ratio when conducting the experiments in varying concentrations of CO.
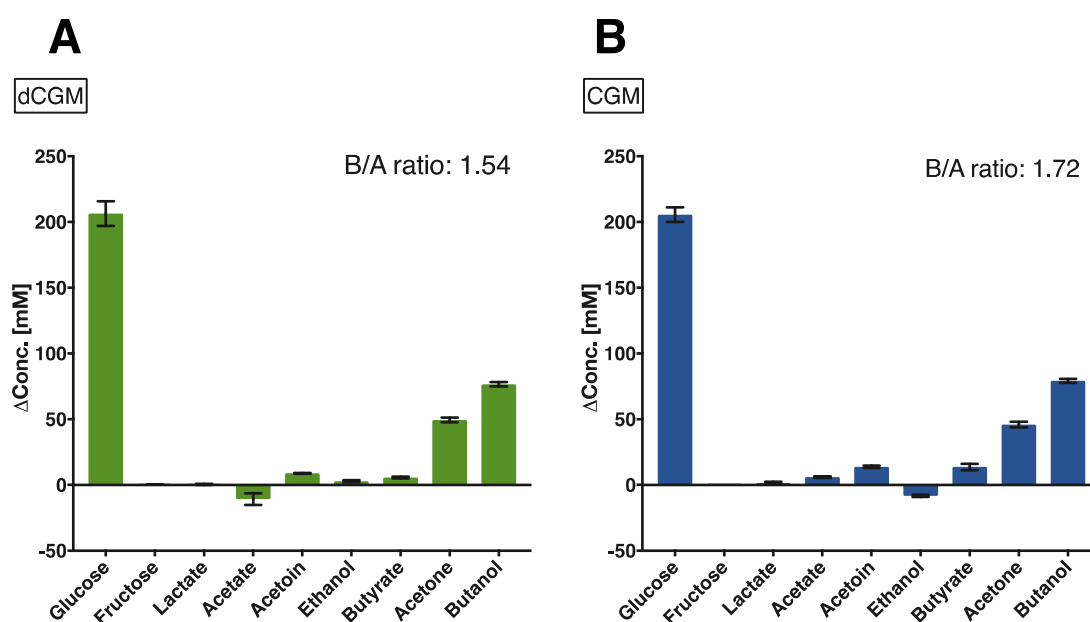
Figure 5.10. Metabolite profile (shown as change in metabolite concentration from 0 to 72 hours) of *C. acetobutylicum* expressing CODH in dCGM (green) or CGM (blue). The ratio of butanol to acetone was ~1.5 for the dCGM media and 1.7 for the CGM media. The use of dCGM in these experiments could have resulted in the lower than usual butanol to acetone ratios. Error bars are the standard deviation of 2 biological replicates.

5.5   Discussion

The heterologously expressed CODH enzyme in *C. acetobutylicum* allowed the engineered strain to function as a whole cell catalyst for the oxidation of CO to CO_2 at 8-10% headspace concentrations. The engineered strain was able to convert between 65 and 80% of CO to CO_2, depending on the initial concentration of CO (.2 and .35 atm CO partial pressure). The increase in conversion rate at the higher partial pressure of CO was due to the higher dissovled CO in the fermentation medium. Solubility is dependent on the partial pressure, so the higher the partial pressure, the more CO is dissolved in the aqeous phase. The higher partial pressure of CO_2 also caused an increase in the isotopic exchange between labeled CO and unlabeled CO_2.

Compared to the control strain, significant differences in total changes in metabolites were seen. The control strain produced less acetone at 0.2 atm CO, and more butanol at 0.35 atm CO. Acetoin and ethanol were also significantly enhanced in the presence of CO for the control strain.

Interestingly, the effect of CO on the metabolites was only observed in the control strain. *C. acetobutylicum* strain expressing the CODH enzyme did not exhibit a different metabolite profile in the presence or absence of CO. This indicates that the engineered strain is able to overcome the toxicity of CO and alleviate the hallmark metabolite profile changes seen in the presence of CO (Figure 5.9). The strains expressing the CODH enzyme exhibited a butanol/acetone ratios of 1.24 to 1.35, which has never been reported before. This was a surprising finding and more research needs to be done to elucidate the mechanisms by which the expression of the CODH influences acetone production.

Even though electrons are derived through the oxidation of CO, metabolism was surprisingly unaffected by the additional reducing equivalents. Oxidation of CO

occurred at a rate proportional to that of glycolysis, indicating a possible link between the two. Both the CO oxidation and glycolysis result in reduced ferredoxin, which is either oxidized by hydrogenases for the production of H_2 or can reduce other electron carriers (NAD(P)H) using the Ferredoxin—NAD(P)(+) reductases. These electron carriers are then responsible for the reduction of acetyl-CoA, butyryl-CoA, or other precursors required for the production of reduced products (ethanol, butyrate, butanol). The increase in reduced ferredoxin therefore also alters the NADH/NAD+ ratio, an important redox indicator that allows the Rex protein to mediate transcriptional changes for the genes involved in solventogenesis. It would be interesting to further investigate the effect of the expression of the CODH in the presence of CO. The oxidation of CO can therefore change the redox pool and lead to metabolite changes.

Our hypothesis was an increased butanol production due to the oxidation of CO, however, this hypothesis was proven to be false. Instead, the most striking effect on increasing butanol production is the presence of CO, as has been previously demonstrated (Meyer, Papoutsakis et al. 1985, Meyer, Roos et al. 1986). However, the ability of the engineered organism to overcome the toxicity of CO is remarkable, as there are visually no differences in the metabolites in the presence or absence of CO. Perhaps experiments employing higher CO concentrations would affect the final metabolites produced, and in doing so, would increase the concentrations of more reduced products, and maybe even abolish acetone production. More research needs to be conducted in order to establish the complex mechanism which controls the fermentations in *C. acetobutylicum*. Our efforts to engineer *C. acetobutylicum* to oxidzie CO have been successful in overcoming the CO toxicity issues seen previously. Clearly, the regulation of metabolites is still poorly understood, and this

work hopes to further expand the understanding of the regulation mechanism for fermentations employing *C. acetobutylicum*.

5.6 Materials and Methods

Strains, culture conditions and medium.

C. acetobutylicum ATCC824 was grown anaerobically at 37°C in either 2xYTG medium (16 g/liter Bacto tryptone, 10 g/liter yeast extract, 4 g/liter NaCl, and 5 g/liter glucose; pH 5.8) or defined clostridial growth medium (dCGM; 0.75 g/liter K_2HPO_4, 0.75 g/liter KH_2PO_4, 0.7 g/liter $MgSO_4·7H_2O$, 0.01 g/liter $MnSO_4·H_2O$, 0.01 g/liter $FeSO_4·7H_2O$, 1 g/liter NaCl, 0.004 g/liter p-aminobenzoic acid, 10 µg/L biotin, 3.3 g/liter $C_2H_3O_2NH_4$ and 40 g/liter glucose; pH 6.8). Recombinant strains were grown on solid 2xYTG media supplemented with 40 µg/ml erythromycin, and single colonies were picked and grown anaerobically in 10ml dCGM as pre-culture. *In vivo* experiments were conducted as described below. Transformations of *C. acetobutylicum* were performed as described (Mermelstein, Welker et al. 1992). All molecular cloning steps were completed in *E. coli*, and strains were grown aerobically at 37°C and 220 rpm in liquid LB medium with shaking at 220 rpm, or on LB with 1.5% agar supplemented with 50 µg/ml ampicillin. *C. carboxidivorans* DSM 15243 was grown anaerobically in American Type Culture Collection (ATCC) medium 1754 with 10 g/l of glucose at 37°C.

Plasmid and Strain Construction.

The vector containing the CODH enzyme was constructed from p94_CODH/ACS derived from the empty plasmid control p94_MCS using site-

directed mutagenesis primers (CODHonly_f & CODHonly_r) and the SDM Kit from

NEB Biolabs. This resulted in a CODH subunit expressed by the strong

phosphotransbutyrylase promoter (p_{ptb}) followed by a terminator sequence.

CODHonly_f	GTAAAAGAGATTGTTTCTAGCTC
CODHonly_r	TAAAATTTATATTCCTAATTTTTTACGTTTTTC

Table 5.2. Primers for construction of strain CODH/ACS and CODH.

Vector transformations.

Vectors were transformed into *E. coli* (NEB Turbo) and isolated using the

Qiaprep Spin Kit (Qiagen). Before transformation into *C. acetobutylicum*, vectors

were transformed into electrocompetent *E. coli* ER2275(pAN3) (Al-Hinai, Fast et al.

2012) for the *in vivo* methylation by the Φ3T I methyl transferase contained on the

pAN3 vector as described (Mermelstein and Papoutsakis 1993). Methylated vectors

were isolated using the Qiaprep Spin Kit (Qiagen) and transformed into *C.*

acetobutylicum ATCC824 using a well-established protocol (Mermelstein, Welker et

al. 1992).

Carbon monoxide oxidation by growing cells at 0.35 atm partial pressure CO.

C. acetobutylicum strains containing either the CODH enzyme or the empty

vector (control) were grown in dCGM to an initial OD of ~1 (OD_{600} 1 and 1.53 for

CODH and Control, respectively). Cells were concentrated 3-fold (final OD_{600} 2.68

and 3.78 for CODH and Control, respectively). The defined media contained 80 g/L of

glucose and was supplemented with erythromycin (100 μg/ml) and 200 μM nickel A

total of 5 ml of the concentrated cells in fresh media were added into 26 ml Wheaton

bottles, and the headspace was charged to ~19 psi and recorded with a handheld
Manometer (Druck DPI705, GE). Then ^{13}CO was filled to ~20.5 psi. The average
percentage of CO in the headspace was ~11%.

Carbon monoxide oxidation by growing cells at 0.2 atm partial pressure CO.

    C. acetobutylicum strains containing either the CODH enzyme or the empty
vector (control) were grown in dCGM to an initial OD of ~2 (OD_{600} 2.2 or 2.5 for
CODH and Control, respectively). Cells were concentrated ~3 fold (final OD_{600} 6 and
7 for CODH and Control, respectively). The defined media contained 40 g/L of
glucose and was supplemented with erythromycin (100µg/ml) and 200 µM nickel. A
total of 10 ml of the concentrated cells in fresh media were added into 160 ml
Wheaton bottles, and the headspace was charged to ~18 psi and recorded with a
handheld Manometer (Druck DPI705, GE). Then ^{13}CO was filled to ~20.5 psi. The
average percentage of CO in the headspace was ~8%.

Media Composition Experiments

    C. acetobutylicum strains containing the CODH enzyme were grown in dCGM
(described above) or Clostridial Growth Media (CGM; 0.75 g/liter K_2HPO_4, 0.75
g/liter KH_2PO_4, 0.7 g/liter $MgSO_4 \cdot 7H_2O$, 0.01 g/liter $MnSO_4 \cdot H_2O$, 0.01 g/liter
$FeSO_4 \cdot 7H_2O$, 2 g/l $(NH_4)_2SO_4$, 1 g/liter NaCl, 2 g/l asparagine, 0.004 g/liter p-
aminobenzoic acid, 10 µg/L biotin, 5 g/l yeast extract, 2.5 g/l sodium acetate, and 80
g/liter glucose; pH 6.8).

Gas Chromatography and Mass Spectrometry

All gas composition measurements were done with a Shimadzu QP-2010 Ultra gas chromatograph-mass spectrometer. Headspace samples of 50 μl were manually collected and injected using an airtight syringe. Gas separation was performed on a Carboxen®-1006 PLOT column (30 m × 0.32 mm, df of 15 μm, Supelco) with injector temperature of 150°C, split ratio of 5, and carrier gas flow of 15.4 psi He (~3 ml/min). The oven temperature was initially held at 30°C for 2.5 min, with ramping at 40°C/min to 120°C. Carbon monoxide separated from nitrogen on the column around .9 minutes. The mass spectrometer was set as a scan speed of ~450 and scanning from 4.00 to 60.00 m/z. Additional SIMs were performed for N_2 (28.00 and 29) and CO_2 (44.00 and 45.00).

Chapter 6

CONCLUSIONS AND RECOMMENDATIONS

The Aim of this work was to interrogate the concept of mixotrophy through first demonstrating mixotrophy in native acetogens (*Clostridium ljungdahlii, Clostridium autoethanogenum, Clostridium carboxidivorans, Moorella Thermoacetica* and *Eubacterium limosum*), and later exploring ways to adopt mixotrophy to *Clostridium acetobutylicum* by engineering the heterologous expression of the carbon monoxide dehydrogenase/acetyl-CoA synthase enzyme. The decarboxylation reaction inherent in microbial fermentation pathways result in an overall decreased mass yield, an undesired process parameter that severely limits microbial platforms for the production of fuels and chemicals. This work validated the theoretical improvements in carbon yield when fermentations are coupled with a biological pathway for carbon fixation. This was achieved by studying acetogens that natively contained the Wood-Ljungdahl pathway. All 5 strains were able to realize superior carbon yields when grown mixotrophically, and low product yields were overcome by the supplementation of additional gases, such as carbon dioxide, hydrogen and carbon monoxide (syngas). The coupling of traditional fermentations of carbohydrates with that of gaseous fermentations achieves higher product yields and a more desired reduced product profile, while simultaneously utilizing cheap and abundant gaseous feedstocks such as industrial waste gases and syngas (Heijstra, Leang et al. 2017).

Besides investigating the coupling of glycolysis to native CO_2 fixation pathways in acetogens, this work set out to pave the way for the incorporation of a

158

synthetic CO_2 fixation pathway in the non-CO_2 fixing host, *Clostridium acetobutylicum*. The carbon monoxide dehydrogenase/acetyl-CoA synthase (CODH/ACS) enzyme from *C. carboxidivorans* was heterologously expressed in *Clostridium acetobutylicum*. The successful expression of the CODH/ACS was demonstrated by observing the tetrameric structure in a native PAGE-gel. The activity of the enzyme complex was tested using whole cell biocatalysts in a closed system, batch fermentation. The CODH/ACS was shown to reduce CO_2 to CO and vice versa. The reactions were interrogated using ^{13}C-carbon tracing.

The effect of the presence of CO on the metabolism of *Clostridium acetobutylicum* when heterologously expressing the carbon monoxide dehydrogenase/acetyl-CoA synthase enzyme was determined. Utilizing gaseous feedstocks to modulate the metabolism of *Clostridium acetobutylicum* towards reduced products provides another process parameter for a "mixotrophic" fermentation of *Clostridium acetobutylicum*. The CO in the headspace was unable to alter metabolism of the engineered strain under the conditions tested. A control strain, however, was shown to be inhibited through the characteristic CO inhibition fermentation profile. This work has demonstrated that the inhibitory effects of CO can be detoxified by the CODH through the oxidation of carbon monoxide to carbon dioxide.

In summary, the hugely positive impact of mixotrophy on traditional fermentations has been demonstrated in native acetogens. Furthermore, the first steps for achieving synthetic mixotrophy have been established. The last sections of this chapter seek to suggest some future research direction for further interrogating synthetic mixotrophy and carbon fixation.

6.1 Future Recommendations

6.1.1 Higher CO partial Pressures to Further Modulate Fermentation Profiles

The most straightforward future work is to further interrogate the effect of CO on *Clostridium acetobutylicum* heterologously expressing the carbon monoxide dehydrogenase/acetyl-CoA synthase. The engineered strain has shown to detoxify the CO found in the headspace (up to 10%), however, at larger CO concentrations, the resulting electrons from CO oxidation should become apparent in fermentation profiles. There is significant evidence that suggest an increase in internal redox potential leads to higher production of alcohols (Meyer, Papoutsakis et al. 1985, Meyer, Roos et al. 1986, Meyer and Papoutsakis 1989). The presence of high concentrations of CO could result into two phenomena: first, the CO will inhibit the hydrogenases, leading to an increase in reduced redox pool (as shown before (Datta and Zeikus 1985, Meyer, Papoutsakis et al. 1985, Meyer, Roos et al. 1986)), and second, the oxidation of CO will further increase the amount of reduced ferredoxin within the cells. Such a strong switch in the electron flow will increases the $NADH/NAD^+$ ratio, which is known to regulate the Rex-protein (Wietzke M 2012). At low $NADH/NAD^+$ ratios, the Rex protein binds to the promoter regions of alcohol forming genes. As the $NADH/NAD^+$ ratio increases, the Rex protein dissociates and transcription of genes for alcohol synthesis increases (Wietzke M 2012, Zhang, Nie et al. 2014). Clearly, by the heterologous expression of the carbon monoxide dehydrogenase, additional electrons can be derived through the oxidation of carbon

monoxide. By employing a continuous system as done by Meyer *et al*. could further enhance the high butanol productions seen previously.

6.1.2   Expression of Formate Dehydrogenase for Synthetic CO$_2$ fixation

Another approach to further pave the way for achieving synthetic CO$_2$ fixation in a non-CO$_2$ fixing host is to overcome the challenges of expressing an acetogenic Formate Dehydrogenase (FDH) enzyme in *Clostridium acetobutylicum*. A focused effort on demonstrating both formate oxidation activities and CO$_2$ reduction activities could provide *Clostridium acetobutylicum* with a way to fix CO$_2$ into the C1-pool, which can be used for the synthesis of serine and methionine. So far, our lab has been unable to successfully show activity of an acetogenic FDH heterologously expressed in *Clostridium acetobutylicum*. One future direction would be to clone the entire operon that is found in acetogenic bacteria, like the one discovered in *Clostridium autoethanogenum,* which was shown to form a complex with a bifurcating hydrogenase (Wang, Huang et al. 2013). The interaction of the FDH with the hydrogenase complex may be important for the function of CO$_2$ reduction rather than formate oxidation. Other FDH's could also be interrogated, such as the FDH found in *Clostridium pasteurianum* (discussed below). This FDH (CLPA_c10260), was shown to fix CO$_2$ into formate (Jungermann, Kirchniawy et al. 1970), however, no more reports of the activity of this enzyme have been published to our knowledge. The FDH complex contains various molybdenum containing proteins (mobE and B), a ferredoxin (Fd), and an electron transport protein (HydN) (Figure 6.1). It may be necessary to express all subunit to achieve proper function. The whole complex (5 kb) should be feasible to express in *Clostridium acetobutylicum*.

Figure 6.1. Operon structure of the formate dehydrogenase found in *Clostridium pasteurianum* (CLPA_c10260 – 10300). The total lenght is 5147 nucleotides.
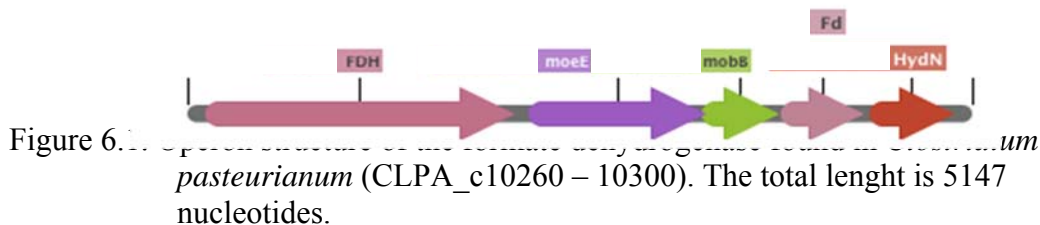
6.1.3 Alternative Hosts for Synthetic CO$_2$ Fixation

Clostridium beijerinckii and *Clostridium pasteurianum* are excellent candidates to further interrogate installing a synthetic CO$_2$ fixation pathway. *Clostridium beijerinckiii* has been shown to contain the recently discovered energy conservation mechanism involving ferredoxin-mediated bifurcated electron transport via a membrane-bound RNF (*Rhodobacter* nitrogen fixation) complex (Poehlein, Solano et al. 2017). This complex could be important for CO$_2$ fixation, as almost all acetogens are found to contain such a complex (Schuchmann and Müller 2014). The RNF complex does not exist in *Clostridium acetobutylicum* (Poehlein, Solano et al. 2017). *Clostridium beijerinckiii* is the only solvent producing clostridium organisms that is also able to produce 2,3 butanediol. It also produces 1,3 propanediol and isopropanol (Poehlein, Solano et al. 2017). Therefore *Clostridium beijerinckiii* exhibits a very wide product profile which could be important for a industrial host for microbial fermentation.

Another potential host is *Clostridium pasteurianum. Clostridium pasteurianum* already contains multiple carbon monoxide dehydrogenases (CLPA_c05080, anaerobic-type carbon monoxide dehydrogenase and CLPA_c34390, carbon-

162

monoxide dehydrogenase catalytic subunit) and a formate dehydrogenase (CLPA_c10260). The activity of the carbon monoxide dehydrogenase has been reported in the 1980's (Fuchs, Schnitker et al. 1974, Diekert, Graf et al. 1979), however, in our lab we were unable to verify the oxidation of CO by *Clostridium pasteurianum (ATCC 6013)*. The presence of the formate dehydrogenase activity has previously been published by Thauer *et al*. (Jungermann, Kirchniawy et al. 1970). The activity of the formate dehydrogenase in *Clostridium pasteurianum* has been verified in our lab. Cells of *Clostridium pasteurianum* were grown in clostridial growth media (CGM), and inoculated into 5 ml of fresh CGM media supplemented with 200 µM nickel. The headspace was 20% CO_2 balance hydrogen (10 psig). The cultures were either supplemented with 50 mM ^{13}C-sodium bicarbonate or 20 mM ^{13}C - sodium formate. A control employing unlabeled ^{12}C-sodium bicarbonate was used. Figure 6.2 shows the increase in labeling in CO_2 during the fermentation of *Clostridium pasteurianum* in the presence of ^{13}C - sodium formate, indicating oxidation of formate towards CO_2 and H_2. To further determine if the CO_2 is incorporated, we completed amino acid analysis in a collaboration with the Antoniewicz lab. Figure 6.3 demonstrates the incorporation of labeling into alanine, serine, aspartate and glutamate in the cultures containing ^{13}C-sodium bicarbonate. Labeling was also observed in alanine and serine for the experiment the cultures containing ^{13}C-sodium formate. The high labeling in serine when exposed to ^{13}C-sodium bicarbonate indicates that the $^{13}CO_2$ is incorporated via the C1-pool. Aspartate and glutamate labeling occurs via the carboxylation of pyruvate to oxaloacaetate (Amador-Noguez, Feng et al. 2010). During the carboxylation step, labeled CO_2 can be incorporated, resulting in the labeled amino acids. From these preliminary results, it is clear that some of the CO_2

fixation enzymes already exist in *Clostridium pasteurianum*, and therefore would require fewer engineering efforts to achieve a complete and functional Wood-Ljungdahl pathway in this strain. Transformation procedures have been developed and are well established (Pyne, Bruder et al. 2014).
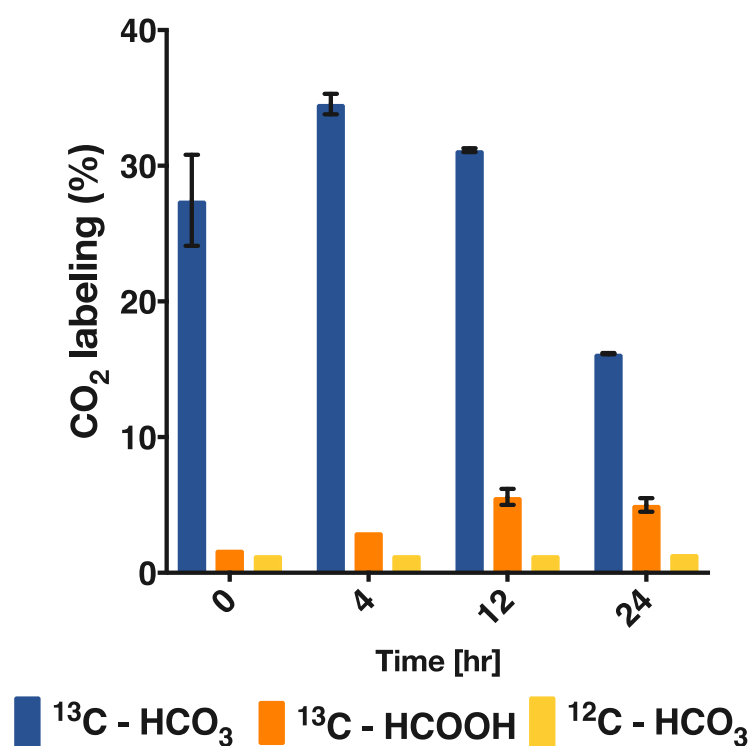
Figure 6.2. Percent labeling in CO_2 of *Clostridium pasteurianum* cultures supplemented with labeled bicarbonate (blue), labeled formate (orange) and unlabeled bicarbonate as control (yellow). The percent labeling in CO_2 is high for the cultures supplemented with labeled CO_2, as expected. The cultures containing the labeled formate also exhibited small amounts of labeling, indicating oxidation of ^{13}C-formate to $^{13}CO_2$ and H_2. The control did not show labeling in CO_2 above natural abundance (~1%).
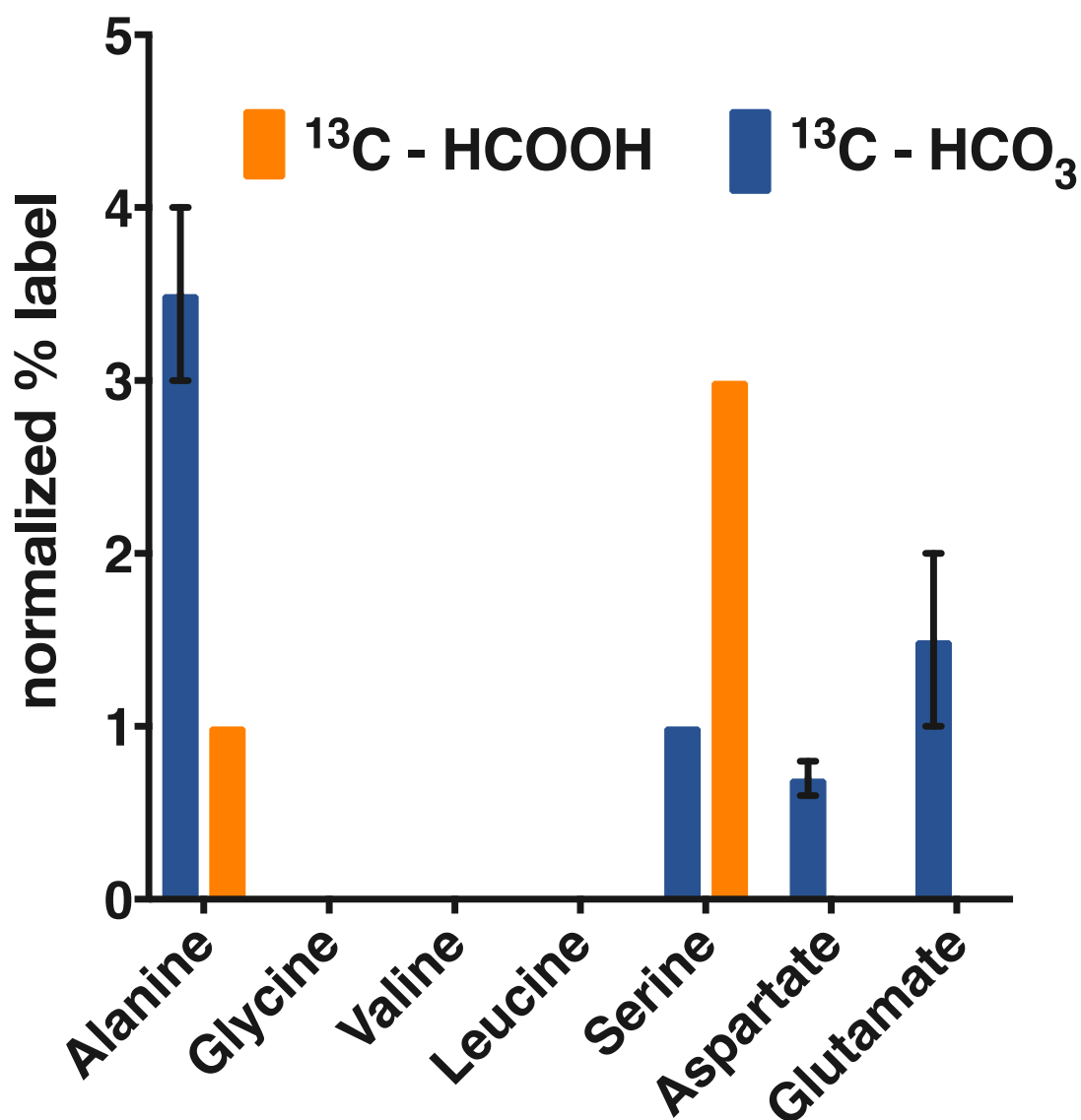
Figure 6.3. Percent labeling in amino acids of *Clostridium pasteurianum* cultures supplemented with labeled bicarbonate (blue), labeled formate (orange). The high labeling in serine indicates $^{13}CO_2$ is reduced towards formate, labeling the internal C-pool and therefore serine. The control did not show labeling in any of the amino acids above natural abundance (~1%). The axis shows the labeling above that of natural abundance.

6.1.4 Interrogating the Last Step of the Wood-Ljungdahl Pathway

The heterologous expression of the carbon monoxide dehydrogenase/acetyl-CoA synthase in *Clostridium acetobutylicum*, already demonstrated the successful function of the CODH enzyme from an acetogen without further codon optimization (Carlson and Papoutsakis 2017). We were unable to be verify the ACS enzyme activity, probably due to the low exchange activity that is observed even in purified enzyme extracts. To further interrogate the ACS enzyme activity, additional genes need to be co-expressed to successfully demonstrate the cleavage of acetyl-CoA into CO and a methyl group. The first set of genes are the Corrinoid-Iron sulfur protein (CFeSP, *acsC* and *acsD*) found in the Wood-Ljungdahl pathway, along with the methyltransferase protein (*acsE*). Together with the ACS (*acsB* and *acsF*), the cleavage of acetyl-CoA to CO and a C1-methyl moiety should be realized. Zhuang *et al.* were able to demonstrate the release of ^{13}CO from 1-^{13}C-acetate in the presence of an incomplete Wood-Ljungdahl pathway (Zhuang, Yi et al. 2014). The authors identified the genes contained in the *Dehalococcoides mccartyi* strain, and found that *acsB, acsF, acsC, acsD* and *acsE* were all contained on the genome, indicating the necessity of these genes to facilitate the release of CO. Because of the sensitivity in our current instrumental set up using GC-MS, the release of the CO molecule can be monitored. The plasmid containing the necessary genes is already constructed in *E. coli*, however, it has yet to be transformed into the *Clostridium acetobutylicum* host successfully. Some preliminary western blots on the *Escherichia coli* strain could confirmed the successful expression of these genes, as they have been expressed in *E. coli* before (Roberts, James-Hagstrom et al. 1989). Amino acid labeling in the presence of both 1-^{13}C-acetate and 2-^{13}C-acetate could further interrogate the functional expression of the genes contained on the plasmid. The successful

transformation and expression of these genes in *Clostridium pasteurianum* would also be interesting, as it is possible that the already existing carbon monoxide dehydrogenases could interact with the ACS complex, thereby providing a complete, synthetic Wood-Ljungdahl pathway.

These suggestions offer many possibilities to further interrogate achieving synthetic CO_2 fixation in a non-native CO_2 fixing host, such as *Clostridium acetobutylicum* or *Clostridium pasteurianum*. With the increasing demand for alternative energies and the imminent threat of the critical levels of atmospheric CO_2 concentrations, research in CO_2 fixation and sequestration has never been more important to the future or our planet.

REFERENCES

Abrini, J., H. Naveau and E. J. Nyns (1994). "*Clostridium autoethanogenum*, sp. nov., an anaerobic bacterium that produces ethanol from carbon monoxide." <u>Archives of Microbiology</u> **161**: 345-351.

Al-Hinai, M. A., A. G. Fast and E. T. Papoutsakis (2012). "Novel system for efficient isolation of clostridium double-crossover allelic exchange mutants enabling markerless chromosomal gene deletions and DNA integration." <u>Applied and environmental microbiology</u> **78**: 8112-8121.

Amador-Noguez, D., X.-J. Feng, J. Fan, N. Roquet, H. Rabitz and J. D. Rabinowitz (2010). "Systems-level metabolic flux profiling elucidates a complete, bifurcated tricarboxylic acid cycle in *Clostridium acetobutylicum*." <u>Journal of bacteriology</u> **192**(17): 4452-4461.

Aresta, M. (2010). "Carbon Dioxide as Chemical Feedstock." <u>Carbon Dioxide as Chemical Feedstock</u>.

Au, J., J. Choi, S. W. Jones, K. P. Venkataramanan and M. R. Antoniewicz (2014). "Parallel labeling experiments validate *Clostridium acetobutylicum* metabolic network model for 13C metabolic flux analysis." <u>Metabolic Engineering</u> **26**: 23-33.

Au, J., J. Choi, S. W. Jones, K. P. Venkataramanan and M. R. Antoniewicz (2014). "Parallel labeling experiments validate Clostridium acetobutylicum metabolic network model for (13)C metabolic flux analysis." <u>Metab Eng</u> **26**: 23-33.

Bar-Even, A., E. Noor and R. Milo (2012). "A survey of carbon fixation pathways through a quantitative lens." <u>Journal of experimental botany</u> **63**: 2325-2342.

Bender, G., E. Pierce, J. a. Hill, J. E. Darty and S. W. Ragsdale (2011). "Metal centers in the anaerobic microbial metabolism of CO and CO_2." <u>Metallomics : integrated biometal science</u> **3**: 797-815.

Bertsch, J. and V. Müller (2015). "CO Metabolism in the Acetogen *Acetobacterium woodii*." <u>Applied and Environmental Microbiology</u> **81**: 5949-5956.

Bogorad, I. W., T.-S. Lin and J. C. Liao (2013). "Synthetic non-oxidative glycolysis enables complete carbon conservation." <u>Nature</u>: 1-6.

Braun, K. and G. Gottschalk (1981). "Effect of molecular hydrogen and carbon dioxide on chemo-organotrophic growth of *Acetobacterium woodii* and *Clostridium aceticum*." <u>Archives of Microbiology</u> **128**: 294-298.

Braun, K. and G. Gottschalk (1981). "Effect of Molecular-Hydrogen and Carbon-Dioxide on Chemo-Organotrophic Growth of Acetobacterium-Woodii and Clostridium-Aceticum." <u>Archives of Microbiology</u> **128**(3): 294-298.

Bruant, G., M.-J. Lévesque, C. Peter, S. R. Guiot and L. Masson (2010). "Genomic analysis of carbon monoxide utilization and butanol production by *Clostridium carboxidivorans* strain P7." PloS one **5**: e13033.

Can, M., F. a. Armstrong and S. W. Ragsdale (2014). "Structure, function, and mechanism of the nickel metalloenzymes, CO dehydrogenase, and acetyl-CoA synthase." Chemical Reviews **114**: 4149-4174.

Carlson, E. D. and E. T. Papoutsakis (2017). "Heterologous Expression of the *Clostridium carboxidivorans* CO Dehydrogenase Alone or Together with the Acetyl Coenzyme A Synthase Enables Both Reduction of CO_2 and oxidation of CO by *Clostridium acetobutylicum*." Applied and Environmental Microbiology: AEM.00829-00817.

Ceccaldi, P., K. Schuchmann, V. Muller and S. J. Elliott (2017). "The hydrogen dependent CO2 reductase: the first completely CO tolerant FeFe-hydrogenase." Energy & Environmental Science **10**(2): 503-508.

Clomburg, J. M., A. M. Crumbley and R. Gonzalez (2017). "Industrial biomanufacturing: The future of chemical production." Science **355**.

Cooksley, C. M., Y. Zhang, H. Wang, S. Redl, K. Winzer and N. P. Minton (2012). "Targeted mutagenesis of the *Clostridium acetobutylicum* acetone–butanol–ethanol fermentation pathway." Metabolic Engineering **14**(6): 630-641.

Cornish, A. J., K. Gärtner, H. Yang, J. W. Peters and E. L. Hegg (2011). "Mechanism of Proton Transfer in [FeFe]-Hydrogenase from Clostridium pasteurianum." The Journal of Biological Chemistry **286**(44): 38341-38347.

Cotter, J. L., M. S. Chinn and A. M. Grunden (2009). "Ethanol and acetate production by Clostridium ljungdahlii and Clostridium autoethanogenum using resting cells." Bioprocess and Biosystems Engineering **32**(3): 369-380.

Covert, M. W. (2014). Fundamentals of Systems Biology: From Synthetic Circuits to Whole-cell Models, CRC Press.

Daniel, S. L., T. Hsu, S. I. Dean and H. L. Drake (1990). "Characterization of the H2- and CO-dependent chemolithotrophic potentials of the acetogens Clostridium thermoaceticum and Acetogenium kivui." Journal of Bacteriology **172**(8): 4464-4471.

Daniels, L., G. Fuchs, R. K. Thauer and J. G. Zeikus (1977). "Carbon monoxide oxidation by methanogenic bacteria." Journal of Bacteriology **132**: 118-126.

Datta, R. and J. G. Zeikus (1985). Modulation of acetone-butanol-ethanol fermentation by carbon monoxide and organic acids. Applied and Environmental Microbiology. **49:** 522-529.

Demuez, M., L. Cournac, O. Guerrini, P. Soucaille and L. Girbal (2007). "Complete activity profile of Clostridium acetobutylicum [FeFe]-hydrogenase and kinetic parameters for endogenous redox partners." FEMS Microbiology Letters **275**(1): 113-121.

Diekert, G. and M. Ritter (1983). "Purification of the nickel protein carbon monoxide dehydrogenase of Clostridium thermoaceticum." FEBS Letters **151**(1): 41-44.

Diekert, G. and R. K. Thauer (1980). "The effect of nickel on carbon monoxide dehydrogenase formation in *Clostridium thermoaceticum* and *Clostridium formicoaceticum*." FEMS Microbiol. Lett. **7**: 187-189.

Diekert, G. B., E. G. Graf and R. K. Thauer (1979). "Nickel requirement for carbon monoxide dehydrogenase formation in Clostridium pasteurianum." Archives of Microbiology **122**(1): 117-120.

Diekert, G. B. and R. K. Thauer (1978). "Carbon monoxide oxidation by *Clostridium thermoaceticum* and *Clostridium formicoaceticum*." J. Bacteriol. **136**: 597-606.

Doukov, T. I., T. M. Iverson, J. Seravalli, S. W. Ragsdale and C. L. Drennan (2002). "A Ni-Fe-Cu center in a bifunctional carbon monoxide dehydrogenase/acetyl-CoA synthase." Science **298**: 567-572.

Drake, H. L., A. S. Gössner and S. L. Daniel (2008). "Old acetogens, New light." Annals of the New York Academy of Sciences **1125**: 100-128.

Drake, H. L., S. I. Hu and H. G. Wood (1980). "Purification of carbon monoxide dehydrogenase, a nickel enzyme from *Clostridium thermoaceticum*." Journal of Biological Chemistry **255**: 7174-7180.

Fast, A. G. and E. T. Papoutsakis (2012). "Stoichiometric and energetic analyses of non-photosynthetic CO_2-fixation pathways to support synthetic biology strategies for production of fuels and chemicals." Current Opinion in Chemical Engineering **1**(4): 380-395.

Fast, A. G., E. D. Schmidt, S. W. Jones and B. P. Tracy (2015). "Acetogenic mixotrophy: novel options for yield improvement in biofuels and biochemicals production." Current Opinion in Biotechnology **33**: 60-72.

Fernández-Naveira, Á., M. C. Veiga and C. Kennes (2017). "H-B-E (Hexanol-Butanol-Ethanol) fermentation for the production of higher alcohols from syngas/waste gas." Journal of Chemical Technology & Biotechnology: 712-731.

Fontaine, F. E. (1942). "A new type of glucose fermentation by Clostridium thermoaceticum." J. Bacteriol. **43**: 701-715.

Fontaine, F. E., W. H. Peterson, E. McCoy, M. J. Johnson and G. J. Ritter (1942). "A new type of glucose fermentation by Clostridium thermoaceticum n sp." Journal of Bacteriology **43**(6): 701-715.

Fuchs, G., U. Schnitker and R. K. Thauer (1974). "Carbon Monoxide Oxidation by Growing Cultures of *Clostridium pasteurianum*." Eur. J. Biochem **49**: 111-115.

Furdui, C. and S. W. Ragsdale (2000). "The role of pyruvate ferredoxin oxidoreductase in pyruvate synthesis during autotrophic growth by the Wood-Ljungdahl pathway." The Journal of Biological Chemistry **275**(37): 28494-28499.

Genthner, B. R. S. and M. P. Bryant (1987). "Additional characteristics of one-carbon-compound utilization by *Eubacterium limosum* and *Acetobacterium woodii*." Applied and Environmental Microbiology **53**: 471-476.

Gray, C. T. and H. Gest (1965). "Biological Formation of Molecular Hydrogen." Science **148**: 186-192.

Gregg, C. M., S. Goetzl, J. H. Jeoung and H. Dobbek (2016). "AcsF catalyzes the ATP-dependent insertion of Nickel into the Ni, Ni-[4Fe4S] cluster of Acetyl-CoA synthase." Journal of Biological Chemistry **291**: 18129-18138.

Hadj-Saïd, J., M. E. Pandelia, C. Léger, V. Fourmond and S. Dementin (2015). "The Carbon Monoxide Dehydrogenase from *Desulfovibrio vulgaris*." Biochimica et Biophysica Acta - Bioenergetics **1847**: 1574-1583.

Heijstra, B. D., C. Leang and A. Juminaga (2017). "Gas fermentation: cellular engineering possibilities and scale up." Microbial cell factories **16**(1): 60.

Hönicke, D., H. Janssen, C. Grimmler, A. Ehrenreich and T. Lütke-Eversloh (2012). "Global transcriptional changes of Clostridium acetobutylicum cultures with increased butanol:acetone ratios." New Biotechnology **29**(4): 485-493.

IEA, I. E. A. (2016). "CO2 emissions from fuel combustion." 166.

Jang, Y.-S., J. A. Im, S. Y. Choi, J. I. Lee and S. Y. Lee (2014). "Metabolic engineering of Clostridium acetobutylicum for butyric acid production with high butyric acid selectivity." Metabolic Engineering **23**: 165-174.

Jeong, J., J. Bertsch, V. Hess, S. Choi, I.-G. Choi, I. S. Chang and V. Müller (2015). "Energy conservation model based on genomic and experimental analyses of a carbon monoxide-utilizing, butyrate-forming acetogen, Eubacterium limosum KIST612." Applied and environmental microbiology **81**(14): 4782-4790.

Jeoung, J.-H. and H. Dobbek (2007). "Carbon dioxide activation at the Ni, Fe-cluster of anaerobic carbon monoxide dehydrogenase." Science **318**(5855): 1461-1464.

Jones, D. T. and D. R. Woods (1986). "Acetone-butanol fermentation revisited." Microbiological reviews **50**: 484-524.

Jones, S. W., A. G. Fast, E. D. Carlson, C. A. Wiedel, J. Au, M. R. Antoniewicz, E. T. Papoutsakis and B. P. Tracy (2016). "CO2 fixation by anaerobic non-photosynthetic mixotrophy for improved carbon conversion." Nature Communications **7**: 12800.

Jones, S. W., C. J. Paredes, B. Tracy, N. Cheng, R. Sillers, R. S. Senger and E. T. Papoutsakis (2008). "The transcriptional program underlying the physiology of clostridial sporulation." Genome Biology **9**(7): R114-R114.

Jungermann, K., H. Kirchniawy and R. K. Thauer (1970). "Ferredoxin dependent CO2 reduction to formate in clostridium pasteurianum." Biochemical and Biophysical Research Communications **41**(3): 682-689.

Kerby, R. L., P. W. Ludden and G. P. Roberts (1997). "*In vivo* nickel insertion into the carbon monoxide dehydrogenase of *Rhodospirillum rubrum:* Molecular and physiological characterization of cooCTJ." Journal of Bacteriology **179**: 2259-2266.

Kim, B., P. Bellows, R. Datta and J. Zeikus (1984). "Control of Carbon and Electron Flow in *Clostridium acetobutylicum* Fermentations: Utilization of." Applied and Environmental Microbiology **48**: 764-770.

Kim, B. H. and G. J. Zeikus (1992). "Hydrogen Metabolism in *Clostridium acetobutylicum* Fermentation." Journal of Microbiology and Biotechnology **2**: 248-254.

Klein, M., M. B. Ansorge-Schumacher, M. Fritsch and W. Hartmeier (2010). "Influence of hydrogenase overexpression on hydrogen production of *Clostridium acetobutylicum* DSM 792." Enzyme and Microbial Technology **46**(5): 384-390.

Kopke, M., C. Held, S. Hujer, H. Liesegang, A. Wiezer, A. Wollherr, A. Ehrenreich, W. Liebl, G. Gottschalk and P. Durre (2010). "Clostridium ljungdahlii represents a microbial production platform based on syngas." Proceedings of the National Academy of Sciences of the United States of America **107**(29): 13087-13092.

Köpke, M., C. Mihalcea, J. C. Bromley and S. D. Simpson (2011). "Fermentative production of ethanol from carbon monoxide." Current opinion in biotechnology **22**: 320-325.

Köpke, M., C. Mihalcea, F. Liew, J. H. Tizard, M. S. Ali, J. J. Conolly, B. Al-Sinawi and S. D. Simpson (2011). "2,3-butanediol production by acetogenic bacteria, an alternative route to chemical synthesis, using industrial waste gas." Applied and environmental microbiology **77**: 5467-5475.

Köpke, M., C. Mihalcea, F. M. Liew, J. H. Tizard, M. S. Ali, J. J. Conolly, B. Al-Sinawi and S. D. Simpson (2011). "2,3-Butanediol Production by Acetogenic Bacteria, an Alternative Route to Chemical Synthesis, Using Industrial Waste Gas." Applied and Environmental Microbiology **77**(15): 5467-5475.

Liew, F., A. M. Henstra, M. Köpke, K. Winzer, S. D. Simpson and N. P. Minton (2017). "Metabolic Engineering of *Clostridium autoethanogenum* for Selective Alcohol Production." Metabolic Engineering.

Liew, F., A. M. Henstra, K. Winzer, M. Köpke, S. D. Simpson and N. P. Minton (2016). "Insights into CO$_2$ Fixation Pathway of *Clostridium autoethanogenum* by Targeted Mutagenesis." mBio **7**: e00427-00416.

Liew, F., M. E. Martin, R. C. Tappel, B. D. Heijstra, C. Mihalcea and M. Köpke (2016). "Gas Fermentation—A Flexible Platform for Commercial Scale Production of Low-Carbon-Fuels and Chemicals from Waste and Renewable Feedstocks." Frontiers in Microbiology **7**.

Liou, J. S.-C., D. L. Balkwill, G. R. Drake and R. S. Tanner (2005). "*Clostridium carboxidivorans* sp. nov., a solvent-producing clostridium isolated from an agricultural settling lagoon, and reclassification of the acetogen *Clostridium scatologenes* strain SL1 as *Clostridium drakei* sp. nov." International journal of systematic and evolutionary microbiology **55**: 2085-2091.

Ljungdahl, L. G. (2009). "A Life with Acetogens, Thermophiles, and Cellulolytic Anaerobes." Annual Review of Microbiology **63**(1): 1-25.

Loke, H. K., G. N. Bennett and P. A. Lindahl (2000). "Active acetyl-CoA synthase from *Clostridium thermoaceticum* obtained by cloning and heterologous expression of acsAB in *Escherichia coli*." Proceedings of the National Academy of Sciences of the United States of America **97**: 12530-12535.

Loke, H. K., X. Tan and P. A. Lindahl (2002). "Genetic construction of truncated and chimeric metalloproteins derived from the alpha subunit of acetyl-CoA synthase from *Clostridium thermoaceticum*." Journal of the American Chemical Society **124**: 8667-8672.

Martin, M. E., H. Richter, S. Saha and L. T. Angenent (2016). "Traits of selected Clostridium strains for syngas fermentation to ethanol." Biotechnology and Bioengineering **113**(3): 531-539.

Maynard, E. L. and P. A. Lindahl (1999). "Evidence of a Molecular Tunnel Connecting the Active Sites for CO_2 Reduction and Acetyl-CoA Synthesis in Acetyl-CoA Synthase from *Clostridium thermoaceticum*." J. Am. Chem. Soc. **121**: 9221-9222.

Maynard, E. L. and P. A. Lindahl (2001). "Catalytic coupling of the active sites in acetyl-CoA synthase, a bifunctional CO-channeling enzyme." Biochemistry **40**: 13262-13267.

Mermelstein, L. D. and E. T. Papoutsakis (1993). "In vivo methylation in *Escherichia coli* by the *Bacillus subtilis* phage phi 3T I methyltransferase to protect plasmids from restriction upon transformation of *Clostridium acetobutylicum* ATCC 824." Applied and Environmental Microbiology **59**: 1077-1081.

Mermelstein, L. D., N. E. Welker, G. N. Bennett and E. T. Papoutsakis (1992). "Expression of cloned homologous fermentative genes in *Clostridium acetobutylicum* ATCC 824." Biotechnology **10**: 190-195.

Meyer, C. L. and E. T. Papoutsakis (1989). "Increased Levels of ATP and NADH Are Associated with Increased Solvent Production in Continuous Cultures of *Clostridium-Acetobutylicum*." Applied Microbiology and Biotechnology **30**(5): 450-459.

Meyer, C. L., E. T. Papoutsakis and J. k. McLaughlin (1985). "The effect of CO on growth and product formation in batch cultures of *Clostridium acetobutylicum*." Biotechnology Letters **7**: 37-42.

Meyer, C. L., J. W. Roos and E. T. Papoutsakis (1986). "Carbon monoxide gasing leads to alcohol production and butyrate uptake without acetone formation in continuous cultures of *Clostridium acetobutylicum*." Applied Microbiology and Biotechnology **24**: 159-167.

Mock, J., Y. Zheng, A. P. Mueller, S. Ly, L. Tran, S. Segovia, S. Nagaraju, M. Köpke, P. Dürre and R. K. Thauer (2015). "Energy conservation associated with ethanol formation from H2 and CO2 in Clostridium autoethanogenum involving electron bifurcation." Journal of bacteriology **197**(18): 2965-2980.

Moersdorf, G., K. Frunzke, D. Gadkari and O. Meyer (1992). "Microbial growth on carbon monoxide." Biodegradation **3**: 61-82.

Mohammadi, M., A. R. Mohamed, G. D. Najafpour, H. Younesi and M. H. Uzir (2014). "Kinetic studies on fermentative production of biofuel from synthesis gas using *Clostridium ljungdahlii*." ScientificWorldJournal **2014**: 910590.

Müller, V. (2003). "Energy Conservation in Acetogenic Bacteria." Applied and environmental microbiology **69**.

Nagarajan, H., M. Sahin, J. Nogales, H. Latif, D. R. Lovley, A. Ebrahim and K. Zengler (2013). "Characterizing acetogenic metabolism using a genome-scale metabolic reconstruction of Clostridium ljungdahlii." Microbial Cell Factories **12**: 118-118.

Nagarajan, H., M. Sahin, J. Nogales, H. Latif, D. R. Lovley, A. Ebrahim and K. Zengler (2013). "Characterizing acetogenic metabolism using a genome-scale metabolic reconstruction of Clostridium ljungdahlii." Microbial cell factories **12**: 118.

Obama, B. (2017). "The irreversible momentum of clean energy." Science **6284**.

Orth, J. D., I. Thiele and B. O. Palsson (2010). "What is flux balance analysis?" Nat Biotech **28**(3): 245-248.

Papoutsakis, E. T. (1984). "Equations and calculations for fermentations of butyric acid bacteria." Biotechnology and Bioengineering **26**(2): 174-187.

Papoutsakis, E. T. (1984). "Equations and calculations for fermentations of butyric acid bacteria." Biotechnol Bioeng **26**(2): 174-187.

Papoutsakis, E. T. (2008). "Engineering solventogenic clostridia." Current Opinion in Biotechnology **19**(5): 420-429.

Papoutsakis, E. T. (2008). "Engineering solventogenic clostridia." Current opinion in biotechnology **19**: 420-429.

Papoutsakis, E. T., C. Wu and K. Venkataramanan (2013). "Transcription factors and genetic circuits orchestrating the complex, multilayered response of *Clostridium acetobutylicum* to butanol and butyrate stress." BMC Systems Biology **7**: 120.

Phillips, J. R., H. K. Atiyeh, R. S. Tanner, J. R. Torres, J. Saxena, M. R. Wilkins and R. L. Huhnke (2015). "Butanol and hexanol production in Clostridium carboxidivorans syngas fermentation: Medium development and culture techniques." Bioresource Technology **190**: 114-121.

Poehlein, A., J. D. M. Solano, S. K. Flitsch, P. Krabben, K. Winzer, S. J. Reid, D. T. Jones, E. Green, N. P. Minton, R. Daniel and P. Dürre (2017). "Microbial solvent formation revisited by comparative genome analysis." Biotechnology for Biofuels **10**(1): 58.

Pyne, M. E., M. Bruder, M. Moo-Young, D. a. Chung, C. P. Chou and C. Perry Chou (2014). "Technical guide for genetic advancement of underdeveloped and intractable Clostridium." Biotechnology advances **32**: 623-641.

Ragsdale, S. W. (1991). "Enzymology of the acetyl-CoA pathway of CO_2 fixation." Critical reviews in biochemistry and molecular biology **26**: 261-300.

Ragsdale, S. W. (2009). "Nickel-based enzyme systems." Journal of Biological Chemistry **284**(28): 18571-18575.

Ragsdale, S. W., J. E. Clark, L. G. Ljungdahl, L. L. Lundie and H. L. Drake (1983). "Properties of purified carbon monoxide dehydrogenase from *Clostridium thermoaceticum*, a nickel, iron-sulfur protein." The Journal of biological chemistry **258**: 2364-2369.

Ragsdale, S. W. and M. Kumar (1996). "Nickel-Containing Carbon Monoxide Dehydrogenase/Acetyl-CoA Synthase." Chemical Reviews **96**(7): 2515-2540.

Ragsdale, S. W. and E. Pierce (2008). "Acetogenesis and the Wood-Ljungdahl pathway of CO_2 fixation." Biochimica et Biophysica Acta **1784**: 1873-1898.

Ramachandriya, K. D., D. K. Kundiyana, M. R. Wilkins, J. B. Terrill, H. K. Atiyeh and R. L. Huhnke (2013). "Carbon dioxide conversion to fuels and chemicals using a hybrid green process." Applied Energy **112**: 289-299.

Roberts, D. L., J. E. James-Hagstrom, D. K. Garvin, C. M. Gorst, J. A. Runquist, J. R. Baur, F. C. Haase and S. W. Ragsdale (1989). "Cloning and expression of the gene cluster encoding key proteins involved in acetyl-CoA synthesis in Clostridium thermoaceticum: CO dehydrogenase, the corrinoid/Fe-S protein, and methyltransferase." Proceedings of the National Academy of Sciences **86**(1): 32-36.

Roberts, D. L., J. E. James-Hagstrom, D. K. Garvin, C. M. Gorst, J. a. Runquist, J. R. Baur, F. C. Haase and S. W. Ragsdale (1989). "Cloning and expression of the gene cluster encoding key proteins involved in acetyl-CoA synthesis in *Clostridium thermoaceticum*: CO dehydrogenase, the corrinoid/Fe-S protein, and methyltransferase." Proceedings of the National Academy of Sciences of the United States of America **86**: 32-36.

Roos, J. W., J. K. McLaughlin and E. T. Papoutsakis (1985). "The effect of pH on nitrogen supply, cell lysis, and solvent production in fermentations of *Clostridium acetobutylicum*." Biotechnology and bioengineering **27**(5): 681-694.

Russell, M. J., W. Nitschke and E. Branscomb (2013). "The inevitable journey to being." Philosophical Transactions of the Royal Society B: Biological Sciences **368**.

Schuchmann, K. and V. Müller (2013). "Direct and reversible hydrogenation of CO_2 to formate by a bacterial carbon dioxide reductase." Science **342**: 1382-1385.

Schuchmann, K. and V. Müller (2014). "Autotrophy at the thermodynamic limit of life: a model for energy conservation in acetogenic bacteria." Nature reviews. Microbiology **12**: 809-821.

Schut, G. J., G. L. Lipscomb, D. M. N. Nguyen, R. M. Kelly and M. W. W. Adams (2016). "Heterologous Production of an Energy-Conserving Carbon Monoxide Dehydrogenase Complex in the Hyperthermophile Pyrococcus furiosus." Frontiers in Microbiology **7**(29).

Seifritz, C., J. M. Fröstl, H. L. Drake and S. L. Daniel (2002). "Influence of nitrate on oxalate- and glyoxylate-dependent growth and acetogenesis by Moorella thermoacetica." Archives of Microbiology **178**(6): 457-464.

Shanmugasundaram, T. and H. G. Wood (1992). "Interaction of ferredoxin with carbon monoxide dehydrogenase from *Clostridium thermoaceticum*." Journal of Biological Chemistry **267**: 897-900.

Shin, W. and P. A. Lindahl (1992). "Function and carbon monoxide binding properties of the nickel-iron complex in carbon monoxide dehydrogenase from *Clostridium thermoaceticum*." Biochemistry **31**: 12870-12875.

Svetlitchnyi, V., H. Dobbek, W. Meyer-Klaucke, T. Meins, B. Thiele, P. Romer, R. Huber and O. Meyer (2004). "A functional Ni-Ni-[4Fe-4S] cluster in the monomeric acetyl-CoA synthase from *Carboxydothermus hydrogenoformans*." Proceedings of the National Academy of Sciences **101**: 446-451.

Tan, X. and P. A. Lindahl (2008). "Tunnel mutagenesis and Ni-dependent reduction and methylation of the alpha subunit of acetyl coenzyme A synthase/carbon monoxide dehydrogenase." Journal of Biological Inorganic Chemistry **13**: 771-778.

Tan, X., H.-K. Loke, S. Fitch and P. a. Lindahl (2005). "The tunnel of acetyl-coenzyme a synthase/carbon monoxide dehydrogenase regulates delivery of CO to the active site." Journal of the American Chemical Society **127**: 5833-5839.

Tan, Y., J. J. Liu, X. H. Chen, H. J. Zheng and F. L. Li (2013). "RNA-seq-based comparative transcriptome analysis of the syngas-utilizing bacterium Clostridium ljungdahlii DSM 13528 grown autotrophically and heterotrophically." Molecular Biosystems **9**(11): 2775-2784.

Thakker, C., I. Martínez, K.-Y. San and G. N. Bennett (2012). "Succinate production in Escherichia coli." Biotechnology journal **7**(2): 213-224.

Tracy, B. P., S. W. Jones, A. G. Fast, D. C. Indurthi and E. T. Papoutsakis (2012). "Clostridia: the importance of their exceptional substrate and metabolite diversity for biofuel and biorefinery applications." Curr. Op. Biotechnol. **23**(0): 364-381

Tracy, B. P., S. W. Jones, A. G. Fast, D. C. Indurthi and E. T. Papoutsakis (2012). "Clostridia: the importance of their exceptional substrate and metabolite diversity for biofuel and biorefinery applications." Current opinion in biotechnology **23**: 364-381.

Tremblay, P.-L., T. Zhang, S. A. Dar, C. Leang and D. R. Lovley (2013). "The Rnf Complex of Clostridium ljungdahlii Is a Proton-Translocating Ferredoxin:NAD+ Oxidoreductase Essential for Autotrophic Growth." mBio **4**(1).

Tummala, S. B., N. E. Welker and E. T. Papoutsakis (1999). "Development and characterization of a gene expression reporter system for *Clostridium acetobutylicum* ATCC 824." Applied and Environmental Microbiology **65**: 3793-3799.

Ukpong, M. N., H. K. Atiyeh, M. J. M. De Lorme, K. Liu, X. Zhu, R. S. Tanner, M. R. Wilkins and B. S. Stevenson (2012). "Physiological response of Clostridium carboxidivorans during conversion of synthesis gas to solvents in a gas-fed bioreactor." Biotechnology and Bioengineering **109**(11): 2720-2728.

Volbeda, A. and J. Fontecilla-Camps (2004). "Crystallographic evidence for a CO/CO$_2$ tunnel gating mechanism in the bifunctional carbon monoxide dehydrogenase/acetyl coenzyme A synthase from *Moorella thermoacetica*." Journal of Biological Inorganic Chemistry **9**: 525-532.

Wang, S., H. Huang, J. Kahnt, A. P. Mueller, M. Kopke and R. K. Thauer (2013). "NADP-specific electron-bifurcating [FeFe]-hydrogenase in a functional complex with formate dehydrogenase in Clostridium autoethanogenum grown on CO." J Bacteriol **195**(19): 4373-4386.

Wang, V. C.-C., S. W. Ragsdale and F. a. Armstrong (2013). "Investigations of Two Bidirectional Carbon Monoxide Dehydrogenases from *Carboxydothermus hydrogenoformans* by Protein Film Electrochemistry." Chembiochem : a European journal of chemical biology **0606**: 1-8.

Wietzke M, B. H. (2012). "The redox-sensing protein Rex, a transcriptional regulator of solventogenesis in *Clostridium acetobutylicum*." Appl Environ Microbiol **96**: 749–761.

Yagi, T. (1958). "Enzymic oxidation of carbon monoxide." Biochimica et Biophysica Acta **30**(1): 194-195.

Yerushalmi, L., B. Volesky and T. Szczesny (1985). "Effect of increased hydrogen partial pressure on the acetone-butanol fermentation by *Clostridium acetobutylicum*." Applied Microbiology and Biotechnology **22**: 103-107.

Yim, H., R. Haselbeck, W. Niu, C. Pujol-Baxley, A. Burgard, J. Boldt, J. Khandurina, J. D. Trawick, R. E. Osterhout, R. Stephen, J. Estadilla, S. Teisan, H. B. Schreyer, S. Andrae, T. H. Yang, S. Y. Lee, M. J. Burk and S. Van Dien (2011). "Metabolic engineering of Escherichia coli for direct production of 1,4-butanediol." Nat Chem Biol **7**(7): 445-452.

Yoo, M., G. Bestel-Corre, C. Croux, A. Riviere, I. Meynial-Salles and P. Soucaille (2015). "A Quantitative System-Scale Characterization of the Metabolism of Clostridium acetobutylicum." mBio **6**(6): e01808-01815.

Zhang, L., X. Nie, D. a. Ravcheev, D. a. Rodionov, J. Sheng, Y. Gu, S. Yang, W. Jiang and C. Yang (2014). "Redox-Responsive Repressor Rex Modulates Alcohol Production and Oxidative Stress Tolerance in *Clostridium acetobutylicum*." Journal of bacteriology **196**: 3949-3963.

Zhuang, W.-Q., S. Yi, M. Bill, V. L. Brisson, X. Feng, Y. Men, M. E. Conrad, Y. J. Tang and L. Alvarez-Cohen (2014). "Incomplete Wood–Ljungdahl pathway facilitates one-carbon metabolism in organohalide-respiring *Dehalococcoides mccartyi*." Proceedings of the National Academy of Sciences of the United States of America **111**: 6419-6424.

Appendix A
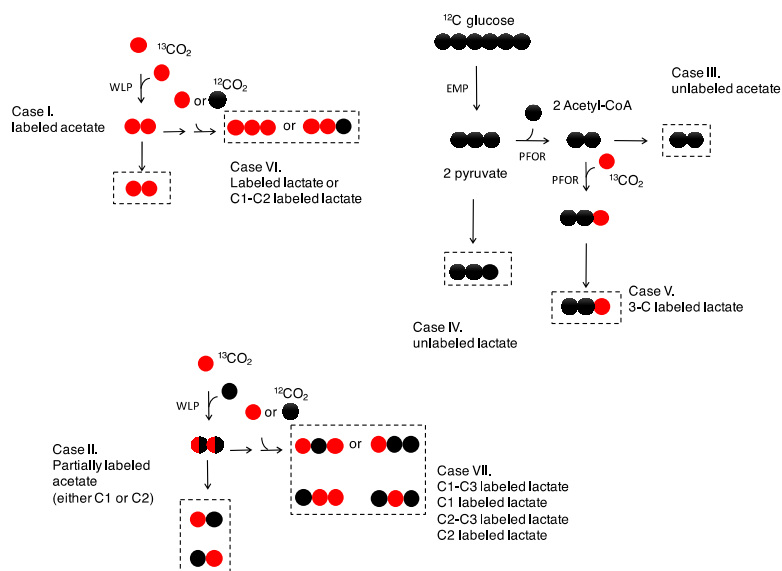
SUPPLEMENTAL MATERIALS FROM CHAPTER 3

Figure S3.1. Labeling in acetate or lactate derived through either the Wood-Ljungdahl pathway or glycolysis with labeled CO_2 or CO.

Table A.1. Percent labeling of the metabolites. Lactate and acetate labeling was measured, and that of ethanol and 2,3-BD was estimated based on the labeling of lactate and acetate, respectively.

	C. autoethanogenum		*C. ljungdahlii*	
	% labeled	total mM labeled	% labeled	total mM labeled
Lactate	21%	0.4	21%	0.5
Acetate	56%	77.1	78%	113.0
2,3-BD	21%	2.7	21%	2.7
Ethanol	56%	45.1	78%	6.4

Appendix B

SUPPLEMENTAL MATERIALS FROM CHAPTER 4

B.1 **Probing the ACS catalytic activity via the acetyl-CoA-exchange reaction using ^{13}C-acetate.**
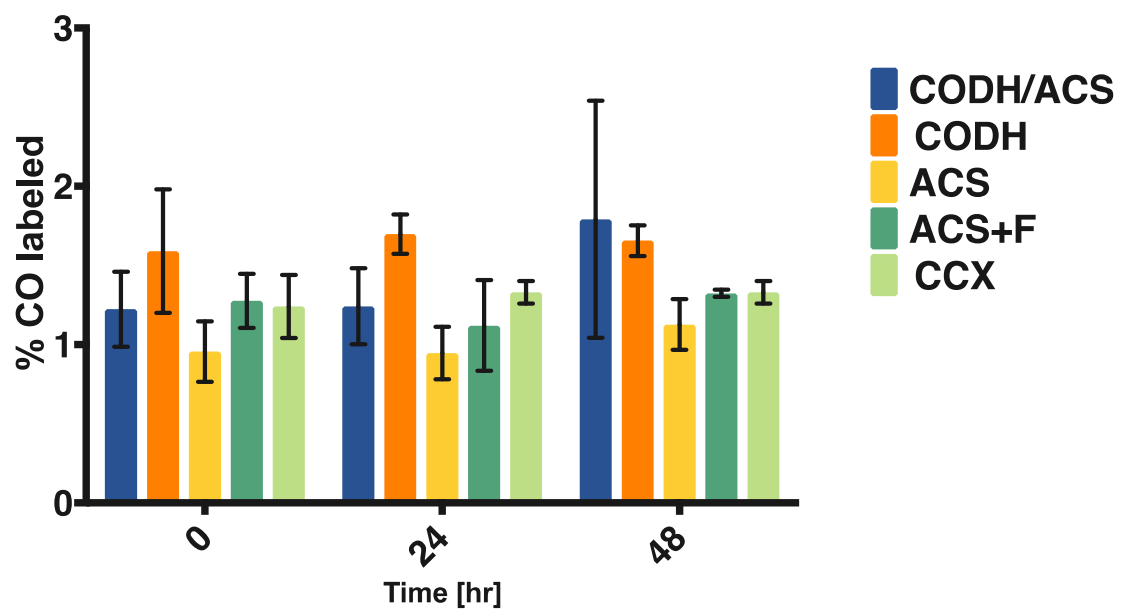
Figure B.1. Probing the ACS catalytic activity via the acetyl-CoA-exchange reaction using ^{13}C-acetate. A) Strains harboring the CODH/ACS, CODH, ACS, ACS and the nickel-accessory protein AcsF (blue, orange, yellow, green, respectively) (displayed left to right) were grown in defined medium with 40 g/L glucose and containing 30 mM sodium 1-^{13}C-acetate. *Clostridium carboxidivorans* (CCX) was used as a native acetogen control (light green). CO concentration was measured in the headspace for all strains of *Clostridium acetobutylicum* after 24 and 48 hours of growth. Even though the CODH/ACS strain exhibited an increase in ^{13}C labeling in CO, it is similar to the labeling pattern of strain expressing CODH alone. The ^{13}C labeling in CO derives from labeled CO_2. ^{13}C isotope labeling in the presence ^{13}C-acetate (carbonyl carbon) results in acetyl-CoA labeling at the carbonyl position. The carbonyl carbon of acetyl-CoA can exchange with CO using ACS. The acetyl-CoA can also be converted to acetone (releasing $^{13}CO_2$), and the CO_2 can be converted to CO using the CODH.

Appendix C

SUPPLEMENTAL MATERIALS FROM CHAPTER 5

C.1   Detailed Gas Consumption and Gas Evolution for *Clostridium acetobutylicum* expressing CODH and Control
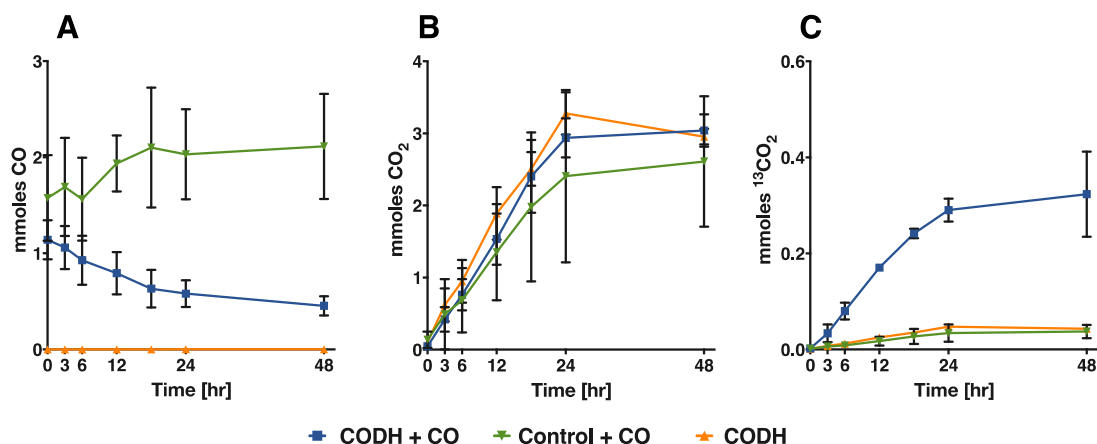
Figure C.1. Gas consumption and evolution during fermentation of *Clostridium acetobutylicum* expressing CODH in the presence of CO (blue), in the absence of CO (orange) or the control in the presence of CO (green). A) Consumption of CO over time. Only the strain containing the CODH is able to consume CO. The plasmid-control strain is unable to consume CO. Error bars are the standard deviation of 3 biological replicates. B) Evolution of total CO_2 over time. C) Evolution of labeled CO_2 over time. Only *Clostridium acetobutylicum* expressing CODH in the presence of CO increased the amount of labeled CO_2 above natural abundance. All experiments were started with high cell densities of late exponentially growing cells (OD_{600} ~1.5) in 40 g/l glucose (10 ml). 0.2 atm CO was added to the headspace (150 ml) to a total of 20 psig. Cultures were shaken at 37°C and 110 rpm.

C.2 Fermentation Profiles Show Similar Trend for *Clostridium acetobutylicum* expressing CODH and Control

The fermentation profiles for the experiment utilizng 0.2 atm of CO in the headspace are shown for the *Clostridium acetobutylicum* strain expressing the CODH enzyme in the presence (top, blue), in the absence of CO (middle, orange) and the control in the presence of CO (bottom, green) in Figure C.2. There is no difference when comparing the profiles of the *Clostridium acetobutylicum* strain expressing the

CODH enzyme in the presence or absence of CO, indicating no effect upon the addition of CO, as previously shown. The time at which acetone and butanol production was initiated was also similar, and appeared to occur shortly after inoculation. This is probably due to the fact that the experiment was started with high density inoculum. The control fermentation did not exhibit a significantly different fermentation profile. One of the biological replicates only consumed 50% of the initial glucose by 24 hours, making the errors large for glucose consumption and product production. Beside this replicate, there was no decrease in glucose consumption.
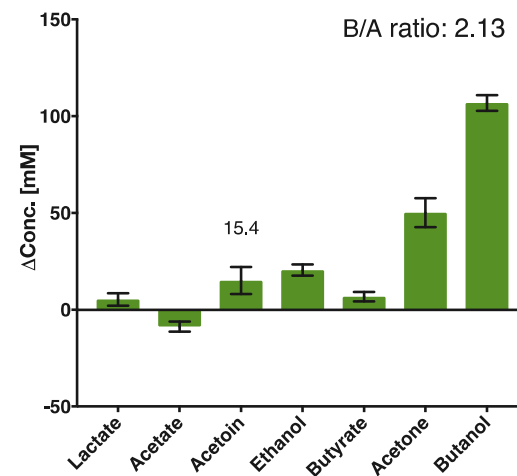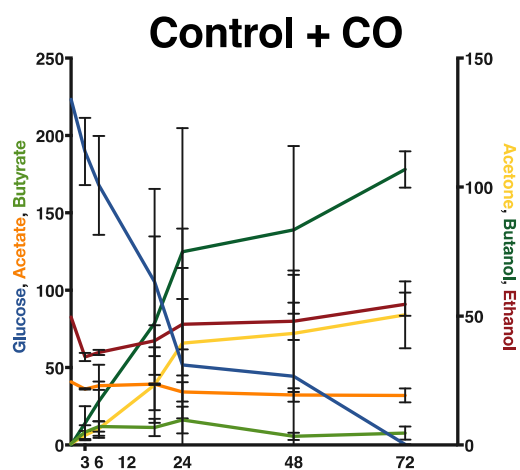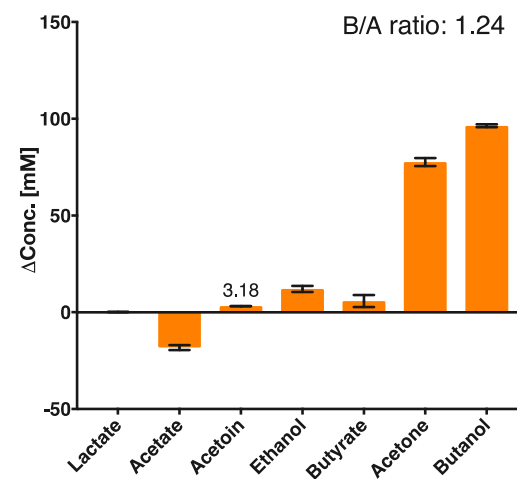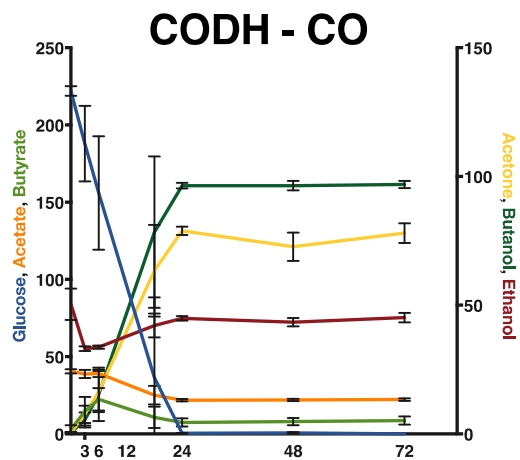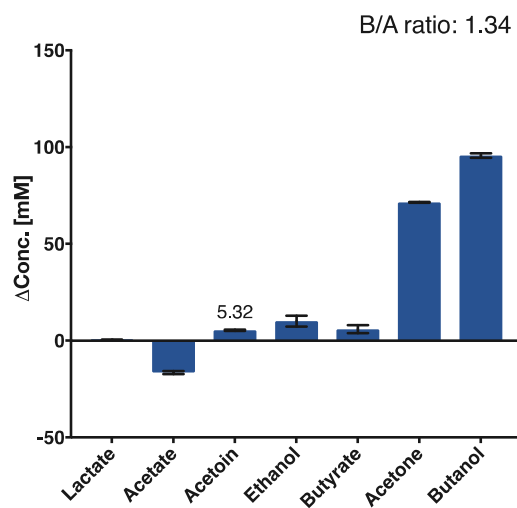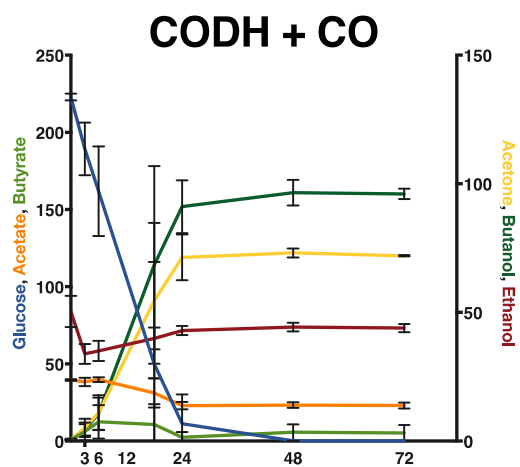
Figure C.2. Fermentation profiles (left side) for *Clostridium acetobutylicum* expressing the CODH in the presence (blue) or absence of CO (orange). The control is shown in green. The butanol to acetone ratios are shown in the box above the final metabolite changes (right side). Error bars are the standard deviations of 3 biological replicates.